

**Exploration of the potential of the hydroxynitrile lyase from *Arabidopsis thaliana* in a micro-aqueous organic solvent system**

Inaugural-Dissertation

zur Erlangung des Doktorgrades  
der Mathematisch-Naturwissenschaftlichen Fakultät  
der Heinrich-Heine-Universität Düsseldorf

vorgelegt von

**Aischarya Brahma**  
aus Dhamanahandi, Indien

Essen, September 2015

---

Aus dem Institut für Bio- und Geowissenschaften 1 (IBG-1: Biotechnology)  
am Forschungszentrum Jülich

Gedruckt mit der Genehmigung der  
Mathematisch-Naturwissenschaftlichen Fakultät der  
Heinrich-Heine-Universität Düsseldorf

Referent: Apl. Prof. Dr. Martina Pohl  
Koreferent: Prof. Dr. Karl-Erich Jäger

Tag der mündlichen Prüfung: 21.10.2015

---

## List of publications

### Peer-reviewed journal

**Brahma, Aischarya**; Musio, Biagia; Siegert, Petra; Jeromin, Gunter; Nikbin, Nikzad; Ley, Steven; Pohl, Martina. "An orthogonal biocatalytic approach for the safe generation and use of HCN in a multi-step continuous preparation of chiral O-acetylcyanohydrins", *Synlett* 2016, 27:262-266.

DOI: 10.1055/s-0035-1560644

### Conference proceedings

**Aischarya Brahma**<sup>a</sup>, Biagia Musio<sup>b\*</sup>, Nikzad Nikbin<sup>b</sup>, Petra Siegert<sup>c</sup>, Günter E. Jerominc, Steven V. Ley<sup>b</sup> and Martina Pohl<sup>a\*</sup> (2015). "Hydroxynitrile lyase catalyzed asymmetric cyanohydrin formation in flow with enzymatic HCN production", Biotrans, 26- 30.07.15, Vienna.

**Aischarya Brahma**<sup>\*</sup>, Amina Frese, Daniel Okrob, Kathrin Scholz, Martina Pohl (2014). "Whole cell biocatalysis for the production of industrially viable cyanohydrins", Biocat, 31.08- 04.09.14, Hamburg.

**Aischarya Brahma**<sup>\*</sup>, Daniel Okrob, Kathrin Scholz, Ulf Hanefeld, Ulrich Krauss, Karl Gruber, Martina Pohl (2013). "Stabilization of hydroxynitrile lyase from *Arabidopsis thaliana* by enzyme engineering and immobilization approaches", BioNoCo summer school, 9- 11.09.13, Aachen.

**Aischarya Brahma**<sup>\*</sup>, Amina Frese, Martina Pohl (2013). "Characterization of a new His-tagged variant of hydroxynitrile lyase in a microaqueous organic solvent system", Biotrans, 21- 25.07.13, Manchester.

---

**Aischarya Brahma\***, Daniel Okrob, Rene Nieguth, Marion Ansorge-Schumacher, Martina Pohl (2012). "Immobilization studies on hydroxynitrile lyase of *Arabidopsis thaliana* for improved biocatalytic applications", Biotrends, 29- 30.11.13, Dortmund

**Aischarya Brahma\***, Daniel Okrob, Rene Nieguth, Marion Ansorge-Schumacher, Martina Pohl (2012). "Characterization of the influences of non-conventional media on the activity and stability of Hydroxynitrile lyase". Biocat, 02.09- 06.09.12, Hamburg.

*\*presenting author*

---

## ACKNOWLEDGEMENT

My doctoral thesis has been a wonderful journey and I would like to express my gratitude to everyone who supported, guided and believed in me throughout this journey.

I fall short of words to express my sincere thanks to Prof. Dr. Martina Pohl for giving me this opportunity to conduct my doctoral thesis in her group. Apart from her scientific guidance and countless discussion sessions, I would like to thank her for her understanding, support and encouragement throughout the project.

I extend my heartiest gratitude to Prof. Dr. Karl-Erich Jäger for his kindness to co-supervise my doctoral thesis and exam.

I would like to acknowledge the effort from Mr. Daniel Okrob during my initial days, when I was being introduced to the project and the techniques. During my doctoral studies I had wonderful Master and Bachelor students working with me. I would like to mention the names of Amina Frese and Arne Billmeier, who not only did a commendable work in their respective thesis but also created an excellent atmosphere in the office and the labs.

I would like to express my gratitude to BioNoCo graduate school for the scholarship and I'd also like to thank all its mentors and members for their fruitful inputs and discussion during the workshops. A special thanks to Dr. Marco Bocola for his kind inputs in my project.

The acknowledgement will be incomplete if I don't express my sincere gratitude to my collaboration partners here:

Prof. Steven Ley from University of Cambridge for giving me an opportunity to work in his lab and learn about flow chemistry. I also appreciate his special interest and several discussions on my project. I extend my thanks to Dr. Biagia Musio for her guidance and support in the lab, Ms. Sonja Kamptmann for her ideas and introducing me to basic flow chemistry techniques and all my colleagues in the Wiffen and ITC lab, for such a friendly

---

working atmosphere, for exciting discussions on flow chemistry and for making life in Cambridge fun and memorable.

Prof. Dr. Ulf Hanefeld from TU Delft for the wonderful cooperation project and for providing me with the opportunity to learn about biotransformation with ketones.

Prof. Günter E Jeromin, Prof. Dr. Petra Siegert and Ulviyya Ismailova from FH Aachen, (campus Jülich) for the nice collaborative work, ideas and discussions.

My sincere gratitude goes to all the supervisors and members of the graduate school BioNoCo for the workshops, feedback, discussions and a friendly atmosphere.

My deep gratitude goes to all my colleagues from the Forschungszentrum Jülich, who were actually a small family for me, away from home. Special thanks to my office mates in Room 305, Anna, Vanessa, Justyna and especially Victoria, who have been pillar of constant support.

I extend my thanks to my car pooling group in Dusseldorf who were kind to give me a ride to Jülich during the days when I didn't own a car.

I cannot imagine my PhD without the loving support of my parents, my parents in law and my entire extended family for constant encouragement even though they were a thousand miles away. Special thanks to my uncle Loknath for being my inspiration since very early days.

My deepest gratitude to my mom who has always believed in me and loved me a lot to let me go so far away for pursuing my dreams.

I would like to thank all my friends spread all across the globe for their support by countless skype, calls, mails, and chats. I extend my thanks to my friend Preseela for being my fellow- PhD buddy and supporting me throughout the journey. I fall short of words to thank my friend Subhajit for his constant motivation, timely feedback and keeping my spirits high.

Finally, last and the most, I want to thank the strongest support system throughout my thesis- my husband Ashish for understanding and believing in me every single day even in the darkest of days. I owe this to you.

---

## DECLARATION

Die vorliegende Dissertation habe ich vollständig und ohne unerlaubte Hilfe angefertigt. Die Dissertation wurde in der vorgelegten oder in ähnlicher Form noch bei keiner anderen Institution eingereicht. Ich habe bisher keine erfolglosen Promotionsversuche unternommen.

Aischarya Brahma

Essen, September 2015

---

## Abbreviations

Ala	alanine
Asn	asparagine
Asp	aspartate
At	<i>Arabidopsis thaliana</i>
c	concentration (mol/L)
cm	centimeter
CSTR	continuous stirred tank reactor
d	day / density
DNA	deoxyribonucleic acid
EC	enzyme class
ee	enantiomeric excess
FAD	Flavin adenosine dinucleotide
FDA	US Food and Drug Administration
GC	gas chromatography
HCN	hydrogen cyanide
HCl	hydrochloric acid
HNL	hydroxynitrile lyase
His	histidine
IMAC	immobilized metal-ion affinity chromatography
Kan	kanamycin
kDa	kilo Dalton
KPi	potassium phosphate
LB	lysogeny broth
Lu	<i>Linum usitatissimum</i>
log	decimal logarithm
Me	<i>Manihot esculenta</i>
MS	Mass spectrometry
MTBE	methyl tert-butyl ether
n.d.	not determined
NTA	nitroacetic acid
OD	optical density
Pa	<i>Prunus amygdalus</i>

---

PBR	packed-bed reactor
Phe	phenylalanine
rpm	rounds per minute
RT	room temperature
SDS	sodium dodecylsulphate
Ser	serine
SFC	supercritical fluid chromatography
<i>Sb</i>	<i>Sorghum bicolor</i>
Thr	threonine
U	unit
UV	ultraviolet
wt	wildtype
w/w	weight per weight

---

## Abstract

There is a growing demand for biocatalytic processes in the industry for synthesis of various bulk and fine chemicals. Cyanohydrins formed by hydroxynitrile lyase (HNL) catalyzed hydrocyanation of aldehydes or ketones serve as valuable chiral building blocks for the pharmaceutical, agro-chemical and fine chemical industry.

In this work the potential of an *R*-selective HNL from *Arabidopsis thaliana* was deeper explored using a new His-tagged variant. The new variant showed an almost double specific activity compared to the wildtype enzyme, due to the higher purity, and otherwise similar pH and temperature optima like the wildtype enzyme. As the expression level is higher and the purification procedure shorter, the yield of purified enzyme is more than doubled.

The new *At*HNL variant (His<sub>6</sub>-*At*HNL) was subsequently used to evaluate the biocatalytic hydrocyanation of aromatic ketones, which are not the preferred substrates of this enzyme. Generally ketones are converted slower and less stereoselective, which is due to the sterical hinderance of the carbonyl function, the lower nucleophilicity, and thermodynamic limitations. However, using a micro-aqueous reaction system, which is well suited for *At*HNL, the conversion of two exemplarily chosen aromatic aldehydes (acetophenone and 2-fluoroacetophenone) could be increased up to 40 % and 48 %, respectively, which is 2-fold higher compared to similar studies in aqueous-organic two-phase systems described in literature. The micro-aqueous reaction system enabled product concentrations of 160-190 mM, demonstrating the potential of HNL-catalyzed reactions in such reaction systems for the synthesis of aromatic ketone cyanohydrins. However, there is strong indication for an enzyme-catalyzed product racemization, which makes careful control of the conversion necessary to obtain the products with high optical purity.

Based on these results also five 2-hydroxy ketones were tested as substrates for the enzyme. Although the respective cyanohydrines could be detected, enzyme catalysis could not specifically be proved for the hydrocyanation of these substrates as the stereoselectivity was almost comparable to the chemical control reaction. However, a weak but clear acceleration in presence

---

of the His<sub>6</sub>-AtHNL as well as of inactive active site variants could be proved for two of the five tested 2-hydroxy ketones. Additional studies to analyze the electrostatic surface potential (ESP) of the His<sub>6</sub>-AtHNL gave hints to the nature of this reaction acceleration by interaction of the reaction partners with the enzyme surface.

The second part of the work includes the transfer of the biocatalytic hydrocyanation from batch to a continuous flow mode. Therefore, a three-step cascade was established using the initial lipase-catalyzed production of HCN from ethyl cyanofornate, a subsequent hydrocyanation step catalyzed by His<sub>6</sub>-AtHNL (on Celite or whole cells), and a final in line acetylation of the resulting cyanohydrins.

Afterwards the flow reactor system was successfully used for the synthesis of six (hetero)aromatic O-acetylated cyanohydrines with excellent conversion and very good *ee*.

---

## Kurzfassung

In der Industrie besteht ein wachsender Bedarf an biokatalytischen Prozessen zur Herstellung von Bulk- und Feinchemikalien. Cyanhydrine, die durch die Hydroxynitrillyase (HNL)-katalysierte Hydrocyanierung von Aldehyden und Ketonen entstehen, sind wertvolle chirale Bausteine für die pharmazeutische, agrochemische Industrie und die Feinchemie.

In dieser Arbeit wurde das Potential einer *R*-selektiven HNL aus *Arabidopsis thaliana* unter Verwendung einer neuen His-getaggten Variante untersucht. Die neue Variante zeigte eine fast doppelt so hohe spezifische Aktivität im Vergleich zum Wildtyp-Enzym, bedingt durch die höhere Reinheit bei ähnlichen pH- und Temperaturoptima. Da der Expressionslevel höher und die Reinigungsprozedur kürzer waren, verdoppelte sich auch die Ausbeute an gereinigtem Enzym.

Die neue AtHNL-Variante (His<sub>6</sub>-AtHNL) wurde anschließend hinsichtlich der Hydrocyanierung von aromatischen Ketonen evaluiert, die nicht zu den bevorzugten Substraten des Enzyms gehören. Allgemein werden Ketone langsamer und meist auch mit geringerer Stereoselektivität umgesetzt, was auf die größere sterische Hinderung der Carbonylfunktion, die damit verbundene geringere Nukleophilie, sowie thermodynamische Gründe zurückzuführen ist. Allerdings konnte durch Verwendung eines mikro-wässrigen Reaktionssystems der Umsatz zweier beispielhaft gewählter Ketone (Acetophenon und 2-Fluoracetophenon) relativ zu Literaturwerten auf 40 % bzw. 48 % verdoppelt werden. Das mikro-wässrige Reaktionssystem ermöglichte Produktkonzentrationen von 160-190 mM, was das Potential solcher Reaktionssysteme für die Synthese von Ketoncyanhydrinen zeigt. Allerdings fanden sich starke Hinweise auf eine Enzym-katalysierte Produktracemisierung, was eine sorgfältige Umsatzkontrolle erfordert, um Produkte mit hoher optischer Reinheit zu erhalten.

Basierend auf diesen Ergebnissen wurden auch fünf 2-Hydroxyketone als Substrate für das Enzym untersucht. Obwohl die entsprechenden Cyanhydrine nachgewiesen wurden, konnte eine spezifischen Enzym-katalysierte Hydrocyanierung dieser Substrate nicht nachgewiesen werden, da die erhaltenen Stereoselektivitäten von ca. 20 % auch in der Enzym-freien Kontrolle auftraten.

---

Allerdings konnte eine schwache, jedoch deutliche Beschleunigung der Reaktion für zwei der untersuchten 2-Hydroxyketone durch His<sub>6</sub>-AtHNL sowie inaktive Varianten dieses Enzyms gezeigt werden. Ergänzende Untersuchungen zur Analyse des elektrostatischen Oberflächenpotentials der His<sub>6</sub>-AtHNL ergaben Hinweise auf die Natur der beobachteten Reaktionsbeschleunigung durch Interaktion der Reaktionspartner an der Proteinoberfläche.

Im zweiten Teil der Arbeit wurde die biokatalytische Hydrocyanierung vom Batch in einen kontinuierlichen Flussmodus übertragen. Dazu wurde eine Dreischritt-Kaskade, bestehend aus der Lipase-katalysierten Freisetzung von HCN aus Ethylcyanoformiat, der anschließenden His<sub>6</sub>-AtHNL-katalysierten (immobilisiert auf Celite oder in ganzen Zellen) Hydrocyanierung und einem dritten chemischen Acetylierungsschritt, etabliert.

Anschließend wurde dieses Flussreaktorsystem zur Synthese von sechs verschiedenen (hetero)aromatischen O-acetylierten Cyanhydrinen mit ausgezeichnetem Umsatz und sehr guten *ee*-Werten erfolgreich eingesetzt.

---

---

# Table of Contents

<b>List of publications</b> .....	<b>I</b>
<b>Abbreviations</b> .....	<b>VI</b>
<b>Abstract</b> .....	<b>VIII</b>
<b>Kurzfassung</b> .....	<b>X</b>
<b>1. Introduction</b> .....	<b>1</b>
1.1 Biocatalysis .....	1
1.1.1 History .....	1
1.1.2 Recent trends .....	1
1.1.3 Biocatalysis in non-conventional media.....	2
1.2 Process modes for biocatalysis .....	5
1.2.1 Batch and fed-batch mode.....	5
1.2.2 Continuous mode .....	5
1.2.3 Packed-bed reactors.....	9
1.3 Flow chemistry .....	10
1.3.1 Biotransformations in flow.....	11
1.4 Biocatalysis as a tool for synthesis of chiral building blocks.....	12
1.5 Hydroxynitrile lyase.....	13
1.5.1 Discovery .....	13
1.5.2 Natural function of hydroxynitrile lyases.....	14
1.5.3 Relevance of HNLs in organic synthesis .....	16
1.5.4 Classification of HNLs .....	17
1.5.5 HNL catalyzed reaction systems.....	19
1.6 HNL from <i>Arabidopsis thaliana</i> (AtHNL) .....	20
1.6.1 Discovery and potential .....	20
1.6.2 Substrate range .....	20

---

1.6.3 Enzyme mechanism.....	21
1.6.4 Enzyme stability.....	23
1.6.5 Immobilization of AtHNL.....	23
1.6.6 Whole cells as natural immobilisates.....	24
1.7 Recent studies on AtHNL-catalyzed synthesis of aldehyde and ketone cyanohydrins.....	24
<b>2. Aim of the thesis .....</b>	<b>27</b>
<b>3. Materials and Methods.....</b>	<b>29</b>
3.1 Materials.....	29
3.1.1 Chemicals .....	29
3.1.2 Bacterial strains and plasmids used .....	29
3.1.3 Kits and standard solutions used .....	30
3.1.4 Enzymes used .....	30
3.1.5 Media components .....	31
3.1.6 Materials.....	31
3.1.7 Devices .....	31
3.1.8 Softwares.....	32
3.1.9 Autoinduction media:.....	33
3.1.10 LB medium:.....	33
3.1.11 LB agar: .....	34
3.1.12 Buffers .....	34
3.2 Methods .....	35
3.2.1 Enzyme production .....	35
3.2.2 Sodium Dodecyl Sulfate PolyAcrylamide Gel Electrophoresis (SDS-PAGE) .....	36
3.2.3 Enzyme purification.....	36
3.2.4 Gel filtration .....	38
3.2.5 Lyophilization .....	38
3.2.6 Determination of protein concentration .....	39

---

3.2.7 HNL activity assay (mandelonitrile cleavage assay) .....	39
3.2.8 Immobilization on Celite .....	41
3.2.9 Preparation of “tea bags” with immobilized enzymes or lyophilized cells.....	42
3.2.10 Generation of HCN in a batch mode .....	42
3.2.11 Synthesis of aldehyde cyanohydrins in a batch mode .....	42
3.2.12 Synthesis of ketone and 2-hydroxyketone cyanohydrins in batch .....	43
3.2.13 Recyclability studies for Celite-His <sub>6</sub> -AtHNL and <i>E. coli</i> -His <sub>6</sub> -AtHNL.....	45
3.2.14 Stability studies for celite-His <sub>6</sub> -AtHNL and <i>E. coli</i> - His <sub>6</sub> -AtHNL in MTBE .....	45
3.2.15 CalB-mediated hydrolysis of ethyl cyanofornate (ECF) in continuous mode .....	46
3.2.16 Stability of lipase-mediated hydrolysis of ECF in a continuous mode .....	47
3.2.17 Synthesis of ( <i>R</i> )-mandelonitrile with Celite- His <sub>6</sub> -AtHNL in continuous mode .....	47
3.2.18 Synthesis of ( <i>R</i> )-mandelonitrile with a 2-step cascade (CalB-His <sub>6</sub> -AtHNL) .....	48
3.2.19 Synthesis of ( <i>R</i> )-mandelonitrile with a 2-step cascade (CalB- <i>E. coli</i> -His <sub>6</sub> -AtHNL).....	49
3.2.20 Three-step cascade synthesis of ( <i>R</i> )-O-acetylcyanohydrins in flow.....	50
3.2.21 General batch procedure for the synthesis of racemic O-acetylcyanohydrins as reference compounds .....	51
3.2.23 Analytics .....	51
<b>4. Results and Discussion.....</b>	<b>57</b>
4.1 Characterization of His <sub>6</sub> -AtHNL .....	57
4.1.1 Synthesis of aldehyde cyanohydrins with lyophilized His <sub>6</sub> -AtHNL.....	59
4.1.2 Recyclability of Celite-His <sub>6</sub> -AtHNL and whole cells in MTBE .....	62
4.2 Ketones as substrates.....	64
4.2.1 Aromatic ketones as substrate.....	64
4.2.2 2-Hydroxy ketones as substrates .....	70
4.3 Biotransformations in flow reactors for continuous synthesis of cyanohydrins .....	77
4.3.1 Step 1- Lipase mediated liberation of HCN .....	78
4.3.2 Stability of the system .....	81

---

---

4.3.3 Step 2: <i>At</i> HNL-catalyzed continuous synthesis of ( <i>R</i> )-mandelonitrile .....	82
4.3.4 Two-step enzymatic cascade.....	83
4.3.5 Evaluation of whole cell biocatalysis in flow .....	84
4.3.6 Stability of the two-step enzyme cascade .....	85
4.3.7 Step 3: Inline acetylation as a third step of the cascade.....	87
<b>Summary.....</b>	<b>92</b>
<b>Outlook.....</b>	<b>97</b>
<b>References.....</b>	<b>100</b>
<b>Appendix.....</b>	<b>118</b>

---

---

## LIST OF FIGURES

Figure 1: Different methods of enzyme immobilization.....	4
Figure 2: Schematic representation of a batch process.....	5
Figure 3: Schematic representation of a continuous process.....	6
Figure 4: Exploded view of a membrane reactor .....	8
Figure 5: Schematic representation of a plug flow reactor .....	9
Figure 6: A schematic depiction of the potential of a simple flow system .....	11
Figure 7: HNL-catalyzed cleavage of cyanohydrins to liberate HCN and the respective aldehydes or ketones.....	13
Figure 8: Synthesis of ( <i>R</i> )-mandelonitrile from benzaldehyde using bitter almond extract (emulsin). .....	13
Figure 9: Biosynthesis, catabolism and detoxification of cyanogenic glycosides.....	14
Figure 10: Biosynthesis of amino acid.....	15
Figure 11: Reactions based on cyanohydrins .....	16
Figure 12: Potential mechanism of AtHNL postulated enzyme mechanism of AtHNL .....	22
Figure 13: IMAC chromatogram for the purification of His <sub>6</sub> -AtHNL.....	37
Figure 14: Cleavage of mandelonitrile .....	40
Figure 15: Procedure for immobilization of AtHNL on Celite .....	41
Figure 16: Derivatization of aldehyde cyanohydrins by acetylation.....	43
Figure 17: Reaction scheme for the a) acetylation using acetic anhydride and 4- dimethylaminopyridine b) O- silylation of cyanohydrin using BSTFA. ....	44
Figure 18: Derivatization of 2-hydroxy ketone cyanohydrins by acetylation.....	45
Figure 19: Packed-bed reactor filled with 277 mg Novozyme 435 (Cal B) .....	47
Figure 20: Picture of an omnifit column .....	48
Figure 21: Reactor setup of the 3-step chemoenzymatic cascade with whole cells (E. coli-His <sub>6</sub> -AtHNL).....	50
Figure 22: Conversion and ee of a) benzaldehyde b) 2-chlorobenzaldehyde and c) hexanal to their respective cyanohydrins.....	59
Figure 23: Synthesis of ( <i>R</i> )-mandelonitrile with Celite-His <sub>6</sub> -AtHNL. ....	61
Figure 24: Conversions and ee with whole cell biotransformation using a) benzaldehyde and b) 2- chlorobenzaldehyde as substrate .....	62
Figure 25: Recyclability of Celite-His <sub>6</sub> -AtHNL (left) and E. coli-His <sub>6</sub> -AtHNL (right) for the synthesis of ( <i>R</i> )- mandelonitrile. ....	63

---

Figure 26: Analysis of the hydrocyanation of 2-F-acetophenone. ....	65
Figure 27: Synthesis of ketone cyanohydrins from a) acetophenone; b) 2-F-acetophenone. ....	66
Figure 28: conversion and ee of the reaction with the enzyme and the ee after removal of the enzyme for a) acetophenone b) 2-fluoroacetophenone.....	69
Figure 29: GC-Chromatogram of diacetylated ( <i>S</i> )-HPP cyanohydrin.....	72
Figure 30: Effect of His-AtHNL concentration on the hydrocyanation and ee of ( <i>S</i> )-HPP.....	75
Figure 31: The electrostatic surface potential (ESP) of the His <sub>6</sub> -AtHNL dimer .....	76
Figure 32: Schematic representation of the 3-step chemoenzymatic cascade .....	78
Figure 33: a) Generation of HCN by hydrolysis of ECF; b) Recyclability of CalB in batch mode; c) Reaction scheme for the hydrolysis of ECF.....	79
Figure 34: Schematic representation of hydrolysis of ECF in a continuous flow set-up. ....	80
Figure 35: CalB-catalyzed hydrolysis of ECF in a continuous flow set-up.....	81
Figure 36: Schematic representation of Celite-His <sub>6</sub> -AtHNL mediated synthesis of ( <i>R</i> )-mandelonitrile .....	82
Figure 37: Schematic representation of the 2-step enzymatic cascade for the synthesis of ( <i>R</i> )-mandelonitrile. ...	84
Figure 38: Schematic presentation of the 2-step cascade .....	85
Figure 39: Conversion and ee of the hydrocyanation of benzaldehyde to ( <i>R</i> )-mandelonitrile in the two-step cascade. ....	86
Figure 40: Schematic presentation of the 3-step cascade .....	88
Figure 41: Schematic representation of the 3-step chemoenzymatic cascade with lipase, E.coli-His <sub>6</sub> -AtHNL and a chemical modification are connected sequentially.....	95

---

---

## LIST OF TABLES

Table 1: Comparative characterization of wt-AtHNL and His <sub>6</sub> -AtHNL [142]. .....	58
Table 2: Substrate screening for the synthesis of 2-hydroxy ketone cyanohydrins. ....	71
Table 3: Hydrocyanation of ( <i>S</i> )-HPP with various control experiments.....	73
Table 4: Optimization of hydrolysis of ECF .....	80
Table 5: Optimization of the reaction parameters for the Celite-His <sub>6</sub> -AtHNL catalyzed synthesis of ( <i>R</i> )- mandelonitrile in the flow set-up.....	83
Table 6: Synthesis of different cyanohydrins in the optimized three-step chemoenzymatic cascade .....	89



# Chapter 1

## INTRODUCTION

---

# 1. Introduction

## 1.1 Biocatalysis

### 1.1.1 History

*“Enzymes are nature’s sustainable catalyst- they’re biocompatible, biodegradable and derived from renewable resources”* Roger Sheldon [1].

In a broader sense, biocatalysis can be defined as the application of enzymes or microbial cells for chemical synthesis [2, 3].

The application of biocatalysis for brewing beer and wine dates back to 7000 years ago [4]. However, it was only in 1767 for the first time ever that Antonie van Leewenhoek observed microorganisms under a microscope and over hundred years later Pasteur postulated that these tiny invisible microorganisms can convert sugars to alcohols by [5]. In 1876, Kühne coined the term “enzymes” and Ostwald coined the term “catalysis” [6] and soon Fischer proposed the famous “lock and key” hypothesis to elucidate the mechanism of enzyme catalysis [7]. It didn’t take long to discover that living organisms are not required to perform catalysis but the cell free extract is sufficient [8]. In 1926, urease was crystallized and it was finally proved that enzymes are actually proteins [9]. Soon a biocatalytic process was patented for the first time ever for the trypsin catalyzed pre-treatment of leather by a German company Röhm GmbH. Since then hundreds of biocatalytic processes have emerged for multiple applications.

### 1.1.2 Recent trends

Enzymes are remarkably brilliant catalysts offering the advantage of excellent chemo and regio selectivity, which makes them very attractive in many industries especially in the pharmaceutical industry and for fine chemical production, where high enantiopurity is an essential [10]. Today in the 21<sup>st</sup> century, with the advancement in molecular biology techniques, the number of industrial applications of enzymes has increased exponentially [11–13]. Industrial processes now are suited

---

to the availability of the biocatalyst rather than the availability of substrate, the nature of the reaction, etc [14]. Moreover, combining enzymes to form a multi-step cascade can help to synthesize complex molecules in an environmentally friendly and sustainable manner [15].

### **1.1.3 Biocatalysis in non-conventional media**

For a very long time, enzymes were only used in an aqueous environment that was regarded as “natural”, although the environment of cytosolic enzymes is far from being aqueous [16]. Application of enzymes in aqueous media, however, limits the scope of biotransformations at preparative scale. These limitations include poor solubility of substrates and products, unwanted side reactions, low product concentrations concomitant with cumbersome product recovery and sometimes even unfavorable thermodynamics in water [17].

In the recent years, biocatalysis in non-conventional media, such as organic solvents, ionic liquids, supercritical fluids, etc. has become increasingly popular [18]. Klibanov first reported the possibility of biocatalysis in organic solvents [19], which shed light on the usually accepted idea that enzymes denature in organic solvents [20]. The reason lies in the fact that water acts as a molecular lubricant and its absence renders the enzyme rigid [21]. It was understood that an optimal degree of hydration is required in non-aqueous media to preserve enzyme flexibility [22].

#### ***1.1.3.1 Effect of organic solvents and water on enantiomeric excess (ee)***

Besides water activity, the choice of the organic solvent plays a very crucial role for the activity, selectivity, and stability of biocatalysts [23]. The enzyme selectivity depends greatly on the solvent used and surprisingly the solvent can even inverse the stereoselectivity [17, 24, 25].

Since water keeps the enzyme flexible, it is indispensable for catalysis. Now, there are two contrasting theories about the effect of enzyme flexibility on enantioselectivity. An early hypothesis of Boos et al., based on studies with subtilisin, stated that with the increase of enzyme flexibility, the enantioselectivity increases [26]. However, these results were contradicted by a subsequent study of the Klibanov group, who found out that subtilisin and  $\alpha$ -chymotrypsin

---

became less enantioselective with increasing water content. They interpreted this effect such that the higher flexibility allows for better binding also of the less preferred enantiomer [17, 27].

### *1.1.3.2 Reaction media*

The most typical reaction media for biocatalysis are aqueous and aqueous/organic solvent systems [28]. There are mono-phasic systems consisting of an aqueous buffer and a small amount of water miscible organic solvent. The second class encompasses two-phase systems consisting of an organic phase and an aqueous phase. Micro-aqueous systems are mono-phasic solvents resulting from hydrophobic organic solvents containing a few percent of dissolved water. The enzymes are either dissolved in the aqueous phase or are applied in immobilized form.

The present work is focused on biocatalysis in micro-aqueous organic media. This small amount of water is crucial for enzyme activity [29]. Nevertheless, biocatalysis in non-aqueous media has been widely used in industry in batch and continuous processes for organic synthesis, however, almost exclusively with hydrolases, such as lipases and esterases. [18, 30, 31]

### *1.1.3.3 Enzyme immobilization*

Enzyme immobilization can be defined as a process of physically confining an enzyme to a defined region in space to retain the catalytic efficiency, which can be recycled continuously [32]. Immobilization can improve the long term operational stability and easy recovery of the enzyme, and sometimes additionally improve the activity and selectivity [33–35].

However, enzyme immobilization also suffers from some limitations such as:

- Loss of activity during immobilization
- Mass transfer limitations
- Cost of the carrier and immobilization procedure

There are different methods to immobilize an enzyme and there is no general method, which can be used for all applications of an enzyme. The choice of an immobilization procedure and/or choice of a support depend on the enzyme and the biocatalytic process. An enzyme can be

---

immobilized by different methods (Figure 1) such as carrier bound on the surface of e.g. silica (Celite) or ion exchangers. This binding is mainly due to weak interactions such as van der Waals forces, ionic interactions, and hydrophobic interactions. To prevent leaching of the biocatalyst, the introduction of covalent bonds is useful. However, this usually requires the use of bifunctional crosslinking agents (e.g. glutaraldehyde), which is often impairs the enzyme activity.

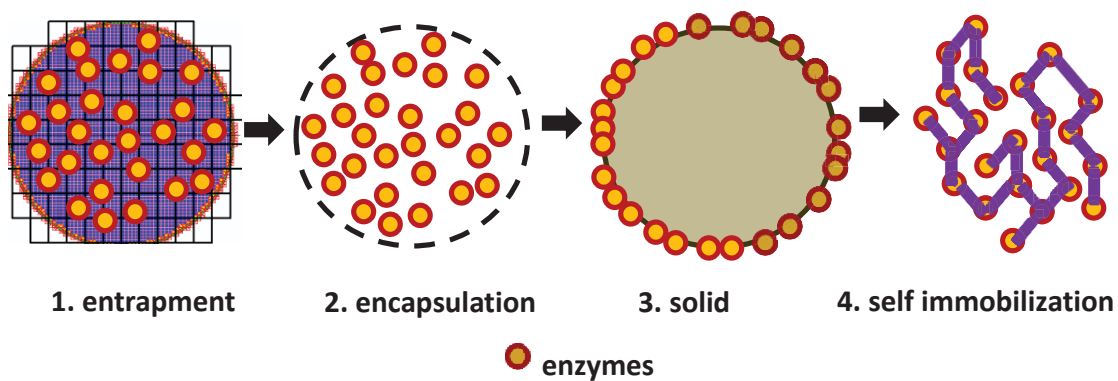


**Figure 1: Different methods of enzyme immobilization. Modified from [36]**

The enzyme can also be entrapped in a polymer network such as silica, sol-gel or a microcapsule. Usually the polymer matrix is synthesized in the presence of the enzyme. Enzyme leaching cannot entirely be prevented by entrapment. The third carrier-free immobilization method is based on direct cross-linking of precipitated enzymes, known as Cross-Linked-Enzyme-Aggregates (CLEAs) [37, 38]. Although this method avoids the costs for the carrier, the general problem arising from crosslinking remains and the specific activity of CLEAS is often much lower compared to the native enzyme. Besides these methods, where the immobilized enzyme is used as a heterogeneous catalyst, the immobilization of soluble enzymes behind a semi-permeable membrane is also a frequently used concept (chapter 1.2.2.1).

---

## 1.2 Process modes for biocatalysis

### 1.2.1 Batch and fed-batch mode

Most conventional biocatalytic processes are performed in batch just like chemical processes and in cases where the catalyst deactivates fast, batch offers a simple and optimal solution [4]. In a typical batch process, the substrate and enzyme molecules have similar residence times within the reactor, although sometimes further addition of substrate or enzyme may be necessary, which is called a fed-batch process mode [39]. Batch processes offer significant advantages like simplicity of process development and controllable environment for slow reactions. Additionally, such processes can be used multiple times for example with immobilized enzymes.

However, when considering scaling up, a batch reactor can be much more laborious and therewith more expensive than a continuous one because of the set-up times. Additionally, it demands extensive labor and services. The reproducibility could also vary from batch to batch, which makes it challenging during a scale up. Since the substrate and product are in a single pot, problems with substrate surplus inhibition or product inhibition may arise.

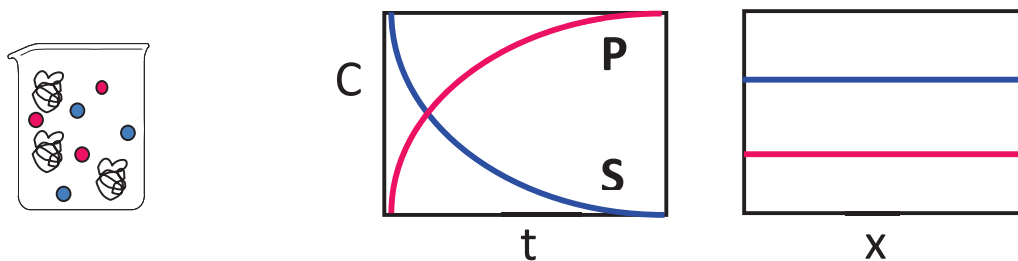


**Figure 2: Schematic representation of a batch process (blue substrate, red product, and black enzyme) (left). In batch the concentrations of substrate and product change over time (middle), whereas in a perfectly mixed system the concentration of both in the reaction vessel at a given time point is constant (right).**

### 1.2.2 Continuous mode

There are two different continuous concepts in biocatalysis: systems that retain a freely flowing biocatalyst behind a semipermeable membrane on the retentate side and plug flow reactors

---

containing a fixed bed of immobilized biocatalysts. Continuous processes have various advantages over batch such as higher space time yields (based on the reactor volume), easier product purification, optimal energy cost, shorter set-up times, etc. [40]. Furthermore, it can be integrated in modern synthetic chemistry approaches using immobilized catalyst (chapter 1.1.4). Immobilized enzymes not only offer catalyst recycling, but also ease the process of product purification and thereby rendering it cost effective [41]. To cope with enzyme inactivation, the residence times can be adjusted by altering the flow rate.

### 1.2.2.1 Continuous stirred tank reactors (CSTR)

CSTRs comprise of a well stirred tank connected to a continuous influx and efflux stream with an immobilized catalyst. Apart from good mixing abilities, a CSTR is simple and versatile. In an ideal case with perfect mixing, the concentrations of all reactants are constant in every volume element and at any time point.

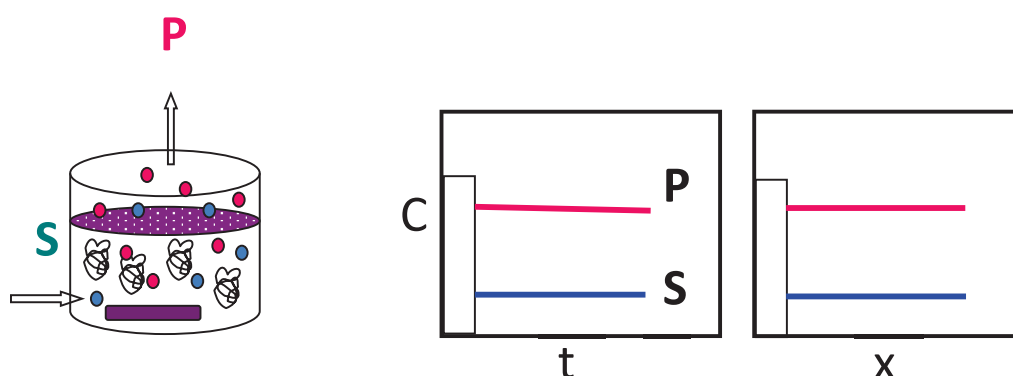


**Figure 3: Schematic representation of a continuous process (blue substrate, red product, black enzyme) (left). In a continuous process, the concentrations of substrate and product remain constant over time (middle), and also the concentration of both at any position (X) in a perfectly mixed reaction vessel is constant (right).**

In a CSTR the enzyme is in a constant environment and the concentrations of substrate(s) and product(s) ideally don't change. Hence such processes are very suitable for enzymes with substrate surplus inhibition. A CSTR can be used as a stand-alone single unit or several CSTRs can

---

be connected in series, this would mimic a packed-bed reactor (PBR). In such cases the product concentration gradually increases over the reactor series [42].

### *1.2.2.2 Membrane reactors*

In most membrane reactors the biocatalyst (isolated enzyme or whole cell biocatalyst) is freely circulating on the retentate side, retained by a semi-permeable membrane, which is permeable for small reaction components, such as substrate and product molecules [43]. Such reactors are operated with flat membranes or with hollow fiber modules [44]. Since enzyme immobilization is achieved through the membrane and thus no additional steps for enzyme immobilization (chapter 1.1.4) are necessary, this concept is not hampered by many typical limitations of heterogeneous immobilization methods (chapter 1.1.3.3).

Membrane reactors are advantageous because of the intensive use of enzymes and thereby high economic viability, continuous product removal, which can contribute a shift in the equilibrium and the possibility of having an integrated process with reaction and separation. In case of an ideal membrane reactor the following applies [43]:

- The enzyme is fully retained and therefore the product is enzyme-free
- There is no loss of enzyme activity over time
- Homogenous reaction conditions between the membrane surface and the core solution
- Enzymes are uniformly distributed (i.e. there is no concentration polarization)
- No membrane fouling

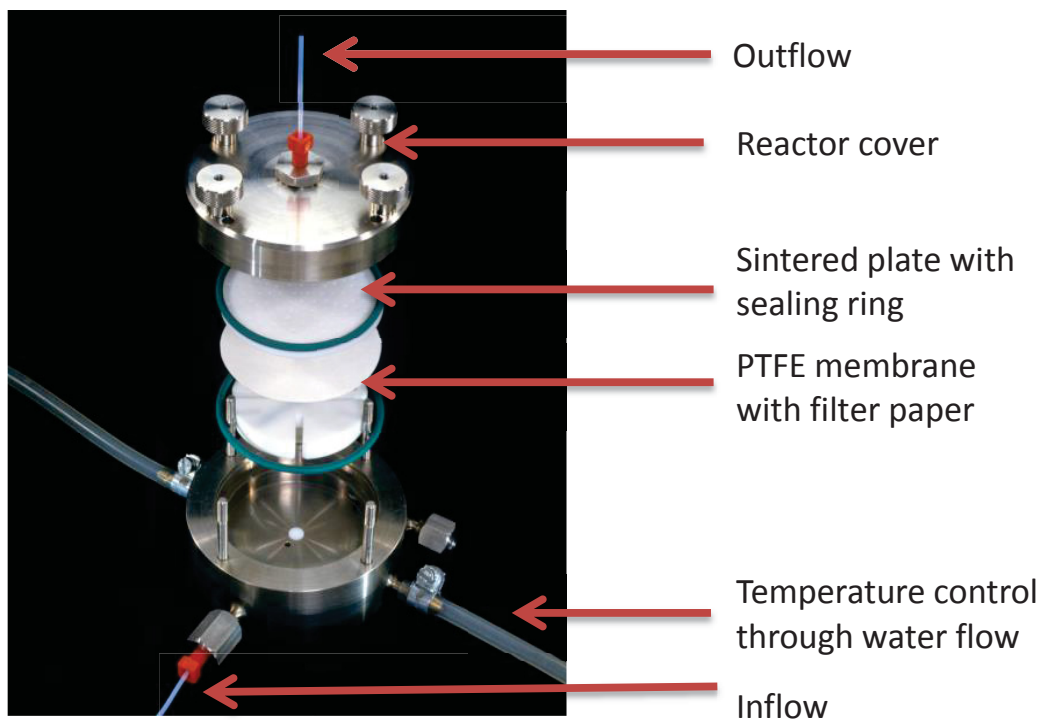


**Figure 4: Exploded view of a membrane reactor [45]**

However, in reality the performance decreases during operation because of enzyme deactivation, mass transfer limitations, leakage of enzyme and enzyme inhibition due to substrates and products. As for all biocatalytic processes, the stability of the biocatalyst under process conditions is decisive. Specifically stirring and pumping poses shear stress to enzymes, and this often leads to a progressive inactivation through denaturation of the protein. In many cases the loss of enzyme activity can be compensated by the addition of fresh enzyme to maintain the productivity of the reactor [46]. However, the deposition of inactive and active enzyme on the membrane often results in mass transfer limitations and fouling, which requires cleaning or replacement of the membrane including additional costs [39, 43].

---

### 1.2.3 Packed-bed reactors

In an ideal packed-bed reactor (PBR) the entire substrate stream flows parallel to the reactor axis with a constant flow rate. It is called a plug flow reactor when a solid/immobilized catalyst is used. In contrast to the CSTR, which offers good mixing, an ideal PBR shows no back mixing. It is quite important to note that a PBR shows a high enzyme/substrate ratio in a small reactor volume. Therefore it offers high space time yield [41]. In case of an ideal plug flow reactor, the following applies:

- the flow is laminar and the reaction medium is uniform throughout the reactor
- the residence time is the same for each volume element
- the reaction rate varies along the length of the reactor
- there are no diffusion or dispersion limitations
- the biocatalyst is fully stable

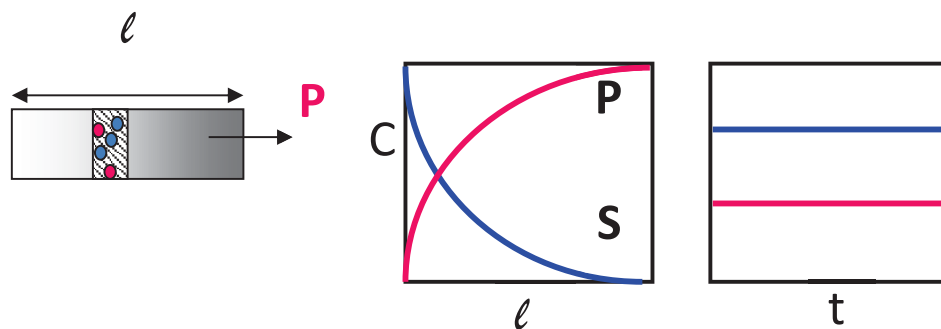


**Figure 5: Schematic representation of a plug flow reactor (blue substrate, red product, black enzyme) (left). In a plug flow reactor, the concentrations of substrate decreases and that of product increases over the length of the reactor (middle), whereas the concentration of both, substrate and product, at any position ( $l$ ) in the reactor at a given time point is constant (right).**

However, in a real case, there is back mixing and also formation of channels within the packed bed. When channel formation occurs, the conversion of the substrate is impaired since the substrate solution has less contact to the catalyst. This can be avoided by the use of a back pressure regulator (BPR) which helps to keep the bed uniformly fluidized. In principle a BPR is a

---

one way valve that opens when a certain set point pressure is reached. Diffusion and dispersion limitations can be minimized by good packaging but unfortunately it cannot be completely avoided.

Apart from the reactors, the modules for the downstream processing such as purification units, etc. are also commercially available. A combination of all the modules to start from the substrate and produce and purify the product and sometimes including recycling opens door to a field called “flow technology”, which is already quite prevalent in the chemical industry.

### 1.3 Flow chemistry

In traditional batch reactions, each step of a multistep synthesis is treated as an isolated system where the respective intermediate product is produced, isolated and applied in the subsequent step. In contrast, all steps of a multi-step reaction including product isolation can be combined with different modules to perform robust and multistep synthesis [47]. Such machine-assisted tools can be assembled together in flow for organic synthesis and with the help of a software all relevant parameters of the process can be controlled [48].

Most interestingly, the reaction can be analyzed in flow by in-line measurements such as infrared spectroscopy, mass spectroscopy, etc. Flow technology is also applied in drug discovery for the synthesis of small molecules [49].

The potential of a simple flow system is as shown in the figure below [50].

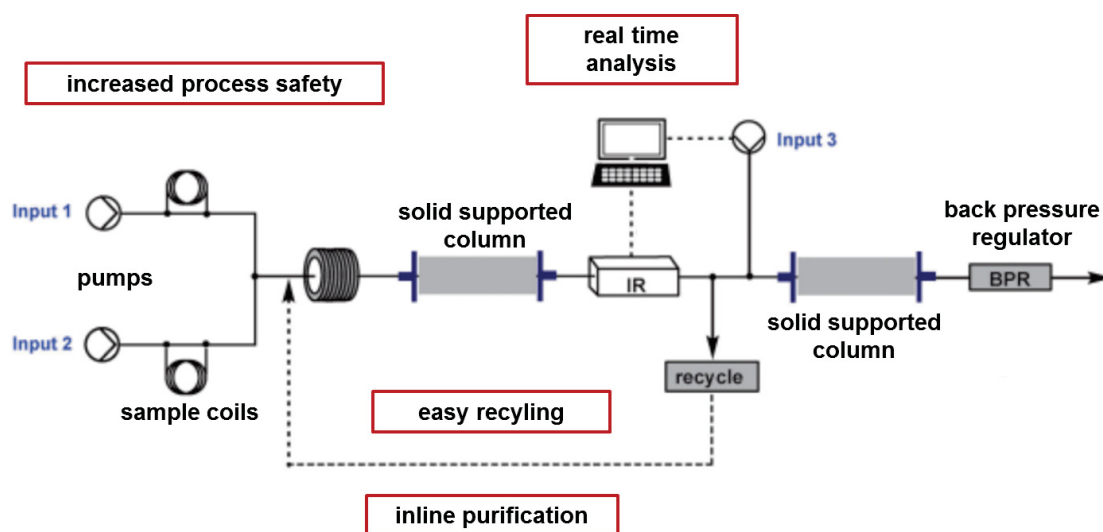


Figure 6: A schematic depiction of the potential of a simple flow system [50]

Besides the possibility to conduct multi-step syntheses without isolation of intermediates, flow technology has further advantages:

- increased process safety, especially for handling toxic compounds
- improved process control
- scale-up is easier
- reactions at temperatures higher than the boiling point of substrate possible
- easier downstream processing

However, a difficulty with flow technology is the transfer of processes from batch to flow, which could be challenging mostly because of differences in the behavior of catalysts in different systems.

Such flow setups are used extensively in the industry with chemical catalysts [50–52].

### 1.3.1 Biotransformations in flow

Despite all the advantages and benefits flow technology has to offer, only few studies have been reported on the use of enzymes in flow technology (see below). Combining flow technology and

---

biocatalysis, however, would increase the potential specifically also of chiral syntheses in in chemo-enzymatic cascade tremendously. There is a growing interest to involve tools and modules of flow reactors for the development of an optimized biocatalytic process to render it time and cost efficient. Most of the reported biotransformations are limited to robust commercially available enzymes like lipases; for example the kinetic resolution of flurbiprofen using whole microbial cells [53].

For retention of the biocatalyst in respective flow modules a sufficiently stable immobilization method must be available. In addition to synthesis with immobilized catalyst, whole cell biotransformation has also been successfully demonstrated in a continuous flow reactor. Such multistep enzyme cascades are also possible by immobilizing the enzyme on the inner side of a glass tubes. An example is the immobilization of two enzymes namely *Aspergillus niger* glucose oxidase (God) and horseradish peroxidase (HRP) using the avidin-biotin system and a polycationic dendronized polymer in order to quantify D-glucose spectrophotometrically [54].

Further, the biocatalytic synthesis of 3-phenylcatechol was reported using a segmented tube in tube reactor with 2-hydroxybiphenyl 3-monooxygenase for hydroxylation reactions [55].

Just recently another flow reactor for the production of protected mandelonitrile has been reported with the *R*-selective hydroxynitrile lyase from almonds using a membrane based phase separation unit [56].

#### **1.4 Biocatalysis as a tool for synthesis of chiral building blocks**

Biocatalysts obviously have an advantage over conventional chemistry owing to their specificity, selectivity, mild reaction conditions and environmental friendliness. They have been therefore implemented in hundreds of biocatalytic processes in industries [14]. Recently, a very interesting article quoted a chemist's prayer- "*I fall upon my knees and pray that all my syntheses may no longer be inferior to those conducted by bacteria*" [57].

---

Many enzymes are being used industrially for the synthesis of chiral compounds. One example is hydroxynitrile lyases which can catalyze the stereoselective carbonylation of achiral precursors.

## 1.5 Hydroxynitrile lyase

### 1.5.1 Discovery

Hydroxynitrile lyases (HNLs) catalyze the reversible cleavage and synthesis of cyanohydrins (Figure 7). The discovery of HNLs dates back to 1837 when Justus and Wöhler observed that bitter almond extract, which he called "emulsin", caused the release of HCN from certain cyanohydrins [58].

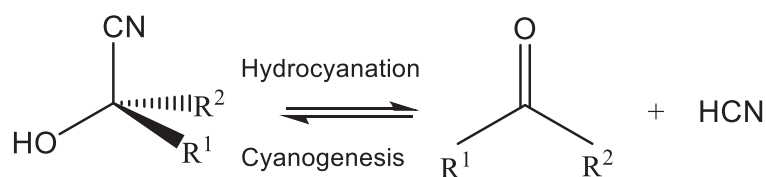


**Figure 7: HNL-catalyzed cleavage of cyanohydrins to liberate HCN and the respective aldehydes or ketones. The reverse hydrocyanation of an aldehyde/ketone is of technical interest.**

Later in 1908, Rosenthaler described that the reverse reaction for synthesis of cyanohydrins from HCN and benzaldehyde can be catalyzed with the "emulsin" reported earlier [59] (**Figure 8**). Subsequently, HNLs were also isolated from many different plant sources for biotechnological processes.

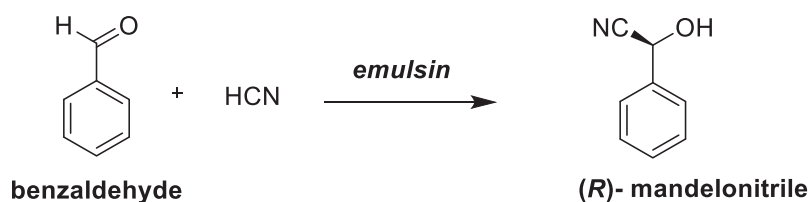


**Figure 8: Synthesis of (R)-mandelonitrile from benzaldehyde using bitter almond extract (emulsin).**

## 1.5.2 Natural function of hydroxynitrile lyases

HNLs occur in certain bacteria, fungi, arthropods as well as in many higher plants [60]. In nature, they are involved in two functions namely cyanogenesis and nitrogen fixation.

### 1.5.2.1 Cyanogenesis

The cleavage of an  $\alpha$ -cyanohydrin to release HCN is part of the plant defense mechanism against predators and this process is called “cyanogenesis” [61]. The fairly unstable cyanohydrins are stored in form of cyanogenic glucosides [62, 63]. The process of cyanogenesis comprises two steps: First the  $\beta$ -glucosidase-mediated degradation of the precursor glycoside to produce the cyanohydrin and second the HNL-mediated cleavage of the cyanohydrin to release HCN. Both enzymes are stored in separate compartments in vacuoles to prevent suicidal cyanogenesis and both only come into contact when the tissue is injured [64–66]. The toxicity of cyanide is attributed to its irreversible binding to the cytochrome oxidase in mitochondria and thus inhibiting the respiratory system [67].

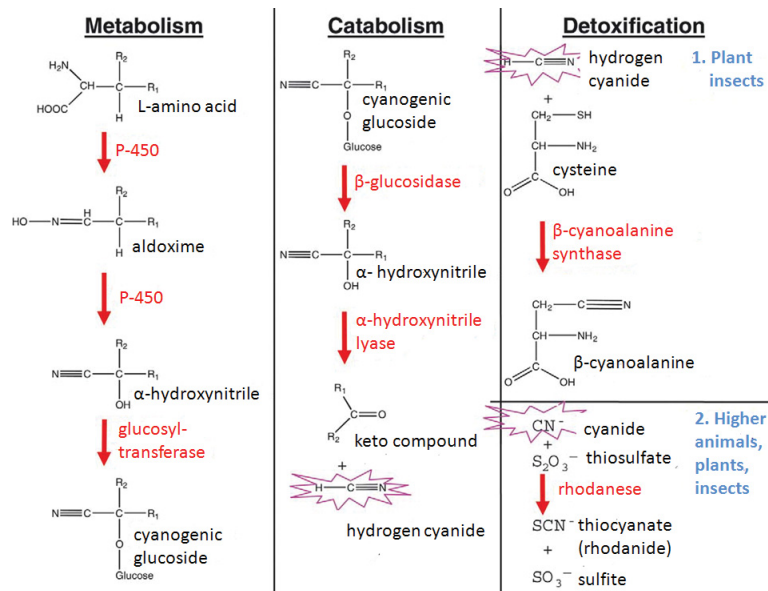


Figure 9: Biosynthesis, catabolism and detoxification of cyanogenic glycosides [68]

Figure 9 shows the anabolism, catabolism and detoxification of cyanogenic glycosides. The first two steps of the metabolism are catalyzed by cytochrome P450 to produce a cyanohydrin and the final step; the glycosylation of the cyanohydrin moiety, is catalyzed by a glycosyltransferase. As explained above, the catabolism is a two-step mechanism including the  $\beta$ -glycosidase mediated breakdown of the cyanogenic glucoside to form an  $\alpha$ -hydroxynitrile. The second route is quite interesting since it is pH-dependent. At pH values above 6, the hydroxynitrile spontaneously degrades into an aldehyde or ketone, sugar and HCN. However, at a lower pH, two pathways are possible. The first pathway involves a rhodanese-catalyzed conversion of HCN to a thiocyanate [69, 70] and this is the common route in vertebrates. The second pathway is part of the nitrogen fixation in plants and insects [65].

### 1.5.2.2 Nitrogen fixation

Apart from its function as a defense mechanism, HCN also serve as a source of nitrogen for the biosynthesis of L-asparagine [71] [72] (Figure 11).

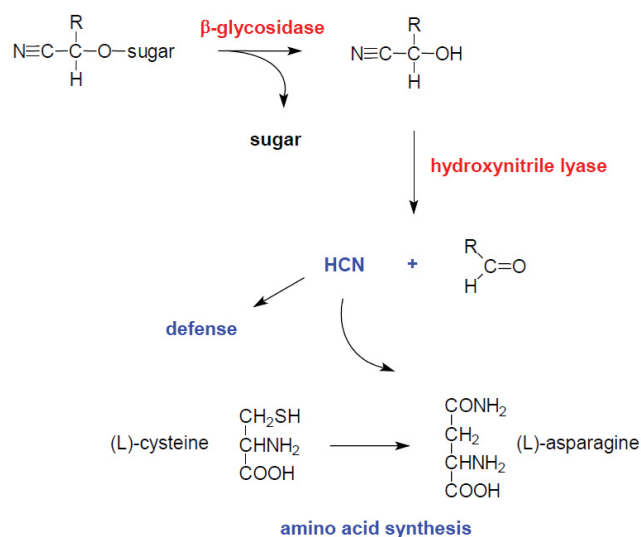


Figure 10: Biosynthesis of amino acid. Modified from [73]

---

This pathway was discovered in germinating seeds of *Hevea brasiliensis* where, although the cyanogenic compounds in the young seedlings was found to decrease, no HCN was released [71]. It was then discovered that the HCN was immediately fixed to form L-asparagine by two enzymes [71]. The first enzyme  $\beta$ -cyanoalanine synthetase refixes the HCN to form  $\beta$ -cyanoalanine together with cysteine. This is then hydrolyzed by the second enzyme  $\beta$ -cyanoalanine hydrolase to form L-asparagine.

### 1.5.3 Relevance of HNLs in organic synthesis

HNLs specifically are attractive in organic synthesis and industrial biotechnology because they can form C-C bonds with high stereoselectivity [74, 75]. Cyanohydrins are excellent chiral synthons as they can be converted to a wide range of valuable compounds by follow up reactions either at the hydroxyl- or the cyanide group [76, 77] (Fig. 11).

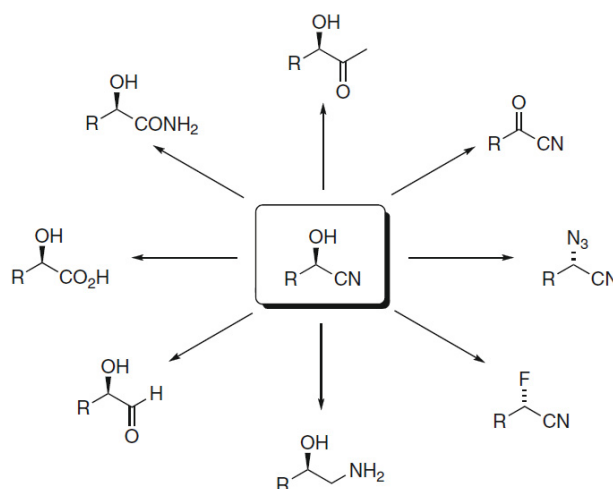


**Figure 11: Reactions based on cyanohydrins. According to [78]**

Usually for HNLs, ketones are less preferred as substrates compared to aldehydes for the synthesis of cyanohydrins mainly because of the lower nucleophilicity of the ketone carbonyl group and the stronger steric hindrance. As the synthesis reaction is thermodynamically limited,

---

full conversion of ketones to the respective cyanohydrines (tertiary alcohols) can hardly be achieved, which poses a challenge to the downstream processing of these products. Further, the ketone cyanohydrines are less thermostable, which hampers storage and instrumental analysis [79–81].

Nevertheless, few HNLs such as the (*S*)-selective HNL from *Manihot esculenta* can yield phenylacetone cyanohydrin with high *ee* [82]. Another example is the HNL from flax (*Linum usitatissimum*, LuHNL), which accepts aliphatic ketones and aromatic methyl and ethyl ketones to synthesize the respective cyanohydrins [83, 84]. This implies that ketone cyanohydrins can be synthesized with high *ee* inspite of the above stated limitations.

#### 1.5.4 Classification of HNLs

Although HNLs have been discovered in certain bacteria and arthropods [85], they have been isolated for biotechnological applications mostly from plant sources. Besides bitter almond extract (*Prunus amygdalus*) [58] similar HNLs were isolated from other prunus species such as *Prunus serotina*, *Prunus lyonii*, *Prunus laurocerasus*, *Prunus capuli*, as well as *Manihot esculenta*, *Hevea brasiliensis*, *Sorghum bicolor*, *Linum usitatissimum*, *Mammea americana*, *Malus communis*, *Phlebodium aureum* and *Arabidopsis thaliana* [86]. Recently HNLs have also been discovered in endophytic bacteria that are similar in sequence to the proteins of cupin superfamily [87]. Among this class, a new HNL from the acidobacterium *Granulicella tundricola* (GtHNL) was biochemically characterized [88].

HNLs are a perfect example for convergent evolution, meaning that the potential to catalyze the cleavage and formation of cyanohydrins was “invented” several times and implemented in quite different structural frame works. Generally, HNLs can be divided into two superfamilies based on the presence or absence of flavin adenine dinucleotide (FAD).

---

#### 1.5.4.1 FAD-dependent HNLs

FAD-dependent HNLs are found in some members of rosaceae family and they accept (*R*)-mandelonitrile as their natural substrate [89]. Amongst this class, the most investigated HNLs are from almonds (*Prunus amygdalus*/*PaHNL*) and cherry (*Prunus serotina*/*PsHNL*) [90–92]. Although FAD is not directly involved in the reaction, it provides structural stability to the structure of the enzyme [93].

#### 1.5.4.2 FAD-independent HNLs

The FAD-independent class of HNLs comprises all HNLs not found in prunus species and is thus very heterogeneous. These enzymes have been isolated from many plant families of Linaceae, Euphorbiaceae, Oleaceae, Passifloraceae, Polypodiaceae, Brassicaceae and Poaceae. As well as from the acidobacterium *Granulicella tundricola* (*GtHNL*) [88]. In contrast to the FAD-dependent HNLs, they have different natural substrates (e.g. acetone cyanohydrine, (*S*)-*p*-hydroxymandelonitrile) and vary with respect to structure, molecular weight, number of subunits, substrate- and stereoselectivity [66].

##### (*S*)-selective HNLs

Among the prominent (*S*)-selective HNLs are those from *Hevea brasiliensis* (*HbHNL*) [94] and *Manihot esculenta* (*MeHNL*) [95] belonging to the Euphorbiaceae family. Both enzymes are highly similar, belong to the  $\alpha/\beta$ -hydrolase superfamily [96] and accept acetone cyanohydrin as their biological substrate [97]. Although the natural substrate is achiral, both catalyze the formation of (*S*)-cyanohydrins from different predominantly aromatic aldehydes [98, 99]. Other prominent *S*-selective HNLs are from *Sorghum bicolor* (*SbHNL*) [100] from the Poaceae family and *Ximenia americana* (*XaHNL*) [101] from the Olaceae family.

##### (*R*)-selective HNLs

Few prominent (*R*)-selective HNLs besides the enzymes from *Prunus* species (1.5.4.1) were found in *Linum usitatissimum* (*LuHNL*) [102] from the family Linaceae, *Phlebodium aureum* (*PhaHNL*)

---

[103], and *Vicia sativa* (VsHNL) [104], and from the family Fabaceae. Another (*R*)-selective HNL discovered few years back is from *Arabidopsis thaliana* with a high catalytic potential and is the focus of this doctoral thesis.

### 1.5.5 HNL catalyzed reaction systems

The enantioselectivity of a HNL catalyzed reaction can be influenced greatly by altering various operational parameters such as reaction media, water content, cyanide source, etc.

#### 1.5.5.1 Reaction media and role of water

The exact mechanism of the influence of water on the enantioselectivity of an enzyme is not yet understood. However, many studies have reported a correlation between the solvent properties and selectivity [24, 25, 105].

In general, the water content in the reaction media is believed to influence the flexibility of the enzyme and consequently its activity and selectivity [106].

#### 1.5.5.2 Cyanide source

An HCN source is always required for the hydrocyanation of an aldehyde/ketone to synthesize the corresponding cyanohydrin. Pure HCN can be produced by acidification of cyanide salts followed by distillation at low temperature. However, this imposes severe safety concerns [107] [67]. Alternatively HCN can be extracted with organic solvents [108]. HCN liberation can also be accomplished from acetone cyanohydrin. However, the excess of acetone formed not only impairs the enzyme [109] but is also highly inflammable, thus rendering it unsafe again.

Alternatively, hydrolysis of certain esters (such as ethyl cyanofornate, ECF) could be used as an HCN source [110]. In 2004 Purkarthofer et al. described the use of ethyl cyanofornate (ECF) for the one-pot synthesis of protected cyanohydrines, using ECF as a cyanide source and protecting agent of the formed cyanohydrins at the same time. Evaluation ECF as both the cyanide source and the protecting agent was therefore a straightforward idea. As proof of concept, the *Pa*HNL-

---

catalyzed formation of (*R*)-mandelonitrile was studied in aqueous buffer at pH 3.3. Although ECF was applied in high excess, only poor derivatization of the formed mandelonitrile was achieved, which was due to the rapid hydrolysis of CFE in water. To enhance the lifetime of ECF, subsequent experiments were performed in micro-aqueous organic solvent (toluene and dichloromethane) using immobilized *Pa*HNL on Celite. However, under these conditions the hydrolytic liberation of HCN was limiting [110].

## 1.6 HNL from *Arabidopsis thaliana* (*At*HNL)

### 1.6.1 Discovery and potential

HNLs are usually found in cyanogenic plants but interestingly an (*R*)-selective HNL was discovered in *Arabidopsis thaliana* which is a non-cyanogenic plant [111]. Until the discovery of this enzyme, it was believed that the *R*-selective HNLs were evolved from the oxidoreductase superfamily (e.g. *Pa*HNL and *Lu*HNL) [83, 90] and the *S*-selective HNLs evolved from the hydrolases with  $\alpha/\beta$  fold (e.g. HNL from *Me*HNL, *Hb*HNL). With the *At*HNL, the first *R*-selective HNL was discovered in the  $\alpha/\beta$ -hydrolase family. *At*HNL exhibits high sequence similarity (68% similar amino acid residues) with the *S*-selective HNLs from *Manihot esculenta* and *Hevea brasiliensis* [112, 113].

### 1.6.2 Substrate range

The substrate range of *At*HNL includes aldehydes and a few ketones which are hydrocyanated with good to excellent *ee*, using an aqueous-organic two-phase system [111]. Benzaldehyde and derivatives thereof are the preferred substrates. In contrast, aromatic ketones are rather challenging substrates which is not only due to their bulky nature, but also because of thermodynamic limitations of the reaction, as was already mentioned above [114]. The enzyme also shows activity towards aliphatic aldehydes and the speed of the reaction varies with the length of the carbon chain. Shorter aldehydes such as hexanal can be converted with excellent enantiomeric excess (*ee*), however with long chained decanal the reaction is slow and relatively less enantioselective [111].

---

### 1.6.3 Enzyme mechanism

The active site of AtHNL is formed by three amino acids Ser81, His236 and Asp208, which form the catalytic triad (Figure 12). The relevance of these residues has been proven by site-directed mutagenesis. The structure was solved without bound substrates and the potential mechanism was deduced upon docking of (*R*)-mandelonitrile into the active site [115].

The reaction mechanism is assumed to occur as follows: As the first step, His236 abstracts a proton from the hydroxyl group of the cyanohydrin. This deprotonation is facilitated by hydrogen bond interactions of the hydroxyl group with Asn12. The second step is the stabilization of the negative charge of the cyano group. It can be assumed that the cyano group is very close to the back bone amide groups of Ala13 and Phe82 and interacts with them. The last step involves the protonation of the cyanide group to produce HCN [115]. Exchange of Asn12 by threonine reduced the catalytic efficiency greatly, because the loss of one H-bond weakens the substrate binding [115].

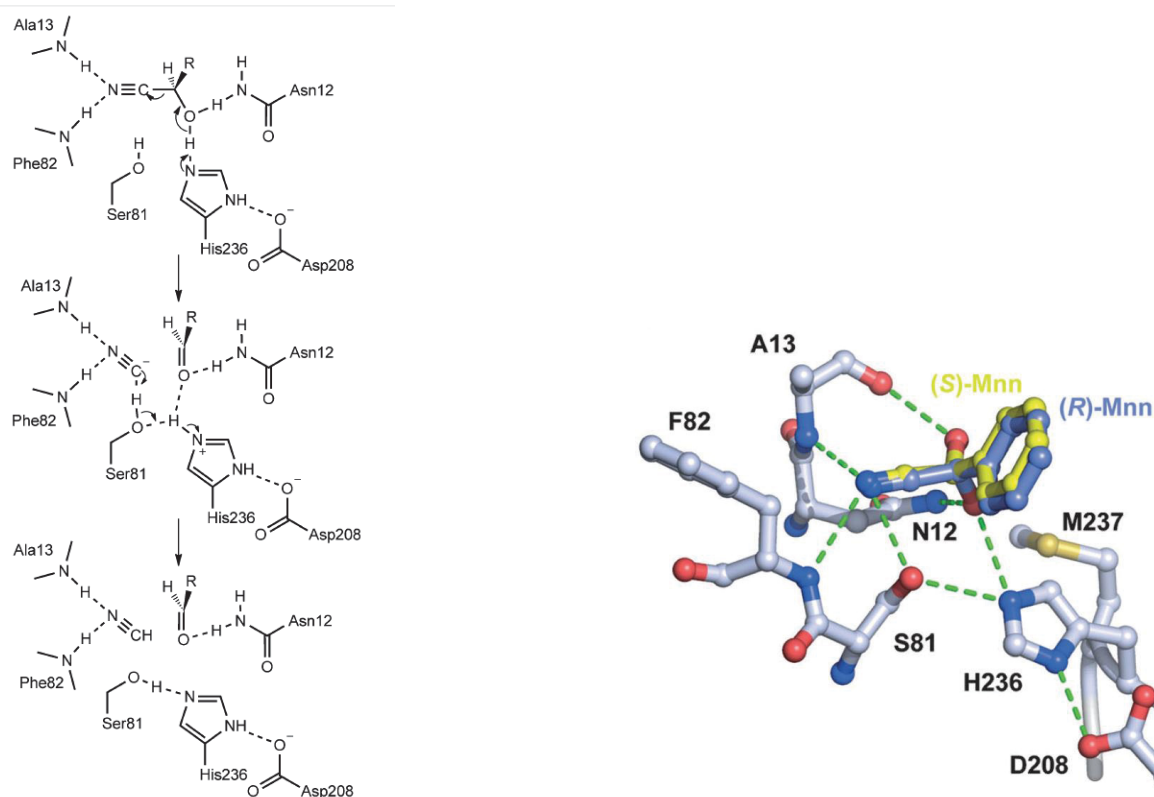


**Figure 12: Potential mechanism of *AtHNL* postulated enzyme mechanism of *AtHNL* (left) and modeled complex of *AtHNL* with (*R*)- and (*S*)-mandelonitrile (Mnn) (right) [115]**

Andexer et al. performed docking studies to explain the high enantioselectivity of the *AtHNL*. The complex structures for the two enantiomers of mandelonitrile were docked into the active site. Deprotonation of the hydroxyl group is more likely to occur with (*R*)-mandelonitrile than the (*S*)-enantiomer, because the hydroxyl group of the (*R*)-enantiomer is closer to His236 that can initiate H-bond formation. Although *AtHNL* shows a broad substrate range with high stereoselectivity, its application in bioorganic synthesis is challenged with respect to stability, which will be addressed in the following.

---

#### 1.6.4 Enzyme stability

Although the HNLs from *Arabidopsis thaliana* and from *Manihot esculenta* are highly similar in sequence and structure, *MeHNL* is much more stable than *AtHNL* [116]. One reason for this is most probably the higher oligomerization state of *MeHNL* in solution, although both enzymes form dimers in the crystal [115]. In a previous study, the amino acid residues on the surface of *AtHNL* and *MeHNL* were compared and by a rational protein engineering approach 11 point mutations were exchanged on the surface of *AtHNL* [117]. This new variant (called “surfmod\_AtHNL”) not only increased its stability at lower pH but also enhanced its activity, although these mutations did not induce tetramer formation as intended. However, higher association states were induced by the fusions with a flavin-based fluorescent protein (FbFP) and a cellulose binding module (CBM) [118, 119], both leading to higher enzyme stability.

The main challenge of enzymatic hydrocyanation in aqueous systems is caused by a chemical background reaction that leads to the formation of the racemic product. In order to achieve high enantiopurity, this side reaction must be suppressed. One way to achieve this is to maintain the pH of an aqueous system below 5. However, wild type (wt) *AtHNL* rapidly inactivates at such low pH [116]. Another approach to reduce the side reaction is to lower the amount of water by using an organic solvent system. Although the enzyme stays active under these conditions, it precipitates in the organic solvent and sticks to the walls of the reactors forming a cloudy sticky mass which cannot be reused. Therefore, in order to enable high stability and recyclability of the enzyme in organic solvent, different immobilization approaches have been evaluated [120].

#### 1.6.5 Immobilization of *AtHNL*

In a previous study, Okrob et al. investigated various immobilization techniques and demonstrated that diatomite (Celite) exhibits high residual activity of 78% after immobilization. Celite-*AtHNL* was further evaluated in micro-aqueous MTBE (methyl *tert*-butyl ether) in batch mode showing excellent activity and enantioselectivity towards benzaldehyde and derivatives thereof. Apart from its ease of preparation (chapter 3.2.8) and usage in organic solvents, it is also

---

recyclable and storable. The interesting effect of humidity on the activity of Celite-AtHNL was reported, where the humidity of dry immobilizate must be carefully adjusted in order to make full use of the enzyme activity [120]. However, immobilization by adsorption is stabilized by weak forces (predominantly H-bonds), which may not be stable over a longer period, especially in the presence of water or other H-bond donating solvents.

#### 1.6.6 Whole cells as natural immobilisates

Whole recombinant *Escherichia coli* cells can be considered as a natural form of immobilization where the enzyme is protected by the cell membrane. The application of whole cells could be an attractive alternative to purified enzymes for biotransformations. Moreover, the need for tedious and expensive enzyme purification and subsequent immobilization can be circumvented. Scholz et al. reported the synthesis of cyanohydrins using recombinant *E.coli* cells expressing AtHNL in micro-aqueous MTBE with high conversions and *ee* [121]. Recently, wt AtHNL and a fusion protein with flavine based fluorescent protein (FbFP) was successfully applied as whole cell biocatalysts in micro-aqueous MTBE [118].

### 1.7 Recent studies on AtHNL-catalyzed synthesis of aldehyde and ketone cyanohydrins

AtHNL being a highly potent *R*-selective enzyme draws attention for its application in biotechnological processes. It accepts a wide range of aldehydes and ketones as substrates [111]. Many studies have been reported on the improvement of this enzyme by rational protein engineering and reaction engineering [117–120]. Various enzyme preparations have been used for synthesis reactions such as purified enzyme, immobilisates, crude cell extracts and whole cells [111, 118, 120]. In 2007, Andexer described the substrate range for the AtHNL with crude cell extract in a biphasic system [111]. In 2011, Okrob immobilized the enzyme on Celite and compared it to the precipitated native enzyme in micro-aqueous MTBE. A year later, Scholz et al. demonstrated that it was also possible to use whole recombinant cells in a micro-aqueous environment instead of isolated AtHNL. The study also depicts the effect of organic solvent on

---

the structural integrity of the enzyme. During the course of this thesis, it was demonstrated that fusion of wt-AtHNL with proteins like the flavine-based fluorescent protein (FbFP) [118] or a cellulose binding module (CBM) [102] could increase its stability.

The quest for ketones as substrates has earlier been investigated with AtHNLs in a aqueous-organic two phase system, however, only poor conversions and *ee* has been reported [111]. As already mentioned, such reactions with ketone are thermodynamically limited because the equilibrium lies on the side of the reactants and therefore the product has a tendency to cleave back to the reactants as soon as it is formed [122]. Andexer et al. reported a conversion of only 7% of acetophenone in an aqueous-organic two phase system with AtHNL [111]. Later, a maximum conversion of 22% was reported with MeHNL in an organic solvent-free system [81]. Nevertheless, ketone cyanohydrins impose analytical challenges because of their instability and they therefore need to be derivatized before analysis. Few methods described in literature for the same are acetylation [111] and silylation [123] of the hydroxyl group of the corresponding cyanohydrin.

It has also been reported that the usage of an organic solvent-free system, meaning a biphasic system of acetophenone derivative and aqueous buffer can help in achieving a higher conversion of ketone cyanohydrins [81]. The synthesis of ketone cyanohydrins have been as well extensively studied on HNLs from other sources, such as the *R*-selective HNL from *Prunus amygdalus* [124, 125] and the *S*-selective HNL from *Manihot esculenta* [80].

---

# Chapter 2

## **AIM OF THE THESIS**

---

## 2. Aim of the thesis

The *R*-selective hydroxynitrile lyase from *Arabidopsis thaliana* has a high potential in catalyzing the hydrocyanation of carbonyl compounds [111] to synthesize chiral cyanohydrins, which are valuable building blocks in industry. This is currently the only *R*-selective HNL, with a similar substrate range to the well-known enzyme from *Prunus amygdalus* (*PaHNL*), which is used also in technical processes. The general aim of this doctoral thesis was to explore the potential of *AtHNL* based on recent studies in order to evaluate the technical applicability of this enzyme. Therefore different preparations of a His-tagged variant should be tested exclusively in micro-aqueous MTBE, which showed best results in previous studies [118, 120, 121].

The **first goal** was to characterize a new *AtHNL* variant with an N-terminal hexa-histidine tag, with respect to its stability and performance in biotransformations and preparations (purified, immobilized, whole cells). This variant was produced to ease the access to purified *AtHNL*.

The **second goal** was to study the substrate scope of His<sub>6</sub>-*AtHNL* in a micro-aqueous organic solvent system by testing simple aromatic ketones and also bulky 2-hydroxy ketones as substrates for the synthesis of the respective cyanohydrins. As discussed (chapter 1.7 and 1.5.3), ketones are the less preferred substrates and so far in previous studies all reported synthesis were performed in aqueous reaction systems and biphasic aqueous-organic systems. In this work, the influence of micro-aqueous organic solvent system on the synthesis of ketone cyanohydrins should be evaluated.

The **third goal** concerns the development of a scalable continuous process including a safer access to HCN. Since, pure HCN imposes severe safety issues (chapter 1.5.5.2), an alternative HCN surrogate will be investigated to ensure a safer generation of HCN to allow scale up of cyanohydrin synthesis.



# Chapter 3

## **MATERIALS AND METHODS**

---

## 3. Materials and Methods

### 3.1 Materials

#### 3.1.1 Chemicals

Chemicals	Supplier
Acetic anhydride	Fluka
Acetophenone	freshly distilled
Agarose	Merck
Benzaldehyde	Freshly distilled
N,O-Bis(trimethylsilyl)trifluoroacetamide (BSTFA)	Sigma aldrich
Citric acid	Fluka
Coomassie brilliant blue G-250	Serva
Dichloromethane	Roth
4-Dimethylaminopyridine (DMP)	Sigma/Aldrich
Dinatrium hydrogenphosphate (Na <sub>2</sub> HPO <sub>4</sub> )	Sigma/Aldrich
Dipotassium phosphate	Roth
Dodecan	Sigma/Aldrich
Ethanol	Roth
Ethyl cyanoformate	Sigma/Aldrich
Hydrochloric acid	Roth
Imidazole	Sigma/Aldrich
Methyl <i>tert</i> -butyl-ether (MTBE)	Roth
Sodium chloride	Roth
Potassium dihydrogen phosphate	Roth
Pyridine	Roth
Sodium cyanide	Sigma/Aldrich

#### 3.1.2 Bacterial strains and plasmids used

Bacterial strain	Genotype	Supplier
<i>E. coli</i> BL21(DE3)	F-ompThsdSb(rB-mB-) gal dcm (λcIts857 ind1Sam7 nin5 lacUV5- T7gene1) [126]	Novagen (Madison, USA)
pET28a	ColE1 lacZ'KanR PT7 Plac	Novagen, Madison, USA

pET28a-wt-AtHNL	Recombinant with 775 bp gene of wt AtHNL (sequence for wt-AtHNL shown in <b>appendix 1</b> )	[120]
pET28a- His <sub>6</sub> -AtHNL	Recombinant with 840 bp gene of His <sub>6</sub> -AtHNL (sequence for His <sub>6</sub> -AtHNL shown in <b>appendix 1</b> )	Dr. Ulrich Krauss

### 3.1.3 Kits and standard solutions used

Kit	Supplier
Plasmid preparation kit (QIAprep <sup>®</sup> Spin Miniprep Kit)	Qiagen
NuPAGE <sup>®</sup> Antioxidant (for SDS gel)	Life Technologies
NuPAGE <sup>®</sup> LDS Sample Buffer (4x)	Life Technologies
NuPAGE <sup>®</sup> MES SDS Running Buffer (20X)	Life Technologies
NuPAGE <sup>®</sup> Sample Reducing Agent (10X)	Life Technologies
SDS-PAGE-Gel (NuPAGE <sup>®</sup> 4-12 % Bis-Tris Gel 1.0 mm)	Life Technologies
SimplyBlue <sup>™</sup> SafeStain	Life Technologies
PageRuler <sup>™</sup> Plus Prestained Protein Ladder (10-250 kDa)	Thermo Scientific
GeneRuler <sup>®</sup> 1 kb Plus	Thermo Scientific
6x MassRuler <sup>™</sup> Loading Dye Solution	Fermentas
GelPilot <sup>®</sup> Loading Dye, 5x	Qiagen

### 3.1.4 Enzymes used

Enzyme	Description	Supplier
Hydroxynitrile lyase (His <sub>6</sub> -AtHNL)	<i>Arabidopsis thaliana</i> with an N-terminal hexahistidine tag	This work protein sequence see <b>Appendix 1</b>
Lipase CalB/Novozyme 435	<i>Candida antarctica</i> immobilized on acrylic resin Commercial name: Novozyme 435	Novozymes

### 3.1.5 Media components

Component	Supplier
Glucose	Roth
Lactose	Merck
Kanamycin sulfate	Roth
Agar-agar	Merck
Peptone	Roth

### 3.1.6 Materials

Materials	Supplier
Nylon mesh (pore size 43 µm)	Millipore
Organic solvent resistant septum G13-D	Chromatographie Services GmbH
Celite R633	World Minerals Inc.
Ni-NTA Agarose	Qiagen
Sephadex G25 matrix	GE healthcare
Column reactor	Kinesis benchmark microbore (omnifit)
Frits and adapters	Kinesis
T-mix adapters	Kinesis
Tubings for flow reactors (PTFE)	Kinesis
Back pressure regulator	Kinesis replacement cartridge

### 3.1.7 Devices

Device	Description	Supplier
Centrifuge	centrifuge 5417r	Eppendorf
	avanti j-20 xp centrifuge	Beckmann coulter
	universal 32r	Hettich Zentrifugen
	centrifuge 5424	Eppendorf

Sterilization	Autoclave systec dx-65	Systec
Incubator	Inforsht	Multitron standard
	thermomixer comfort 5335r	Eppendorf
Spectrophotometer	uv-1610	Shimadzu
	uv-1800	Shimadzu
pH measurement	pH meter standard buffer solutions (pH 4.0, 7.0, 9.0)	Methrom Roth
Gas chromatography	gas chromatograph 6890n with FID	Agilent technologies
	cp-chiralsil-dex cb	Chromatographie services GmbH
NMR	Bruker Avance DPX-400	Bruker
SFC	Aurora SFC systems, Hydra	Chiral Technologies
GC-MS	Saturn 2000 GC/MS/MS	Agilent technologies
Enzyme purification	ups-200s Ultraschallprozessor	Dr. Hielscher
	Äkta explorer protein purification system	GE healthcare
SDS PAGE	Electrophoresis	
	XCell SureLock™	Invitrogen
	Novex mini cell	Invitrogen
HCN detector	PAC III	Dräger
Flow reactor	Glass column reactor	Kinesis
	Frits and O-rings	Kinesis
	Syringe pump	Syrris Asia pumps

### 3.1.8 Softwares

Software	Supplier
ChemBio Office 2008	Cambridge soft
GC software	GC Chemstation

GC-MS software	Saturn GC/MS workstation
NMR software	Brucker Topspin™ software
References	Mendeley
MS Office 2010	Microsoft
Clone manager 9	Clone manager
Origin 8.5G	Origin Lab
Skanit 2.4.2	Shimadzu

### 3.1.9 Autoinduction media:

Components	Composition	Volume (ml)
Media component	15 g/L peptone, 30 g/L yeast extract	80
Potassium phosphate buffer	1 M, pH 7.0	9
Lactose	20 g/L	10
Glucose	50 g/L	1
Kanamycin	50 µg/µL	100 µL
sterilized by autoclaving at 121 °C, 2 bar for 3 h		

### 3.1.10 LB medium:

Components	Composition
Trypton	10 g/L
Yeast extract	5 g/L
Sodium chloride	10 g/L
sterilized by autoclaving at 121 °C, 2 bar for 3 h [127]	

### 3.1.11 LB agar:

Components	Composition
Agar-Agar	15 g/L (in LB medium)
sterilized by autoclaving at 121 °C, 2 bar for 3 h	

### 3.1.12 Buffers

Activity assay (chapter 3.2.7)		
Mandelonitrile cleavage Assay	Citrate phosphate buffer (substrate buffer)	3 mM, pH 3.5
	Potassium phosphate buffer	5 mM, pH 6.5
	Citrate phosphate buffer	50 mM, pH 5.5

Protein purification (chapter 3.2.3)		
Lysis buffer	Potassium phosphate buffer	50 mM, pH 7.5
	Lysozyme	1 mg/ml
IMAC purification	Equilibration buffer	300 mM NaCl 10 mM potassium phosphate buffer in Millipore water, pH 7.5
	Washing buffer	300 mM NaCl 50 mM potassium phosphate buffer 50 mM imidazole in Millipore water, pH 7.5
	Elution buffer	300 mM NaCl 50 mM potassium phosphate buffer 300 mM imidazole in Millipore water, pH 7.5
Gel Filtration	Desalting buffer	10 mM potassium phosphate buffer in Millipore water, pH 7.5

---

## 3.2 Methods

### 3.2.1 Enzyme production

N-terminally hexa-histidine tagged *AtHNL* plasmid was kindly provided by Dr. Ullrich Krauss from the Institute for Molecular Enzyme Technology, Heinrich-Heine-University of Düsseldorf & Forschungszentrum Jülich. The gene map and the sequence are shown in the Appendix 1-2.

#### 3.2.1.1 Transformation

50 µl of chemically competent *E. coli* BL21(DE3) cells [128] were thawed on ice and then transformed with 1 µl of pET28a-His<sub>6</sub>*AtHNL* plasmid by a heat shock (30 min, 4 °C; 90 s, 42 °C; 5 min, 4 °C). 500 µl LB medium was added to each vial and subsequently incubated at 37 °C for 1 h. 200 µl from these vials were plated on an agar plate containing kanamycin (50 µg/ml). As a negative control, competent cells without the plasmid were plated on a separate agar plate. The plates were then incubated overnight at 37 °C.

#### 3.2.1.2 Overexpression

In order to obtain large amounts of enzyme, the gene was overexpressed in *E. coli*. The culture was carried out in autoinduction medium as described by Studier et al. [129]. A single colony was picked from the transformed cells with a pipette tip to inoculate 5 ml LB medium containing kanamycin (50 µg/ml) in a test tube. This pre-culture was then incubated at 37 °C overnight. For the preparation of the main/primary culture, 1 L autoinduction medium was freshly mixed (chapter 3.1.9) in a 5 L shake flask with baffles. 1 ml of the pre-culture was used to inoculate the main culture and incubated at 120 rpm for 72 hours. For the first 3 hours, it was incubated at 37 °C to allow sufficient cell growth. Then the temperature was lowered to 17 °C to avoid the formation of inclusion bodies during gene expression. In order to harvest the cells, the culture broth was centrifuged at 10,000 rpm for 50 min at 4 °C. The formation of the target protein was then determined by SDS-PAGE (chapter 3.2.2).

---

### 3.2.2 Sodium Dodecyl Sulfate PolyAcrylamide Gel Electrophoresis (SDS-PAGE)

SDS-PAGE is an electrophoresis technique wherein the proteins are denatured and separated based on their size [130]. This method was applied to analyze the recombinant enzyme production. The gel, samples, and electrophoresis unit were prepared and setup as described in the manual from supplier (Invitrogen). The optical density (OD) of the main culture (chapter 3.2.1.4) was adjusted such that 10 µg protein were loaded per lane. Electrophoresis was carried out at 100 mA, 200 V and 150 W for 35 min.

The SDS gel was then dyed with Coomassie brilliant blue G 250 (SimplyBlue™ SafeStain) [131] at room temperature for 1 h. Subsequently the gel was washed twice with Millipore water, sealed in a plastic bag and analyzed by visual inspection.

### 3.2.3 Enzyme purification

#### 3.2.3.1 Cell disruption

The recombinantly produced enzyme (chapter 3.2.1) accumulated in the *E. coli* cytosol. In order to get access to the target protein, the cells must be disrupted and in this work, the cells were disrupted by ultrasonication.

9 g *E. coli* His<sub>6</sub>-AtHNL cells were weighed (chapter 3.2.1) and resuspended in lysis buffer (chapter 3.1.11) on ice. The sonotrode S14D was used and the sonicator was adjusted to amplitude of 40% and a cycle of 0.5 minutes. The disruption lasted 28 min, with alternating pulses of ultrasonic waves and a break of 4 min in between to avoid overheating. It is important to keep the system cooled during the whole process in order to avoid heat denaturation. Cell debris was then removed by centrifugation at 35000 rpm for 45 min at 4 °C. The supernatant (lysate) was collected and was used as crude cell extract for further purification.

---

### 3.2.3.2 Immobilized Metal-ion Affinity Chromatography (IMAC)

IMAC is an affinity chromatography method to purify proteins in a single step and the principle is based on the specific interaction of the polyhistidine residues (6-10 His residues) which binds to a specific metal-chelate of different transition metal ions like  $\text{Ni}^{2+}$ ,  $\text{Cu}^{2+}$  and  $\text{Co}^{2+}$  complexed on a matrix [132].

The freshly prepared crude cell extract (chapter 3.2.3.1) was filtered through a  $0.45\ \mu\text{m}$  sterile filter to remove any suspended cell debris. Nitriloacetic acid (NTA) complexed with nickel ions ( $\text{Ni}^{2+}$ ) was used as the column material. The Ni-NTA column (diameter 1.5 cm, volume 17 ml) was equilibrated with 3 column volumes of equilibration buffer (300 mM NaCl, 10 mM KPi, pH 7.5). The filtered crude cell extract was then loaded onto the column with a flow of 2 ml/min. The absorption was monitored via a detector at 280 nm. Non-bound proteins were washed out (“flow through”) with the equilibration buffer until the baseline was reached. On applying a low concentration of imidazole (50 mM), the nonspecifically bound proteins were eluted (Figure 13) which was followed by applying a high concentration of imidazole (200 mM) to elute the target protein with His-tag.

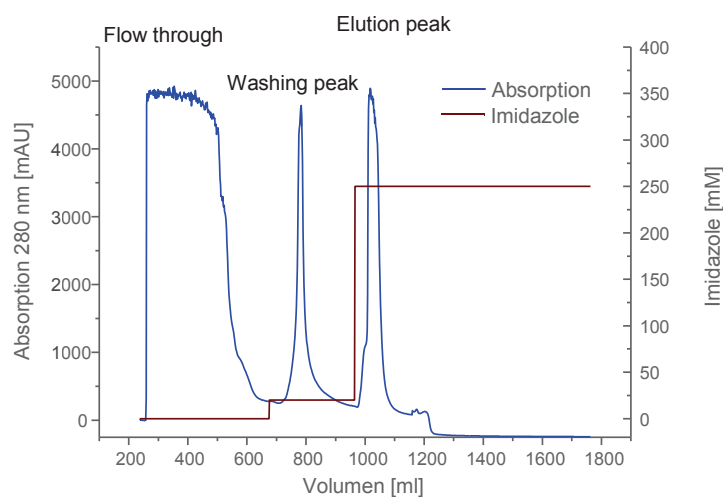


**Figure 13: IMAC chromatogram for the purification of His<sub>6</sub>-AthNL**

---

The active eluate fractions were collected and subsequently desalted using gel filtration.

### 3.2.4 Gel filtration

The purified eluent from the IMAC contains a high concentration of imidazole and buffer salts which might be harmful for the stability of the protein. In order to remove the salts (“desalting”) from the target protein, gel filtration or size exclusion chromatography was performed which is a chromatographic separation method based on the size (hydrodynamic volume) of the molecules. The salts elute first followed by the larger protein molecules. The column (diameter 5 cm, volume 800 ml, filled with Sephadex-G25 material) was equilibrated with 2 column volumes of desalting buffer (chapter 3.1.12) with a flowrate of 10 ml/min. The protein fraction was monitored by measuring the absorption at 280 nm. The eluate was collected in a crystallization bowl and stored in the freezer at - 20 °C overnight.

### 3.2.5 Lyophilization

This is commonly called as “freeze-drying” and involves the removal of excess water at low pressure and low temperature.

- a) *Purified enzyme*: The frozen eluate fractions after desalting were placed in a lyophilizer at – 35 °C under a vacuum of 0.22 mbar for 3 days. The lyophilized enzyme was then collected in a falcon tube and stored at – 20 °C for further use. 1 mg of lyophilisate contained 0.82 mg of pure protein.
  
- b) *Whole cells*: The recombinant *E. coli*-His<sub>6</sub>-AtHNL cells obtained after centrifugation (chapter 3.2.1) were spread in a transparent plastic bag and stored in the freezer at -20 °C overnight. The frozen cell pellet was then broken into pieces and placed in a beaker and then lyophilized for 4 days at – 35 °C and 0.22 mbar. The dried cells were then lightly crushed with a glass spatula to form a powder and stored at 4°C in a screw-capped bottle for further use.

---

### 3.2.6 Determination of protein concentration

Quantification of the protein amount was performed by Bradford assay [133]. This is a simple calorimetric method which is based on the wavelength shift of absorption maxima of Coomassie brilliant blue from 465 nm to 565 nm on binding to a protein. The dye solution was prepared by dissolving 100 mg Coomassie G250 blue in 50 ml ethanol followed by the addition of 100 ml phosphoric acid and the suspension was stirred in dark for 1 hour. The solution was then filled up to 1 L in a flask with distilled water and boiled. The resulting mixture was then cooled and filtered through a filter paper to remove any suspended particles.

A calibration curve was prepared with defined concentrations of bovine serum albumin of 0.01 mg/ml to 0.1 mg/ml as a standard by plotting the concentration-dependent absorption at 595 nm. 900  $\mu$ l Bradford reagent was added to 100  $\mu$ l of the protein sample dissolved in potassium phosphate buffer (pH 6.5) in a plastic cuvette. As a control, 900  $\mu$ l Bradford reagent was added to 100  $\mu$ l of buffer (without protein). The cuvettes were incubated at room temperature (RT) in the dark for 10 min to allow the binding of the dye to the protein. The absorbance was then measured at 595 nm and the protein concentration was deduced from the calibration curve.

#### **Estimation of the AtHNL content in lyophilized *E. coli* cells**

The His<sub>6</sub>-AtHNL content was estimated from the total amount of purified enzyme attained from the recombinant *E. coli* cells (chapter 3.2.1). From 9 g of fresh wet His<sub>6</sub>-AtHNL-*E. coli* BL21 (DE3) cells, 300 mg of purified His<sub>6</sub>-AtHNL was obtained. Thus, 1 g of recombinant wet cells (or 280 mg lyophilisate) contains about 33 mg His<sub>6</sub>-AtHNL.

### 3.2.7 HNL activity assay (mandelonitrile cleavage assay)

Hydroxynitrile lyases catalyze the reversible cleavage and synthesis of cyanohydrins. To determine the activity of HNLs, the reaction of mandelonitrile to benzaldehyde (Figure 14) was performed and the increase of the benzaldehyde concentration was followed photometrically at 280 nm over 2 min [134].

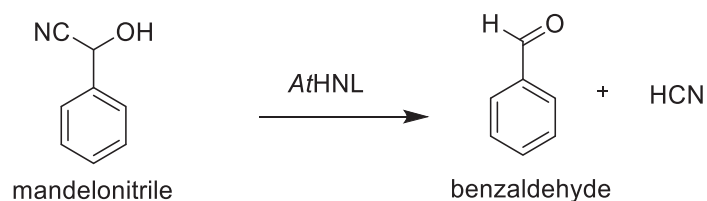


**Figure 14: Cleavage of mandelonitrile**

To perform the cleavage activity assay, first the substrate solution was prepared by dissolving 40  $\mu\text{l}$  racemic mandelonitrile in 5 ml substrate buffer (3 mM citrate-phosphate buffer, pH 3.5) and it was then vortexed until the mandelonitrile was completely dissolved. An enzyme solution was prepared by dissolving lyophilized His<sub>6</sub>-AtHNL in KPi buffer (5 mM, pH 6.5) such that a final protein concentration of 0.3 mg/ml to 0.8 mg/ml was measured by Bradford assay (chapter 3.2.6). The assay was performed in quartz cuvettes with a path length of 1 cm.

100  $\mu\text{l}$  enzyme solution was added to 700  $\mu\text{l}$  citrate phosphate buffer (50 mM, pH 5.5). The reaction was started by addition of 200  $\mu\text{l}$  mandelonitrile solution and mixed inside the cuvette with a plastic spatula. The increase of absorbance at 280 nm was measured immediately in a photometer and was followed for 2 min with an interval of 5 sec at 25 °C.

However, there always occurs a background reaction without the enzyme and to subtract this, a control measurement was done with 100  $\mu\text{l}$  of KPi buffer (5 mM, pH 6.5) (without the enzyme). The volumetric activity of His<sub>6</sub>-AtHNL was calculated as follows:

$$\text{Volumetric activity [U/ml]} = \frac{V * \Delta A}{v * \epsilon * d * \text{min}} \frac{\mu\text{mol}}{\text{min} * \text{ml}}$$

with

V: total volume (1 ml)

$\Delta A/\text{min}$ : resulting slope

v: sample volume (0.1 ml)

$\epsilon$ : extinction coefficient for benzaldehyde (1.376 L/mmol/cm)

D: path length (1 cm)

---

In order to calculate the specific activity, the volumetric activity is divided by the protein concentration.

### 3.2.8 Immobilization on Celite

Celite is a porous diatomaceous material used very often for immobilization, because of its high surface area, low polarity and low cost [135]. Immobilization of His-AtHNL on Celite is a simple adsorptive technique where the enzyme is immobilized via hydrogen bonds.

For the preparation of the immobilizates, the same protocol was followed as described by Okrob et al. [120] (Figure 15). First, 100 mg Celite (grade R-633; pore size 0.2-0.5 mm) was weighed and placed in a glass bowl. 25 mg pure His<sub>6</sub>-AtHNL (corresponding to 31.2 mg lyophilizate) was dissolved in 900  $\mu$ l of 10 mM potassium phosphate buffer (pH 6.5) and subsequently the enzyme solution was carefully dropped over the Celite particles with the help of a pipette. The enzyme-Celite mixture was placed in a desiccator with molecular sieve and silica gel and dried under a vacuum of 20 mbar for at least 12 h at RT. The Celite-AtHNL was then stored in the fridge at 4 °C in tightly screwed glass vials.

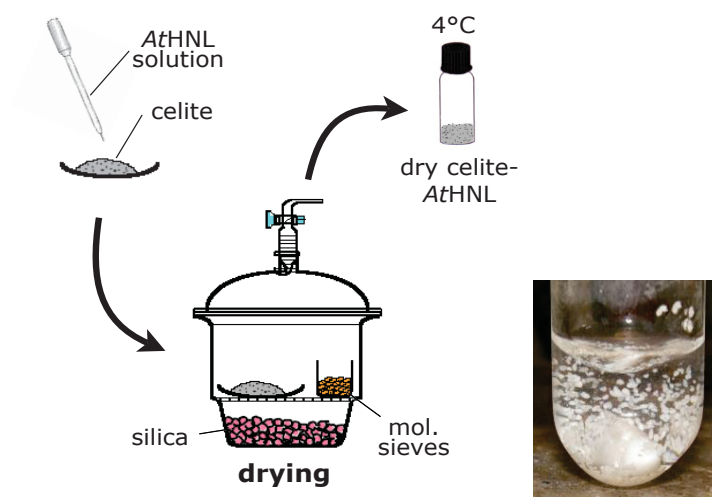


Figure 15: Procedure for immobilization of AtHNL on Celite [120]

---

### 3.2.9 Preparation of “tea bags” with immobilized enzymes or lyophilized cells

The concept of catalyst-filled “tea bags” is prevalent in biocatalysis since a very long time [136, 137]. “Tea bags” can be prepared from various materials. In this work nylon membrane with a pore size of 43  $\mu\text{m}$  was used. A rectangular piece of the material was cut, folded and heat sealed on three sides in shape of a bag and the fourth side was used to fill in immobilized enzyme or lyophilized whole cells.

### 3.2.10 Generation of HCN in a batch mode

#### *a) Chemical synthesis*

HCN was synthesized chemically by the acidification of sodium cyanide as described in literature [120]. 4.9 g of sodium cyanide, 25 ml MTBE and 10 ml water were added to a round bottomed flask and stirred vigorously on ice for 20 min. 10 ml of 30 % aq. HCl was added dropwise through a dropping funnel and the mixture was then allowed to warm slowly to room temperature. The aqueous and organic phases were separated by a separating funnel. The aqueous phase was extracted twice with 7 ml MTBE. The organic phases were stored over 50 mM citrate phosphate buffer with pH 5.5. Thus 1.5 M HCN was prepared in micro-aqueous MTBE.

#### *b) Lipase-mediated synthesis*

HCN can be released by the lipase catalyzed hydrolysis of ethyl cyanoformate [110]. 1 M ethyl cyanoformate dissolved in 1 ml buffer saturated MTBE was placed in a glass vial with a magnetic stirrer. 40 mg CalB (commercial name: Novozyme 435) was added and the mixture was stirred at room temperature for 1.5 hour. The formation of HCN was followed by measuring the depletion of ethyl cyanoformate using GC analysis (GC program: chapter 3.2.23.1)

### 3.2.11 Synthesis of aldehyde cyanohydrins in a batch mode

His<sub>6</sub>-AtHNL catalyzed synthesis of aldehyde cyanohydrin was performed in a 4 ml glass vials with a screw cap fitted with an organic solvent resistant septum. 3 mg of pure His<sub>6</sub>-AtHNL or 20 mg

---

Celite-His<sub>6</sub>-AtHNL or 100 mg lyophilized *E. coli*-His<sub>6</sub>-AtHNL cells (chapter 3.2.5) were placed in the 4 ml glass vial. An argon atmosphere was created by piercing two needles into the septum of the closed glass vial. Argon was continuously passed through one needle while removing air from the other needle. 1 ml of a 1.5 M HCN-MTBE (3.2.10.a) solution was added to the vial with a plastic syringe. 500 mM of the respective aldehyde (benzaldehyde, 2-chlorobenzaldehyde, hexanal or furfural) and 100 mM dodecane (as internal standard) were injected with a Hamilton pipette. The reaction was followed at regular intervals for 150 min by withdrawing samples (50 μl).

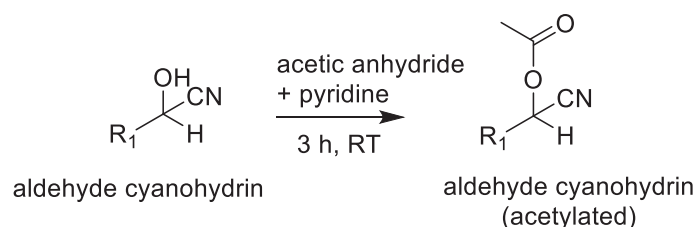


**Figure 16: Derivatization of aldehyde cyanohydrins by acetylation**

**Experimental conditions: 50 μl of the reaction sample was diluted with 850 μl dichloromethane and acetylated with 50 μl each of pyridine and acetic anhydride followed by 3 h incubation at RT. The modified products were analyzed on a chiral GC (GC program: chapter 3.2.23.1)**

### 3.2.12 Synthesis of ketone and 2-hydroxyketone cyanohydrins in batch

His<sub>6</sub>-AtHNL catalyzed synthesis of ketone cyanohydrin was performed in 4 ml glass vials with a screw cap fitted with an organic solvent resistant septum. 3 mg of lyophilized His<sub>6</sub>-AtHNL was applied as biocatalyst. An argon atmosphere was created by piercing two needles into the septum of the closed glass vial, argon was continuously passed through one needle while removing air from the other needle. 1 ml of a 1.5 M HCN-MTBE solution (3.2.10.a) was added to the vial with a plastic syringe. 400 mM of the respective ketone (acetophenone, 2-fluoroacetophenone, 2-hydroxy ketones) and 100 mM dodecane (as internal standard) was injected with a Hamilton pipette. The reaction was followed at regular intervals for 50 h by withdrawing sample (50 μl), which were diluted with 950 μl dichloromethane. Initially derivatization was carried out by acetylation with an excess of acetic anhydride and 4-dimethylaminopyridine. However, this

---

method later turned out not to be complete (Figure 17a). Better results were obtained upon modification with 50  $\mu$ l N,O-bis(trimethylsilyl)trifluoroacetamide (BSTFA) followed by incubation for 12 to 20 h at RT [123] (Figure 17b).

For the set-up of the analytics for ketone cyanohydrins, the ketone cyanohydrins were acetylated.

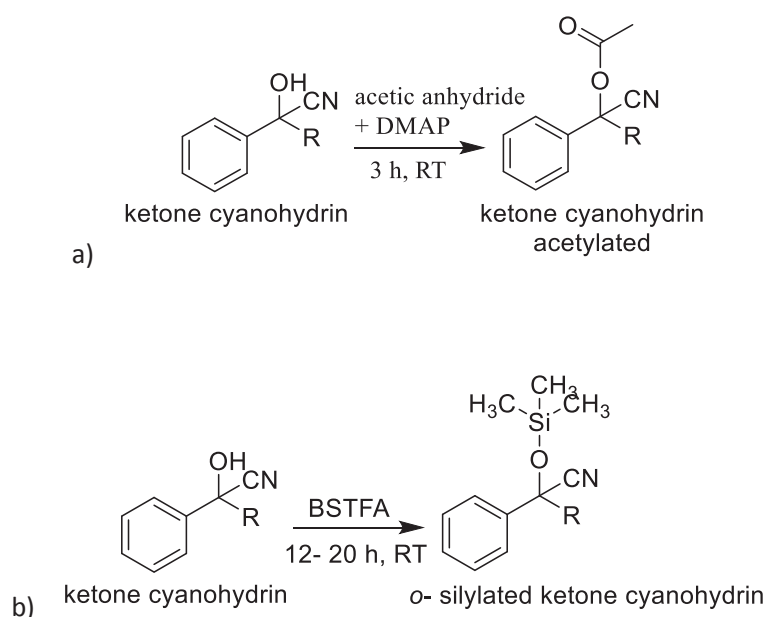


**Figure 17: Reaction scheme for the a) acetylation using acetic anhydride and 4- dimethylaminopyridine b) O-silylation of cyanohydrin using BSTFA.**

**Experimental conditions: a) 50  $\mu$ l of the reaction sample was diluted with 850  $\mu$ l dichloromethane and acetylated with 50  $\mu$ l each of 4-dimethylaminopyridine and acetic anhydride followed by 3 h incubation at RT. The modified products were analyzed on a chiral GC (GC program: chapter 3.2.23.1)**

**b) 50  $\mu$ l of the reaction sample was diluted with 900  $\mu$ l isopropanol and silylated with 50  $\mu$ l BSTFA. The mixture was incubated for 12-20 h at RT**

For the synthesis of cyanohydrins from 2-hydroxy ketones, the derivatization was done with an excess of acetic anhydride and dimethyl amino pyridine (Figure 18).

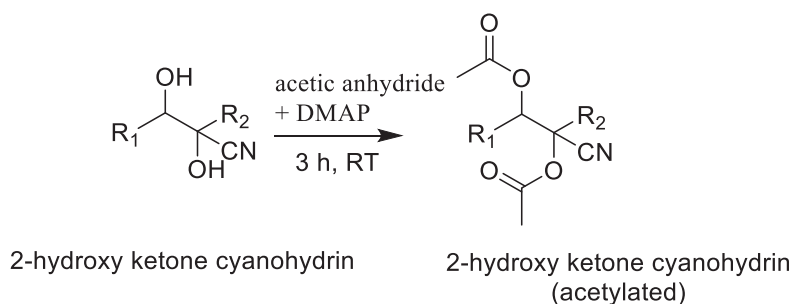


**Figure 18: Derivatization of 2-hydroxy ketone cyanohydrins by acetylation**

**Experimental conditions: same as Figure 17a)**

### 3.2.13 Recyclability studies for Celite-*His*<sub>6</sub>-*At*HNL and *E. coli*-*His*<sub>6</sub>-*At*HNL

To determine the recyclability, 20 mg of Celite-*His*<sub>6</sub>-*At*HNL or 100 mg lyophilized *E. coli*-*His*<sub>6</sub>-*At*HNL was sealed in nylon “tea bags” (chapter 3.2.9). These catalyst-filled bags were used for the synthesis of (*R*)-mandelonitrile. Samples of 50 μL were taken at regular intervals over 1 h. At the end of each synthesis reaction (60 min) the “tea bag” was removed from the reaction vessel and washed three times in fresh, pure MTBE. A new synthesis reaction was then started by inserting the washed “tea bag” into a fresh reaction vessel containing 1 ml of 1.5 M HCN-MTBE, 500 mM benzaldehyde and 100 mM dodecane. The synthesis reaction was analyzed by GC in the same procedure as described before (chapter 3.2.11).

### 3.2.14 Stability studies for celite-*His*<sub>6</sub>-*At*HNL and *E. coli*-*His*<sub>6</sub>-*At*HNL in MTBE

Stability of Celite-*His*<sub>6</sub>-*At*HNL and *E. coli*-*His*<sub>6</sub>-*At*HNL was studied in pure MTBE at RT. For the catalyst preparation, a “tea bag” with 20 mg Celite-*His*<sub>6</sub>-*At*HNL or 100 mg lyophilized *E. coli*-*His*<sub>6</sub>-*At*HNL was used. To determine the residual activity over time the synthesis reaction of (*R*)-mandelonitrile (chapter 3.2.8) was performed with these catalyst-filled “tea bags” 5 times in 14 days and in between stored in a fridge in pure MTBE in a glass vial with screwing lid. Each synthesis reaction was carried out for 30 min. As initial rate activities could not be measured due to the experimental setup, the initial activity was defined as the conversion after 10 minutes which was

---

considered as 100%. A loss of activity was then followed for subsequent reaction cycles relative to the first measurement.

### **3.2.15 CalB-mediated hydrolysis of ethyl cyanofornate (ECF) in continuous mode**

HCN was generated in a continuous mode by the Cal B (Novozyme 435) mediated hydrolysis of ECF (Figure 19). A packed-bed reactor was formed by packing in 277 mg Novozyme 435 into a 10 cm long (diameter 3 mm) omnifit glass column (kinesis microbore 3 mm) and closed at both ends by end fittings. The column was connected to a syringe pump (Syrri Asia Syringe pump) by PTFE tubings.

In order to ensure a unidirectional flow of substrate and to keep the uniformity of the packed bed, a back pressure regulator (BPR), set to 5 bar, was installed in-line with the column. The BPR contains a unidirectional valve, which opens only when the set point pressure (5 bar) is reached. Since these omnifit glass columns could sustain a maximum pressure of 80 bar, the presence of BPR did not impose any risk on the column stability.

Micro-aqueous MTBE was prepared by mixing pure MTBE and 50 mM potassium phosphate buffer with pH 6.5 (in the ratio 3:1). The mixture was allowed to settle in a separation funnel until the phases separated and the organic phase (saturated with the buffer with approx. 10% v/v) was used for all subsequent reactions.

1 M ECF in micro-aqueous MTBE was continuously pumped through the reactor at a flow rate of 0.04 ml/min. The liberation of HCN was measured from the depletion of ECF by GC analysis (chapter 3.2.23.1). A picture of the packed bed reactor with Cal B is shown below (Figure 19).



**Figure 19: Packed-bed reactor filled with 277 mg Novozyme 435 (Cal B)**

For the optimization of this setup, various parameters were considered such as flow rate, amount of catalyst and residence time.

### **3.2.16 Stability of lipase-mediated hydrolysis of ECF in a continuous mode**

The stability test was performed to investigate how long the continuous system could be run for the liberation of HCN without significant deactivation of the catalyst. Therefore, the reactor was set up as described above (chapter 3.2.15) and 1 M of ECF in micro-aqueous MTBE was continuously pumped through this reactor setup for 8 h with a flow rate of 0.04 ml/min. The product stream was collected in fractions and analyzed offline by GC. The liberation of HCN was measured by the depletion of ECF by GC analysis (GC program: chapter 3.2.23.1).

### **3.2.17 Synthesis of (*R*)-mandelonitrile with Celite- His<sub>6</sub>-AtHNL in continuous mode**

This step involves the His<sub>6</sub>-AtHNL-mediated hydrocyanation of benzaldehyde to (*R*)-mandelonitrile. To form a packed-bed reactor, 100 mg celite-His<sub>6</sub>-AtHNL (chapter 3.2.8) was packed into a 5 cm omnifit glass column (kinesis microbore 3 mm) and both ends were sealed by end fittings (Figure 20). The column was connected to a syringe pump (Syrris Asia Syringe pump) by PTFE tubings. Meanwhile, 1 ml of 1 M HCN in micro-aqueous MTBE was produced separately in batch mode (chapter 3.2.10 b) and to this 500 mM benzaldehyde was added. This substrate mixture

---

containing HCN and benzaldehyde was passed through the reactor with a flow rate of 0.04 ml/min.



**Figure 20: Picture of an omnifit column (length: 5 cm, diameter: 3 mm) filled with 100 mg Celite-His<sub>6</sub>-AtHNL**

The product stream was collected in fractions and acetylated off-line in small vials with an excess of pyridine and acetic anhydride. The modified product was subsequently analyzed on chiral GC (GC program: chapter 3.2.23.1).

### **3.2.18 Synthesis of (*R*)-mandelonitrile with a 2-step cascade (CalB-His<sub>6</sub>-AtHNL)**

A two-step cascade was designed with the liberation of HCN as the first step and the hydrocyanation of aldehydes to the respective cyanohydrins as the second step. The synthesis of (*R*)-mandelonitrile was used as an example to optimize the setup.

Two different approaches were undertaken to realize this cascade and they are described as follows: In order to synthesize (*R*)-mandelonitrile in a two-step cascade, the reactor setups with CalB (chapter 3.2.15) and with Celite-His<sub>6</sub>-AtHNL (chapter 3.2.17) were connected sequentially by PTFE tubings.

---

#### **a) combined substrates in flow**

A substrate mixture of 1 M ethyl cyanoformate and 500 mM benzaldehyde in micro-aqueous MTBE was pumped continuously through the reactors at a flow rate of 0.04 ml/min using a syringe pump (Syrris Asia Syringe pump).

The product was collected in 500  $\mu$ l fractions and each fraction was acetylated with acetic anhydride and pyridine and subsequently analyzed by GC (GC program: chapter 3.2.23.1)

#### **b) separate substrates in flow**

In order to improve the two-step enzymatic setup for the synthesis of (*R*)-mandelonitrile, the substrates (ECF and benzaldehyde) were pumped in separately through two different syringe pumps. 1 M ECF in micro-aqueous MTBE was pumped through the lipase column (10 cm) containing 277 mg CalB at a flow rate of 0.04 ml/min. While a 500 mM benzaldehyde solution in micro-aqueous MTBE was pumped by a second pump which was connected such that its influx meets the efflux of the first stream by means of a “T-piece” assembly. Both streams flew through the second PBR containing 100 mg Celite-AtHNL now with a cumulative flow of 0.08 ml/min (Figure 20).

The entire setup was kept pressurized at 5 bar by a back pressure regulator. The product was collected in fractions and each fraction was acetylated with acetic anhydride and pyridine and subsequently analyzed by GC (GC program: 3.2.23.1)

### **3.2.19 Synthesis of (*R*)-mandelonitrile with a 2-step cascade (CalB-*E. coli*-His<sub>6</sub>-AtHNL)**

To test the 2-step enzymatic cascade with whole cells instead of immobilized His<sub>6</sub>-AtHNL. An omnifit glass column (l=10 cm, d=3 mm) was filled with 250 mg lyophilized *E. coli*-His<sub>6</sub>-AtHNL cells and was closed on both sides using end fittings. Meanwhile, 1 M ECF in micro-aqueous MTBE was pumped via syringe pump through the first column (l=10 cm, d=3 mm) containing 277 mg CalB at a flow rate of 0.04 ml/min (Figure 21). 500 mM benzaldehyde in micro-aqueous MTBE was pumped by a second pump, which was connected such that its influx meets the efflux of the first

---

stream by means of a “T-piece” assembly. Both streams flow through the second column with a cumulative flow of 0.08 ml/min. The entire setup was kept pressurized at 5 bar by a back pressure regulator. The product was collected in fractions and each fraction was modified with an excess of acetic anhydride and pyridine and subsequently analyzed by GC for conversion and *ee* (GC program: chapter 3.2.23.1).

### 3.2.20 Three-step cascade synthesis of (*R*)-*O*-acetylcyanohydrins in flow

In order to ensure rapid *O*-acylation of the hydroxynitrile formed in of the 2-step cascade (3.2.19), an in-line acetylation unit was setup through a reaction coil using a third HPLC pump (Knauer), which added a mixture of pyridine/acetic anhydride (1:1, v/v). The resulting solution was passed through a PTFE coil (2 ml) and finally collected in different fractions. The products were analyzed by chiral GC to measure conversions and *ee* (GC program: chapter 3.2.23.1). The reactor set-up was made as described above (chapter 3.2.19). Figure 21 shows the assembly of the system.

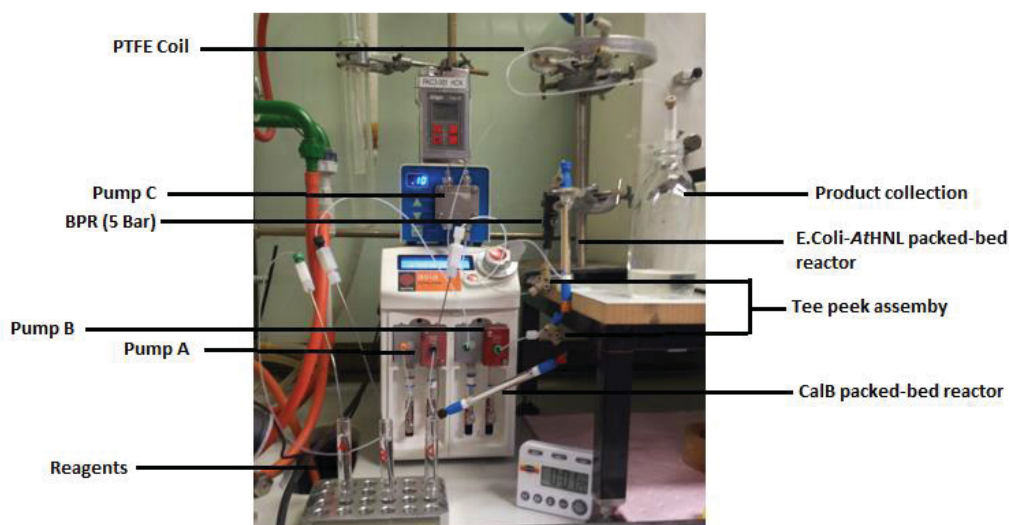


**Figure 21: Reactor setup of the 3-step chemoenzymatic cascade with whole cells (*E. coli*-His<sub>6</sub>-AtHNL)**

A 2 ml coil was set up in-line with the product stream and an additional third pump was used to pump in a mixture of acetic anhydride and pyridine at a FR of 0.01 ml/min. The product stream and the modification stream meet via a T-shaped mixer before passing through the 2 ml coil.

---

### 3.2.21 General batch procedure for the synthesis of racemic *O*-acetylcyanohydrins as reference compounds

A mixture of the respective aldehyde (benzaldehyde, 2-chlorobenzaldehyde, 4-bromobenzaldehyde, 4-methoxybenzaldehyde, 2-nitrobenzaldehyde, 4-(trifluoromethyl)benzaldehyde and 2-furfural) (1 mmol) and ECF (2 mmol) in MTBE was filled in a 8 ml GC vial. Novozyme 435 (50 mg) and a 2 ml of KPi-buffer (pH 8.5) were added consecutively.

The vial was closed and the resulting mixture was stirred gently for 5 h. A sample (0.05 ml) was taken from the reaction mixture and diluted in dichloromethane (1 ml) in a clean vial. A mixture of pyridine (0.05 ml) and acetic anhydride (0.06 ml) was added and the resulting mixture was stirred at RT for 180 min, affording racemic *O*-acetylcyanohydrins.

These experiments were performed by Dr. Biagia Musio at the University of Cambridge, UK. The retention times are listed in chapter 3.2.23.2

### 3.2.23 Analytics

#### 3.2.23.1 Gas chromatography

Syntheses of cyanohydrins were followed by chiral gas chromatography on a Shimadzu gas chromatograph GC-14B equipped with an FID detector, a beta-cyclodextrin column (CP-Chirasil-Dex CB 25 m x 0.25 mm) and Hydrogen as the carrier gas. Samples were derivatized prior to analysis using the procedures described in chapter 3.2.11 und 3.2.12.

##### 3.2.23.1.1. GC method for CalB mediated hydrolysis of ECF

	ECF
<b>Start</b>	40 °C
<b>Gradient</b>	15 °C/min till 180 °C
<b>hold</b>	0 min
<b>post run</b>	180 °C, 2 min
<b>retention time</b>	2.1 min

### 3.2.23.1.2 GC method for synthesis of cyanohydrins from aldehydes

	benzaldehyde*	2-chlorobenzaldehyde	hexanal
<b>start</b>	120 °C, 3 min	110 °C, 5 min	70 °C, 6 min
<b>gradient</b>	15 °C/min till 200 °C	5 °C/min till 200°C	15 °C/min till 200°C
<b>hold</b>	200 °C, 1 min	140 °C, 5 min	200 °C, 1 min
<b>gradient2</b>	0 min	15 °C/min till 180°C	0 min
<b>post run</b>	0 min	0 min	180 °C, 1 min
<b>retention time</b>	1.9 min	3 min	10 min

\*This method was used for the synthesis of o-acetylcyanohydrins [1-6] shown in the table below

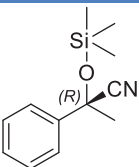
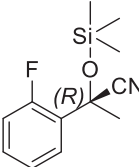
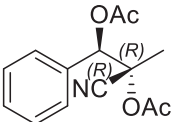
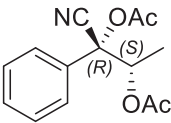
#### Retention times of reported O-acetylcyanohydrins

No.	Compound	Structure	Enantiomer 1 T1 (min)	Enantiomer 2 T2 (min)
1	(R)-2-O-acetyl-2-phenyl acetonitrile		4.9 min	5.3 min
2	(R)-2-O-acetyl-2-(4-bromophenyl) acetonitrile		18.3 min	19.1 min
3	(R)-2-O-acetyl-2-(4-methoxyphenyl) acetonitrile		17.6 min	18.6 min
4	(R)-2-O-acetyl-2-(2-nitrophenyl) acetonitrile		18.7 min	18.8 min
5	(S)-2-O-acetyl-2-(furan-2-yl) acetonitrile		4.8 min	6.4 min
6	(R)-2-O-acetyl-2-[4-(trifluoromethyl) phenyl] acetonitrile		10.1 min	12.2 min
7.	(R)-(2-chlorophenyl)(cyano)methyl acetate		9.3 min	9.5 min
8.	1-cyanoethyl acetate		7.8 min	7.9 min

### 3.2.23.1.3 GC method for synthesis of cyanohydrins from ketones and 2-hydroxy ketones

	Ketones (acetophenone, 2- F-acetophenone)	2-hydroxy ketones (R-PAC, S-HPP)
start	100 °C, 3 min	100 °C, 3 min
gradient	7 °C/min till 180 °C	4 °C/min till 180 °C
hold	5 min	5 min
gradient2	0 min	5 °C/min till 200 °C
hold	0 min	3 min
retention time	3 min, 3.6 min	11.8 min, 12 min

Retention times of reported ketone and 2-hydroxy ketone cyanohydrins (derivatized)

No.	Compound	Structure	Enantiomer 1 T1 (min)	Enantiomer 2 T2 (min)
1	(R)-2-phenyl-2-((trimethylsilyl)oxy)propanenitrile		15.4	16.3
2	2-(2-fluorophenyl)-2-((trimethylsilyl)oxy)propanenitrile		18.5	19.0
3	(1R,2R)-2-cyano-1-phenylpropane-1,2-diyl diacetate		19.5	19.7
4	(1R,2S)-1-cyano-1-phenylpropane-1,2-diyl diacetate		18.5	18.8

### 3.2.23.3 Supercritical Fluid Chromatography (SFC)

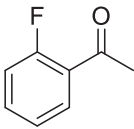
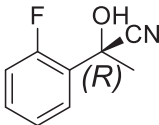
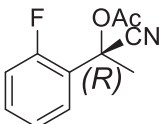
Supercritical Fluid chromatography is an efficient and rapid analytic technique for enantio-resolutions where a supercritical fluid constitutes the main part of the mobile phase [138]. An Aurora SFC-Hydra from Chiral technologies was fitted with a chiralpak IF column (Amylose tris(3-

chloro-4-methylphenylcarbamate) immobilized on 5  $\mu\text{m}$  silica gel). A mixture of supercritical  $\text{CO}_2$  and methanol in the ratio 90:10 were used as the mobile phase at a flow rate of 2 ml/min.

### 3.2.23.3.1 Parameters for SFC program

Pump	SFC	Sampler	Column Compartment	DAD
flow 2 ml/min	BPR pressure	inj. volume 5 $\mu\text{L}$	temp. 30°C	200 nm
90 % $\text{CO}_2$	150 bar	overflow 15 $\mu\text{L}$		210 nm
10 % MeOH	BPR temp. 60°C			230 nm
time: 15 min				250 nm
				(all wavelengths with bandwidth 4 nm)

### 3.2.23.3.2 Retention times of reported compounds on SFC

No.	Compound	Structure	Retention time
1.	2-F-acetophenone		2.0 min
2	2-(2-fluorophenyl)-2-hydroxypropanenitrile		2.5 min, 2.8 min
3	(R)-1-cyano-1-(2-fluorophenyl)ethyl acetate		1.7 min and 1.9 min

### 3.2.23.4 Mass Spectrometry

A GC system (Varian CP 3800) was coupled with a mass spectrometer (Saturn 2000 MS) was used. Electron ionization was used with an ionization energy of 70 eV, using helium as the carrier gas. The analyzer was set between  $m/z$  40 and  $m/z$  300, respectively. The spectra were analyzed by SaturnView and the molecules were identified based on their fragmentation pattern (see Appendix 10-13).

---

### 3.2.23.5 Nuclear Magnetic Resonance (NMR)

<sup>1</sup>H-NMR spectra were recorded on either Bruker Avance DPX-400 or Bruker Avance DPX-600 spectrometer, as specified, with the residual solvent peak as the internal reference (CDCl<sub>3</sub> = 7.26 ppm). <sup>1</sup>H resonances are reported to the nearest 0.01 ppm. <sup>13</sup>C-NMR spectra were recorded on the same spectrometer, as specified, with the central resonance of the solvent peak as the internal reference (CDCl<sub>3</sub> = 77.00 ppm). All <sup>13</sup>C resonances are reported to the nearest 0.01 ppm. The multiplicity of <sup>1</sup>H signals are indicated as: s = singlet, d = doublet, dd = doublet of doublet, ddd = doublet of doublet of doublet, t = triplet, q = quadruplet, sext = sextet, m = multiplet, br = broad, or combinations of thereof. Coupling constants (*J*) are quoted in Hz and reported to the nearest 0.1 Hz. Where appropriate, averages of the signals from peaks displaying multiplicity were used to calculate the value of the coupling constant.

#### 3.2.23.4.1 Spectroscopic characterization of compound 1-5 (chapter 3.2.23.1.2).

The spectroscopic data of 1 [139], 2 [140], 3, 5 [141] and 6 [133] are as reported in literature.

**(*R*)-2-*O*-Acetyl-2-(2-nitrophenyl) acetonitrile (4).** <sup>1</sup>H NMR (400 MHz, CDCl<sub>3</sub>) δ 2.21 (s, 3H), 7.09 (s, 1H), 7.68 (dt, *J* = 8.2, 1.4 Hz, 1H), 7.80 (dt, *J* = 7.7, 1.3 Hz, 1H), 7.93 (dd, *J* = 7.8, 1.2 Hz, 1H), 8.20 (dd, *J* = 8.2, 1.2 Hz, 1H). <sup>13</sup>C NMR (150 MHz, CDCl<sub>3</sub>) δ 20.1, 59.6, 115.0, 125.8, 129.3, 131.3, 134.5, 147.0, 168.3. IR (Neat, cm<sup>-1</sup>) 3123, 3036, 2333, 1756, 1399, 1116, 1064. HRMS *m/z* calculated for C<sub>10</sub>H<sub>9</sub>O<sub>4</sub>N<sub>2</sub> [M + H]<sup>+</sup> 221.0557, found 221.0547.



# Chapter 4

## **RESULTS AND DISCUSSION**

---

## 4. Results and Discussion

### 4.1 Characterization of His<sub>6</sub>-AtHNL

The wt-AtHNL demonstrates excellent activity and enantioselectivity towards aldehydes, however, the purification via anion chromatography is challenging not only with respect to yields and purity but it is also tedious and time consuming [120].

Therefore, a new variant of wt-AtHNL with an N-terminal hexahistidine tag was tested to facilitate an easier and effective purification of the protein (Appendix 3). The overexpression and purification for this variant was optimized as described in chapter 3.2.1.

Compared to the purification of wt-AtHNL, which required three chromatographic steps, including desalting of the crude cell extract, anion exchange chromatography and a final desalting step, the new protocol yields a higher amount of purer enzyme per gram recombinant *E. coli* cells. This new variant not only provided a faster purification protocol, but also resulted in a higher expression level of the enzyme in *E. coli*. In case of wt-AtHNL, 100 mg protein was obtained from 9.5 g wet *E.coli*\_BL21-AtHNL cells whereas the His-tagged version yielded 220 mg enzyme from the same amount of cells, with a 2.3-fold higher specific activity (Table 1).

To make sure that the His-tag did not impair the enzyme properties, the variant was first characterized relative to the wt-enzyme with respect to pH-optima and stability as well as the synthesis of different aldehyde cyanohydrins using three different enzyme preparations.

Many of these studies were done in the Master thesis of Amina Frese, which was supervised in the context of this doctoral thesis [142].

The main important results are summarized in Table 1.

**Table 1: Comparative characterization of wt-AtHNL and His<sub>6</sub>-AtHNL [142].**

**Experimental condition: The enzymes were applied in purified soluble form. Kinetic parameters ( $V_{max}$ ,  $K_M$ ) were determined by the mandelonitrile cleavage assay (chapter 3.2.7)**

Parameters	wt-AtHNL	His <sub>6</sub> -AtHNL
<b>pH-optimium</b>	5.5-6.0	5.5-6.0
<b>t<sub>1/2</sub> at pH 4.5 (min)</b>	4	4
<b>t<sub>1/2</sub> at pH 5.5 (min)</b>	211	220
<b>T-optimium (°C)</b>	35-45	35-45
<b>V<sub>max</sub> (U/mg)</b>	32 ± 1.43	75 ± 4.26
<b>K<sub>M</sub> (mM)</b>	0.12 ± 0.04	0.13 ± 0.06

The pH optima curves for wt-AtHNL and His<sub>6</sub>-AtHNL are similar to each other in the range of 5.5 to 6.0, with a maximum at pH 5.75 for both the variants and the activity falls sharply at pH values lower than 5.0. The lower activity can be partly explained because of the inactivation due to the partial unfolding of the protein in acidic environment [116].

To avoid the non-enzymatic side reaction yielding racemic cyanohydrins, the enzyme-catalyzed synthesis of enantiopure cyanohydrins can be performed at lower temperatures (10 °C). However, this would require additional cooling and therefore all the following mandelonitrile cleavage assays were performed at 25 °C. In addition to the pH-optimium, the stability of the His<sub>6</sub>-AtHNL was determined in comparison to the wt-AtHNL at low pH values. In summary both the variants have similar half-lives (211-220 min) at pH 5.5 and are rapidly inactivated at lower pH.

In summary, the N-terminal hexahistidine-tag has no effect on the pH-optimium and stability of AtHNL in the range tested [142]. Additionally not only is the purification protocol simpler, it also offers a higher expression and thereby a higher specific activity as compared to the wt-AtHNL. His<sub>6</sub>-AtHNL was purified and lyophilized as described in chapter 3.2.5.

## 4.1.1 Synthesis of aldehyde cyanohydrins with lyophilized His<sub>6</sub>-AtHNL

### 4.1.1.1 lyophilized His<sub>6</sub>-AtHNL

In order to compare the synthetic potential of the His-tagged variant with the wt-enzyme, three different aldehydes (benzaldehyde, 2-chlorobenzaldehyde, hexanal) were evaluated as substrates for His<sub>6</sub>-AtHNL in micro-aqueous MTBE

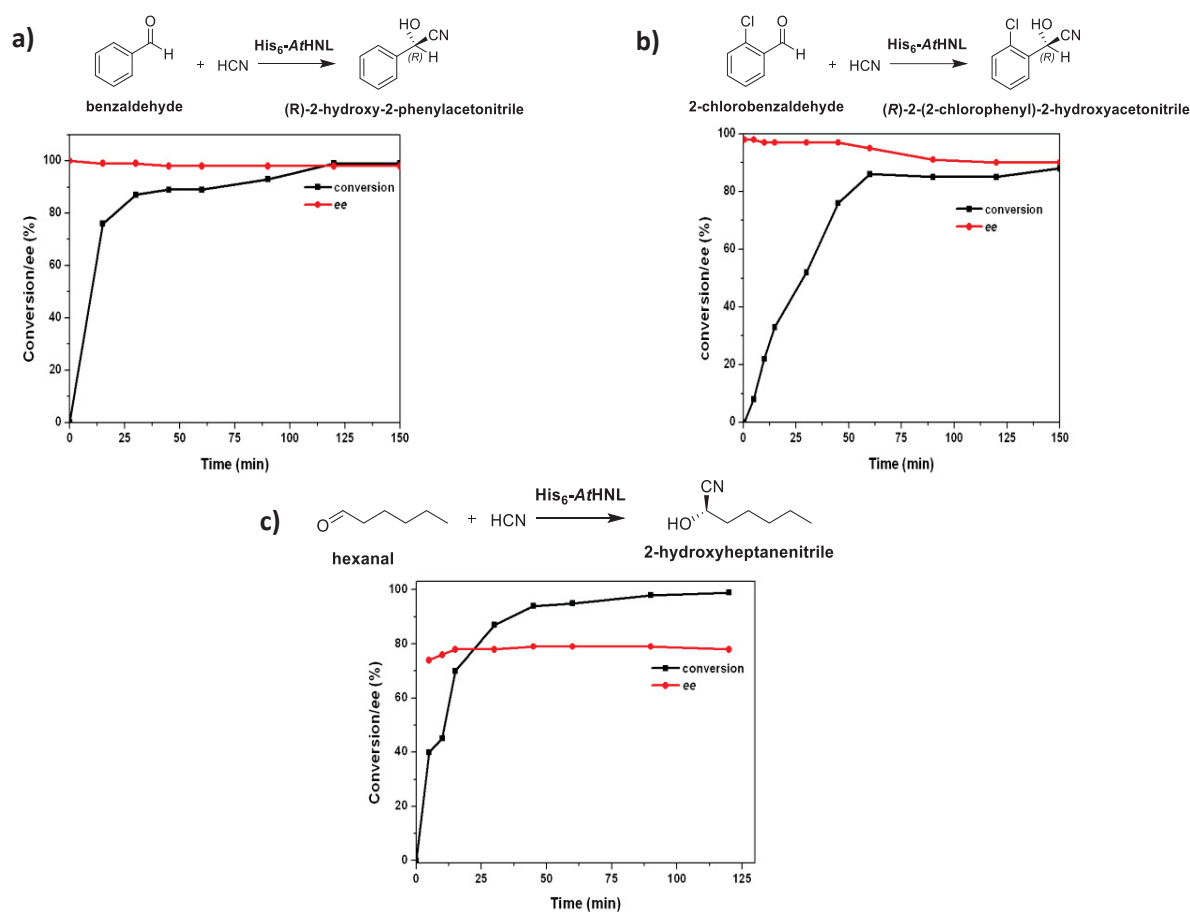


Figure 22: Conversion and *ee* of a) benzaldehyde b) 2-chlorobenzaldehyde and c) hexanal to the respective cyanohydrins. Reaction conditions: 500 mM aldehyde (freshly distilled), 1.5 M HCN-MTBE, 3 mg His<sub>6</sub>-AtHNL stirred at RT for 2 hours. His<sub>6</sub>-AtHNL was weighed and added to 1 ml 1.5 M HCN-MTBE (micro-aqueous MTBE) and the reaction was started by adding 500 mM of each substrate (chapter 3.2.11). A non-enzymatic control reaction was performed in parallel to monitor the chemical background reaction. The products were acetylated in small batches and then subsequently analyzed on chiral GC (chapter 3.2.23.1). Data of a single experiment are shown.

---

To keep the water content low, the enzyme was added in dry form to the reaction media. This was in contrast to previous studies with wt-AtHNL where the enzyme was resuspended in 50  $\mu$ l buffer [120].

However, the enzyme behaved in a similar way by forming a cloudy precipitate that stuck to the walls of the reaction vessel, which did not impair the activity and full conversion was achieved in all cases after 1-2 hours.

Conversion and *ee* were plotted over time and from Figure 22 we see that after 120 minutes, the reaction with benzaldehyde (BA) was the fastest to attain full conversion. The reaction rate decreased in the series: benzaldehyde > 2-Cl-benzaldehyde > hexanal.

A non-enzymatic chemical reaction was not detected in case of benzaldehyde under these reaction conditions, however a very low conversion of 4 % was observed with 2-chlorobenzaldehyde. In case of hexanal the conversion due to the chemical reaction increased up to 40 % after 2 hours.

Excellent *ee* of 99 % was attained with benzaldehyde throughout the course of reaction. In case of the synthesis reaction with 2-chlorobenzaldehyde, the *ee* remained at 98 % for 1 hour and then decreased to 90 %. Hexanal, on the other hand, showed a low overall *ee* of 75 % which can be explained by the high velocity of the non-enzymatic chemical reaction.

#### **4.1.1.2 Celite-His<sub>6</sub>-AtHNL**

Celite was shown to be a useful matrix for the immobilization of wt-AtHNL [120]. Celite-His<sub>6</sub>-AtHNL was prepared as described in chapter 3.2.8. The advantage of this immobilization technique is not only its ease of preparation but also as much as 78 % residual activity [120] is retained after the procedure. Moreover, it has been already shown that in a batch reaction with Celite-AtHNL, there is no leaching of active enzyme into the reaction medium [120]. Syntheses reactions were performed as described in Figure 23.

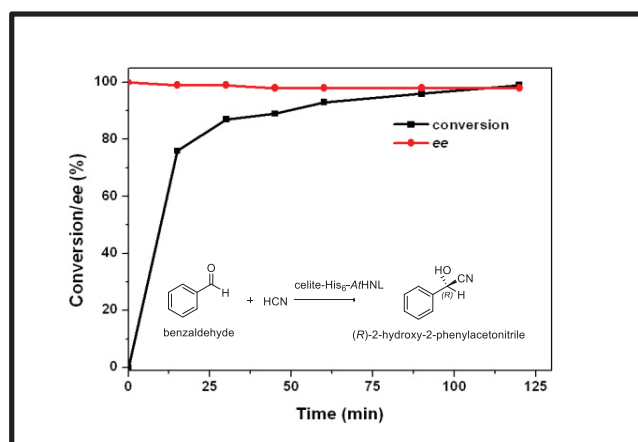


**Figure 23: Synthesis of (*R*)-mandelonitrile with Celite-His<sub>6</sub>-AtHNL.**

**Reaction conditions: 500 mM benzaldehyde, 1.5 M HCN-MTBE, 20 mg celite-His<sub>6</sub>-AtHNL stirred at RT for 2 hours. The products were acetylated in small batches and then subsequently analyzed on chiral GC (chapter 3.2.23.1). Data of a single experiment are shown.**

High conversions and *ee* were achieved comparable to those reported above with the lyophilized enzyme (chapter 4.1.3), which is again comparable to previous studies with wt AtHNL.

#### 4.1.1.3 whole cell biocatalysis

The synthesis of chiral cyanohydrins with whole cells in micro-aqueous MTBE has already been reported in previous studies for wt-AtHNL [118]. A cell load of 100 mg was used in previous studies with wt-AtHNL, similar to the present study. Because of higher expression levels of His<sub>6</sub>-AtHNL, not only is the purification of His<sub>6</sub>-AtHNL faster and more efficient, it is also advantageous to apply them in whole cells as biocatalyst.

Using recombinant *E. coli*-BL21-AtHNL cells excellent conversion and *ee* was achieved with benzaldehyde (Figure 24a) and these results are comparable to those obtained with purified and immobilized His<sub>6</sub>-AtHNL (chapter 4.1.1.2). The synthesis reaction with 2-chloromandelonitrile (Figure 24b) resulted in similar conversion and *ee* as with purified His<sub>6</sub>-AtHNL (chapter 4.1.1.1).

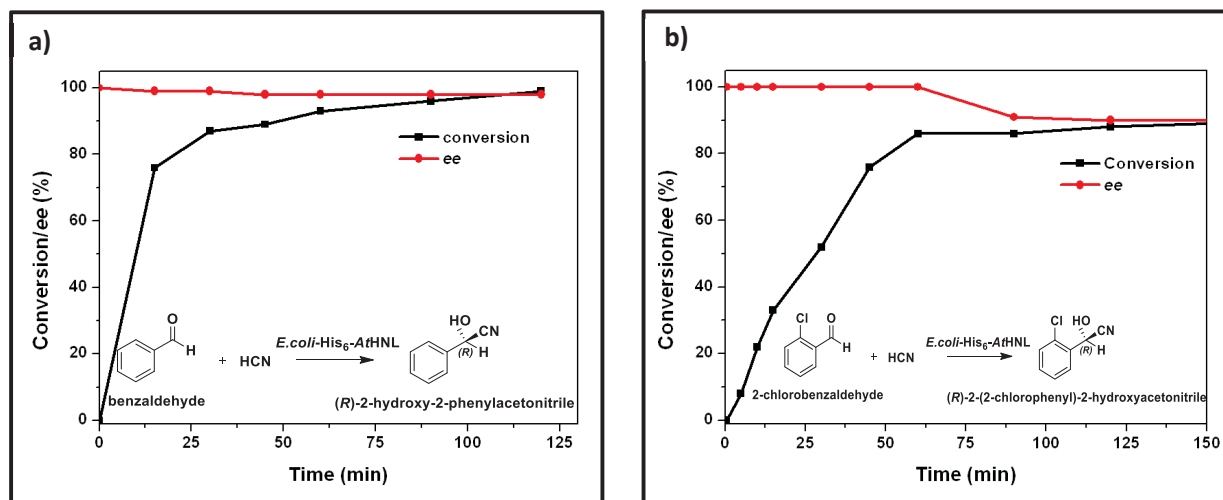


**Figure 24: Conversions and ee with whole cell biotransformation using a) benzaldehyde and b) 2-chlorobenzaldehyde as substrate**

**Reaction conditions:** Lyophilized *E. coli*-BL21-His<sub>6</sub>-AtHNL cells were prepared (chapter 3.2.1) and 100 mg of them were packed into a “tea bag” as described in chapter 3.2.9. Two synthesis reactions were started by the addition of 500 mM of substrate into a 4 ml GC vial containing 1 ml of 1.5 M HCN-MTBE and the “tea bag” containing 100 mg lyophilized cells. Data of a single experiment are shown

In a previous study, the difference in behavior of fresh wet cells and lyophilized cells was reported [118]. However, in case of His<sub>6</sub>-AtHNL no difference in activity and ee was observed using wet cells or lyophilized cells as catalysts for the synthesis of mandelonitrile (data not shown). Nevertheless, since lyophilized cells are easier to handle especially while packing them into “tea bags”, subsequent experiments with whole cells were performed with lyophilized cells only.

#### 4.1.2 Recyclability of Celite-His<sub>6</sub>-AtHNL and whole cells in MTBE

Further recyclability tests were performed with Celite-His<sub>6</sub>-AtHNL and *E. coli*-His<sub>6</sub>-AtHNL in micro-aqueous MTBE (chapter 3.2.9). In both cases, high conversions were achieved for all four cycles (Figure 25). The ee, on the other hand, decreased slowly and in the 4<sup>th</sup> cycle a total decrease of 8-10 % in ee was observed with Celite-His<sub>6</sub>-AtHNL and whole cells, respectively.

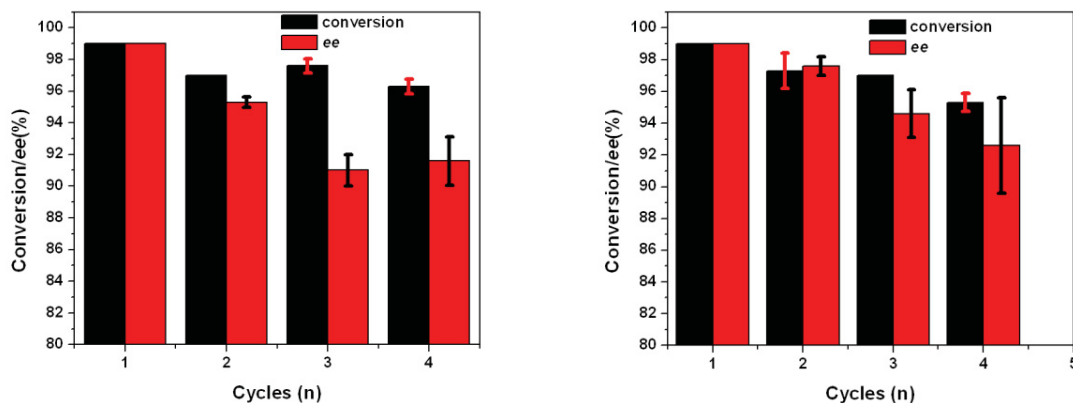


**Figure 25: Recyclability of Celite-His<sub>6</sub>-AtHNL (left) and *E. coli*-His<sub>6</sub>-AtHNL (right) for the synthesis of (*R*)-mandelonitrile.**

**Reaction conditions: 500 mM benzaldehyde, 1.5 M HCN-MTBE, 20 mg celite-His<sub>6</sub>-AtHNL or 100 mg *E. coli*-His<sub>6</sub>-AtHNL sealed in a “tea bag”, stirred at RT for 2 hours. In between the cycles, the “tea bag” was washed thrice with buffer-saturated MTBE to remove excess substrate and a new reaction was started with the same “tea bag” by the addition of fresh substrate. Measurements were done in triplicate.**

Good recyclability of Celite-wt-AtHNL has been already reported without any loss of *ee* [120, 121]. However, in the present study with Celite-His<sub>6</sub>-AtHNL a loss of *ee* was observed with every consequent cycle, which could be explained by the intermediate washing steps with MTBE. Since the MTBE used for the washing steps was not exchanged, there is a possibility that accumulated water triggered the chemical reaction. The same explanation holds for the results observed with whole cells.

#### **4.1.2.1 Stability of Celite-His<sub>6</sub>-AtHNL and whole cells in MTBE**

Further the stability of Celite-His<sub>6</sub>-AtHNL and whole cells was studied in MTBE. A “tea bag” containing Celite-His<sub>6</sub>-AtHNL or whole cells, respectively, was incubated in MTBE and their residual activities were tested each day by measuring the formation of mandelonitrile [142]. The results demonstrated that a high conversion of 98 % with a decent *ee* of 95 % was achieved up to the third day of incubation in MTBE. However, conversion and *ee* decreased continuously. In

---

contrast, the whole cells incubated in MTBE exhibited a high conversion and *ee* of 89 % and 96% respectively even on the 15<sup>th</sup> day of incubation [142]. It is noteworthy, that the amounts of cells used for this experiment were adjusted such that they contained the same amount of enzyme as their Celite-immobilized counterpart. The higher stability of the whole cells in MTBE under the tested conditions can be explained by the presence of the cell membrane which acts as a natural immobilization. The effect of organic solvents on whole cells have been studied by microscopic analysis demonstrating partially ruptured membranes [137] and shrunken cells [121] upon prolonged incubation in MTBE.

## 4.2 Ketones as substrates

As already stated in the introduction (chapter 1.5.3), the substrate scope of *AtHNL* includes a broad range of aldehydes and some ketones. Besides the initial studies from Andexer et al. [111] in an aqueous/organic two-phase system, no further investigations to optimize conversion and *ee* of the biocatalytic hydrocyanation of ketones were performed.

In this chapter, the possibility to influence these parameters using His<sub>6</sub>-*AtHNL* in micro-aqueous MTBE was evaluated with two aromatic ketones (acetophenone and 2-F-acetophenone). Further, the enzyme was tested with new ketone substrate, namely 2-hydroxy ketones, to evaluate the access to the corresponding cyanohydrins in a stereospecific manner. The HCN used for all reactions was prepared as described in chapter 3.2.10a.

### 4.2.1 Aromatic ketones as substrate

#### 4.2.1.1 Analytics for ketone cyanohydrins

The instability of ketone cyanohydrins at GC temperatures imposes analytic challenges and therefore they must be derivatized. The 2-F-acetophenone cyanohydrin was synthesized as described in chapter 3.2.12. Various approaches were evaluated for the esterification of the tertiary alcohol group. The first approach involved acetylation with an excess of acetic anhydride and pyridine (chapter 3.2.12). This procedure, however, led to only 7 % conversion in 24 h under

the tested conditions. As a second approach, pyridine was replaced by the stronger base 4-dimethylaminopyridine (DMAP). This led to a higher conversion of 22 % but was nevertheless incomplete (Appendix 4). The extent of this derivatization was analyzed by Supercritical Fluid Chromatography (SFC) (chapter 3.2.23.2). As demonstrated in Figure 26 acetylation with acetic anhydride and DMAP was incomplete under the tested conditions.

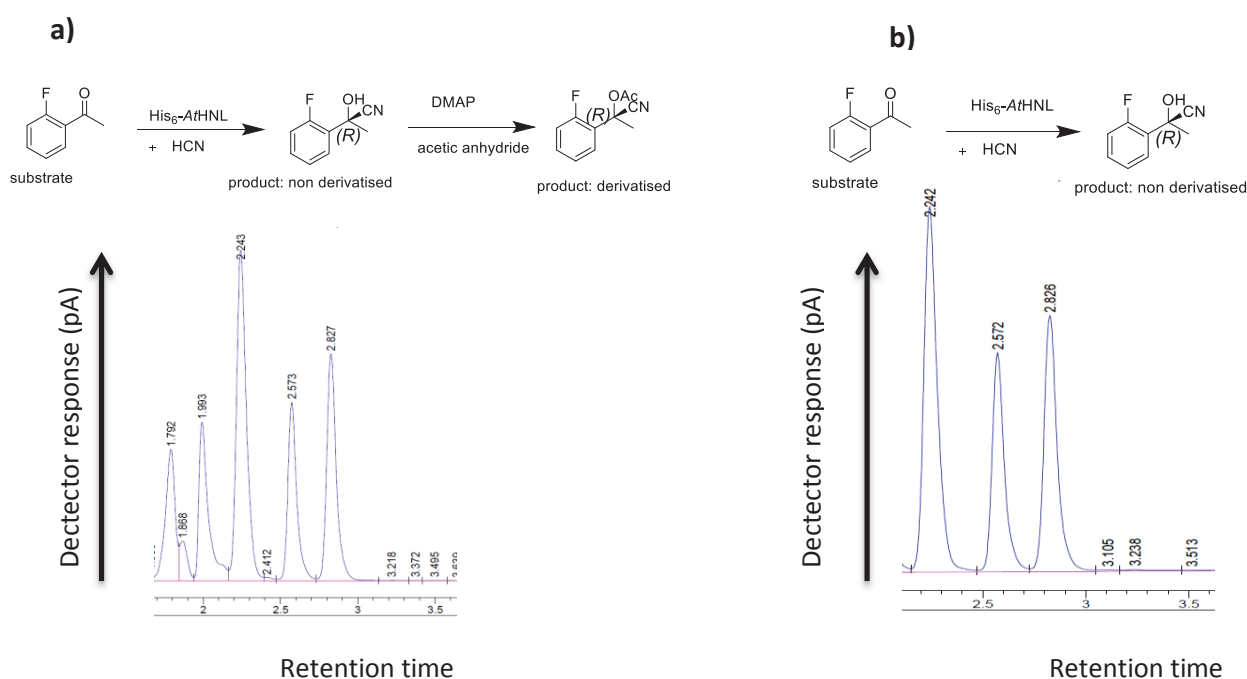


**Figure 26: Analysis of the hydrocyanation of 2-F-acetophenone ( $t=2.24$  min) using SFC (chapter 3.2.23.2). Left: both enantiomers of the non-derivatized product ( $t=2.5$  min and  $t=2.8$  min) Right: additional peaks of both enantiomers of the derivatized product ( $t=1.72$  min and  $t=1.99$  min).**

**Experimental conditions:** Synthesis reaction was performed with 400 mM 2-F-acetophenone, 1.5 M HCN-MTBE and 3 mg His<sub>6</sub>-AthNL. After 24 h 50  $\mu$ l of reaction mixture was a) diluted with 950  $\mu$ l isopropanol, incubated for 12-20 h, RT and analyzed on SFC: b) diluted with 850  $\mu$ l dichlormethane, modified with 50  $\mu$ l each of acetic anhydride and dimethyl aminopyridine for 3 h at RT and subsequently analyzed on SFC.

Therefore, a third approach was evaluated from a recently reported method [123], where the alcohol group of the ketone cyanohydrin is silylated with N,O-bis(trimethylsilyl)trifluoroacetamide (BSTFA) (chapter 3.2.12). The product was derivatized with an excess of BSTFA for 12-20 hours at RT and was subsequently analyzed on SFC. This procedure of derivatization by silylation leads to almost complete derivatization (Appendix 5).

#### 4.2.1.2 Synthesis of two aromatic ketone cyanohydrins

Acetophenone and 2-F-acetophenone were biocatalytically hydrocyanated in micro-aqueous MTBE following the procedure in chapter 3.2.12. The progress curves for each of the substrate are shown in Figure 27.

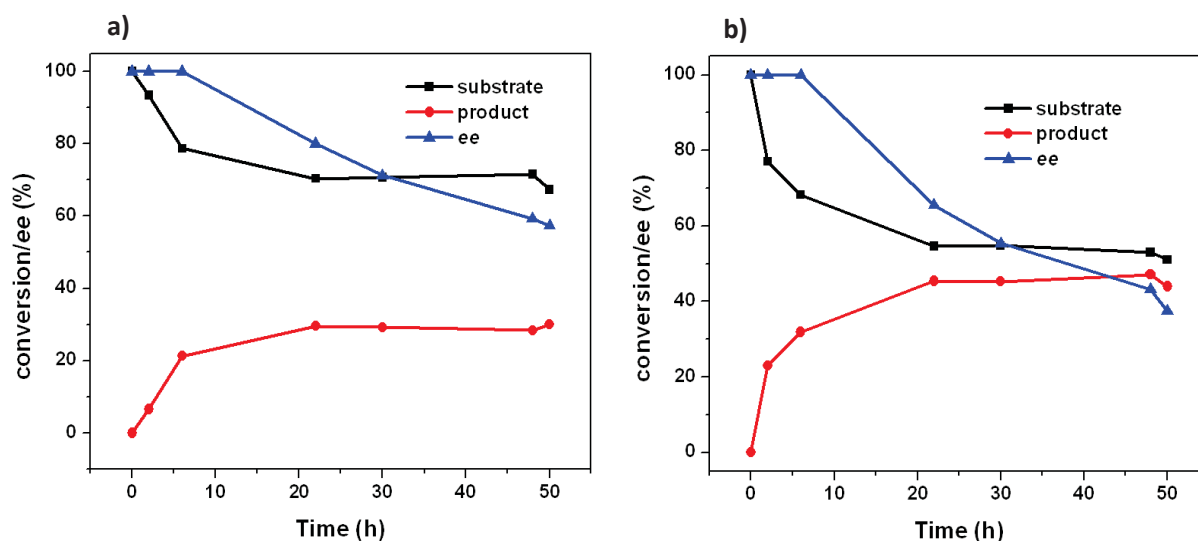


Figure 27: Synthesis of ketone cyanohydrins from a) acetophenone; b) 2-F-acetophenone.

Reaction conditions: 1 ml of 1.5 M HCN-MTBE, 400 mM substrate, 3 mg His<sub>6</sub>-AtHNL (lyophilized). Samples were taken at t=0, 2, 6, 20, 30, 48 and 50 h respectively. 50 µl of sample at each time point was derivatized in 50 µl BSTFA and 750 µl of dichloromethane and subsequently incubated for 12-20h at RT before GC analysis (chapter 3.2.23.1). The products were confirmed by GC/MS analysis (Appendix 10-11). Data of a single experiment are shown.

---

For both, acetophenone and 2-F-acetophenone a maximum conversion of 40 % and 48 % was obtained, respectively, which refers to product concentrations of 160-190 mM.

Thus, this reactions system provides very good results compared to an earlier study by von Langermann et al., where *MeHNL* was used as a catalyst in an aqueous organic two-phase system either with diisopropyl ethyl ether (DIPE) or pure aromatic ketone substrate as the organic phase [81].

The authors studied the effect of various reaction media on the yield of acetophenone cyanohydrin and demonstrated a maximum of 22 % conversion using acetophenone as the organic phase and a 5-fold excess of HCN [81].

In the present study, the use of micro-aqueous MTBE increased the conversion to 40 % using only a 3-fold excess of HCN, which is 3.7 fold higher than the reported values. The biggest advantage of the micro-aqueous system is attributed to the high substrate concentration (400 mM) and thereby high product yields.

Introducing an electron withdrawing fluorine substituent in *ortho* position of the aromatic ring was shown to increase the conversion and this behavior has been explained by the formation of intramolecular H-bonds [81]. 2-F-acetophenone was also faster transformed than acetophenone by *MeHNL* in biphasic reaction systems.

Therefore, it was also evaluated as a substrate for *His<sub>6</sub>-AtHNL* in micro-aqueous MTBE and a maximum conversion of 48 % was achieved. Although these conversions are much higher than the reported values with *MeHNL*, the reactions with ketones as substrates are much slower compared to aldehydes, which is attributed partly to the intrinsic bulky nature of ketones, which imposes steric hindrance, and partly due to the thermodynamic limitations of such reactions [81]. This effect was further studied by increasing the catalyst load (see 4.2.1.3). Further, following the development of *ee* over the conversion of acetophenone and 2-F-acetophenone gave an interesting result: Although almost enantiopure (*ee* 99%) products were formed during the first

---

8 h of the reaction, there was a steady decrease of *ee* observed when the reaction was continued (Figure 27). This effect was further studied as described in chapter 4.2.1.4.

#### ***4.2.1.3 Effect of catalyst load on conversion***

In order to confirm that the observed conversions of 40 % and 48 %, respectively, is not attributed to inactivation of the enzyme, additional doses of enzyme were pulsed into the reaction and the effect on conversion was analyzed. Therefore, a synthesis reaction was started with 400 mM acetophenone, 1.5 M HCN-MTBE and 2.5 mg lyophilized His<sub>6</sub>-AtHNL. After 8 h, double the enzyme amount (5 mg) was added to the reaction and the conversion was further monitored.

There was hardly any increase of conversion visible even on doubling the amount of enzyme, which demonstrates firstly that the increase of the catalyst load has no effect on the conversion of the reaction and secondly that the reaction equilibrium was reached.

Furthermore, it was also confirmed that the enzyme was still active in the reaction mixture by injecting 500 mM benzaldehyde into to the reaction mixture at t=24 h and nearly a full conversion to (*R*)-mandelonitrile was observed within an hour (data not shown).

#### ***4.2.1.4 Enzyme-catalyzed product racemisation***

As mentioned already above, the *ee* of both ketone cyanohydrins started to decrease continuously after about 8 hours reaction time. In order to test, whether this effect was enzyme-coupled, synthesis reactions were performed with a “tea bag” containing Celite-His<sub>6</sub>-AtHNL. The “tea bag” was then removed after 8 h, which resulted in a constantly high product *ee* in the reaction mixture (Figure 28).

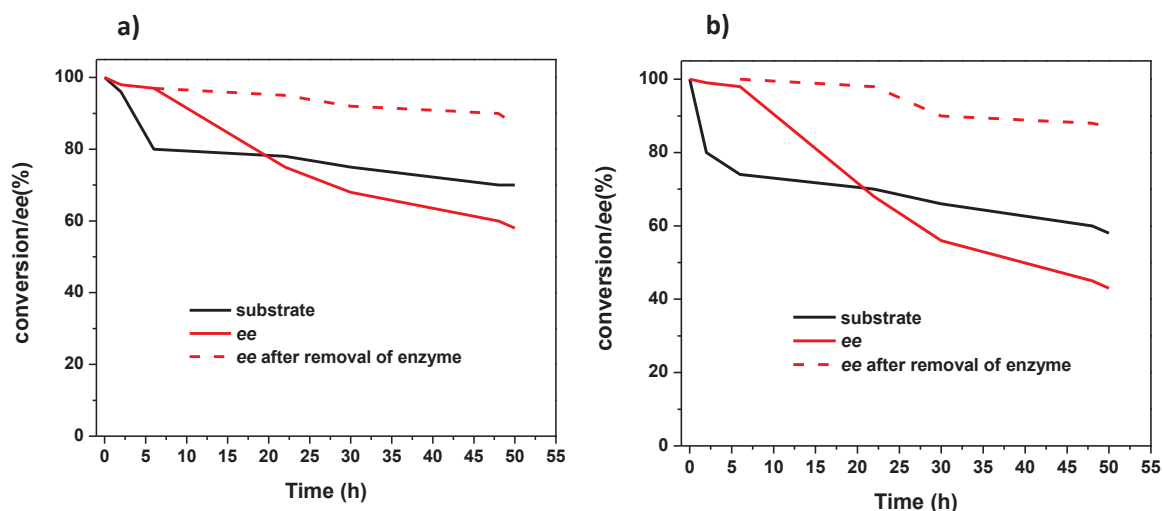


**Figure 28: Conversion and *ee* of the reaction with the enzyme and the *ee* after removal of the enzyme for a) acetophenone b) 2-fluoroacetophenone.**

**Reaction conditions: same as in Figure 27 (chapter 4.2.1.2). Celite- $\text{His}_6$ -*At*HNL was removed from the reaction after 8 h and the reaction was followed till 50 h.**

The observed decrease in *ee* is not because of the non-enzymatic chemical reaction, which is up to 8-10%. These results strongly hint to an enzyme-catalyzed product racemisation. Under the tested condition the reaction equilibrium is reached after about 10 hours. To that point the enzyme catalyzes the formation of the respective ketone cyanohydrine. However, HNLs catalyze also the cleavage of cyanohydrines. Depending on the  $K_M$ -value the velocity of the cleavage reaction increases the more cyanohydrine is formed. As *At*HNL is an *R*-selective enzyme it prefers also (*R*)-cyanohydrines over the *S*-enantiomers for the cleavage reaction.

As a consequence the *S*-enantiomer accumulates in the reaction mixture. It should be noted here that the rate of the synthesis can be very different compared to the cleavage. It is possible that the cleavage is much faster than the synthesis reaction. It is therefore essential to stop the reaction as soon as the equilibrium is reached to avoid product racemization.

Previous studies have reported the synthesis of acetophenone cyanohydrin using the *S*-selective *Me*HNL, where a maximum conversion of 22 % with an *ee* of 97 % was reported in an organic

---

solvent free system [81]. The high *ee* in such system could be explained by its short reaction time of 6 hours, which was probably not sufficient to cleave the product cyanohydrin. Moreover, such behavior of HNL-catalyzed product racemization has not been reported in previous studies.

It is interesting to note here that this behavior of product racemization is only pronounced, if the reaction is allowed to proceed till the chemical equilibrium is reached. The reason why this behavior has not been observed with aldehyde cyanohydrins is probably because the reactions are usually stopped after 2 hours when almost complete conversion was achieved.

In this study, His<sub>6</sub>-AtHNL-catalyzed reactions in micro-aqueous MTBE (Figure 27), gave a maximum conversion of 40-48 % with acetophenone and 2-F-acetophenone, respectively, and an increase of the catalyst load did not lead to an increased conversion. The reason lies in the fact that the thermodynamic equilibrium is attained at this point. Further studies with solvent engineering and in-situ product removal could lead to a shift of the equilibrium.

Von Langermann et al. studied the synthesis of cyanohydrins in different reaction media such as aqueous systems, two-phase systems and organic solvent free systems and explained how different reaction media can affect the thermodynamic equilibrium [81]. Applying Le Chatlier's principle, a relatively higher conversion could be attained by increasing the concentration of HCN in the system; however, the enzyme stability is greatly challenged in such systems.

#### 4.2.2 2-Hydroxy ketones as substrates

Besides the acetophenone derivatives described above, different 2-hydroxy ketones shown in Table 2 were evaluated as substrates for His<sub>6</sub>-AtHNL. The formation of 2-hydroxy ketones by carbonylation of aldehydes catalyzed by thiamine diphosphate-dependent enzymes has been studied extensively in the Biocatalysis & Biosensors group at IBG-1 [143]. Stereoselective hydrocyanation of chiral 2-hydroxy ketones would open a broader range of chiral dihydroxy-nitriles, which could further be transformed by modification of the nitrile group (chapter 1.5.3), yielding highly functionalized molecules with more than three stereo centers.

#### 4.2.2.1 Analytics for 2-hydroxy ketone cyanohydrins

Owing to their instability at GC temperatures, the respective 2-hydroxy ketone cyanohydrins must be derivatized before analysis. In this study, the products were acetylated with an excess of acetic anhydride and dimethyl aminopyridine (chapter 3.2.12) and the diacetylated products were identified by GC/MS (Appendix 12-13). In this case the completeness of acetylation was not studied, as described for the acetophenone cyanohydrins above. This could lead to underestimation of the conversions of 2-hydroxy ketones.

#### 4.2.2.2 Substrate screening

As shown in Table 2, five different 2-hydroxy ketones were tested as substrates and compounds **1** and **2** yielded higher concentrations of the respective cyanohydrins in the presence of the enzyme compared to the chemical control.

**Table 2: Substrate screening for the synthesis of 2-hydroxy ketone cyanohydrins.**

**Reaction conditions: 400 mM substrate, 1.5 M HCN and 3 mg His<sub>6</sub>-AtHNL were used in micro-aqueous MTBE. The reaction was carried out in a 4 ml glass vial with a small magnetic stirring bar at room temperature. A chemical background reaction was always performed in parallel as a negative control. The products were acetylated as described in chapter 3.2.12 and subsequently analyzed by GC/MS.**

No.	Substrate trivial name and [IUPAC nomenclature]	Structure
1	( <i>R</i> )-Phenylacetylcarbinol (PAC) [( <i>R</i> )-1-hydroxy-1-phenylpropan-2-one]	
2	( <i>S</i> )-Hydroxypropiophenone (HPP) [( <i>S</i> )-2-hydroxy-1-phenylpropan-1-one]	
3	( <i>R</i> )-Hydroxypropiophenone (HPP) [( <i>R</i> )-2-hydroxy-1-phenylpropan-1-one]	
4	Acetoin [3-hydroxybutan-2-one]	
5	Propioin [4-hydroxyhexan-3-one]	

Acetoin **4** and propionin **5**, on the other hand, showed no higher conversion in the presence of enzyme compared to the non-enzymatic control (Appendix 6-7). Interestingly, both the enzymatic and the non-enzymatic reactions gave products with the same low *ee* of about 20 % in all cases (Table 3).

The chiral GC-chromatogram of the (*S*)-HPP cyanohydrin is shown exemplarily in Figure 34. After 24 hours, for *S*-HPP (**2**) a conversion of 30 % and an *ee* of 22 % were measured. Conversions were determined from the depletion of substrate.

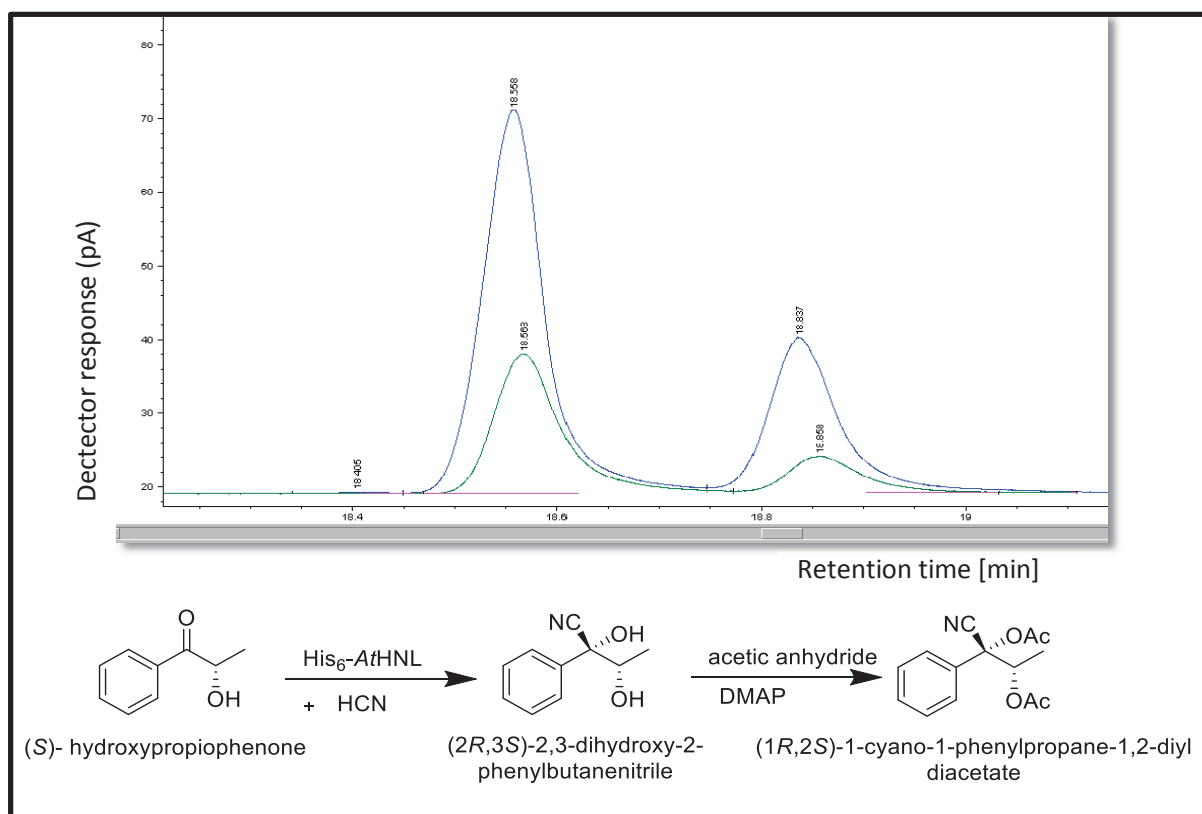


**Figure 29: GC-Chromatogram of diacetylated (*S*)-HPP cyanohydrin**

**Reaction conditions: 400 mM (*S*)-HPP, 1.5 M HCN and 3 mg His<sub>6</sub>-AtHNL were used in micro-aqueous MTBE. The reaction and derivatization was carried out as described in chapter 3.2.12. The enzymatically produced product is showed as a blue line. A chemical background reaction (green line) was always performed in parallel as a negative control.**

Three inactive variants of AtHNL namely S81A, D208N and H236F, each of them containing a mutation from the active site triad, were cloned and overexpressed as described in chapter 3.2.1. Synthesis reactions were again performed with the crude cell extract of the three inactive AtHNL variants, BSA, heat inactivated His<sub>6</sub>-AtHNL, crude cell extract of His<sub>6</sub>-AtHNL and a non-enzymatic chemical control. Surprisingly, all these controls yielded products with an *ee* of 22 %. Similar reactions were performed with (*R*)-PAC (Appendix 9) along with all the same controls.

**Table 3: Hydrocyanation of (*S*)-HPP with various control experiments**

**Experimental conditions: 400 mM (*S*)-HPP resp. (*R*)-PAC, 1.5 M HCN-MTBE (micro-aqueous). For each of the synthesis reactions a negative control without the enzyme was performed in parallel. Catalyst used in each reaction was (from left to right) 3 mg each of His<sub>6</sub>-AtHNL, as well as variants with the following point mutations: S81A, D208N, H236F; 3 mg/ml BSA, and 3 mg His<sub>6</sub>-AtHNL heat inactivated at 100 °C for 20 min. Protein concentrations were determined by Bradford assay. The reaction was allowed to run for 24 hours and conversion was measured by chiral GC (chapter 3.2.6) by depletion of the substrate.**

Substrate		Conversion	<i>ee</i>
<i>(S)</i> -HPP	His <sub>6</sub> -AtHNL	30	22
	S81A	28	22
	D208N	30	22
	H236F	31	22
	BSA	9	22
	Heat inactivated His <sub>6</sub> -AtHNL	10	21
	chemical control	9	23
<i>(R)</i> -PAC	His <sub>6</sub> -AtHNL	20	18
	S81A	18	18
	D208N	18	18
	H236F	20	18
	BSA	10	18
	Heat inactivated His <sub>6</sub> -AtHNL	10	20
	chemical control	10	18

---

In every control experiment (Table 3), the *ee* for the respective diacetylated hydroxyketone cyanohydrine remained constant. However, the presence specifically of the active and inactive *AtHNL* variants resulted in an about 3-fold higher conversion relative to BSA, heat inactivated His<sub>6</sub>-*AtHNL* and the chemical control without any protein. So there is a weak but clear accelerating effect by *AtHNL*, but it is most probably not caused by a specific interaction with the active site. Rather a non-specific protein catalysis, probably on the surface of the enzyme, can explain these results [144, 145]. Such non-specific protein catalysis has also been reported for the formation of olefinic bonds by protein impurities found in porcine pancreas lipase [144]. The authors further reported the ability of BSA to accelerate the transformation of products from a series of aldehydes with active methylene groups as substrate. As the stereoselectivity of all hydrocyanation reactions including the non-enzymatic control, is 20 %, a chiral induction of the neighboring stereo center in the chiral substrate next to the reacting carbonyl group is most likely. The results suggest a direct influence of the correctly folded enzyme surface. In order to evaluate this effect further, the enzyme concentration was increased. As demonstrated in Figure 30, a proportional acceleration of the hydrocyanation reaction was observed with increasing enzyme concentration, whereas the *ee* remained constant.

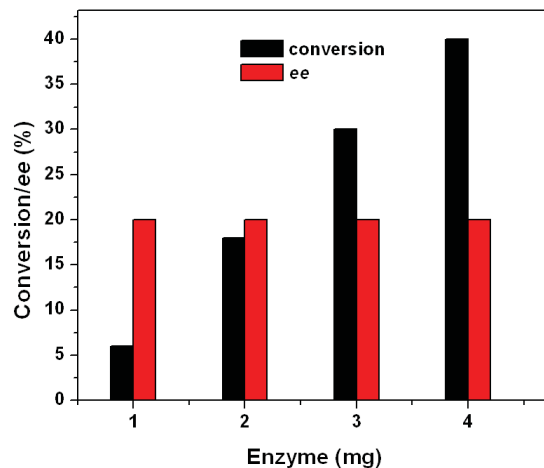


**Figure 30: Effect of His-AtHNL concentration on the hydrocyanation and ee of (*S*)-HPP**

Reaction conditions: 1.5 M HCN-MTBE, 400 mM S-HPP, 1 mg, 2 mg and 4 mg AtHNL (lyophilized) were added to three different synthesis reactions respectively. Samples were taken at t=0 and 24 h. 50  $\mu$ l of sample at each time point was derivatized in 50  $\mu$ l acetic anhydride, 50  $\mu$ l pyridine, 750  $\mu$ l of dichloromethane, and subsequently was incubated for 3 h at RT. Conversions and ee were measured by chiral GC (chapter 3.2.23.1).

In order analyze a potential enzyme surface-induced reaction acceleration further, the respective distribution of charges and hydrophobic sites on the enzyme surface were calculated taking a pH of 5.5 (from citrate buffer used to saturate the MTBE, chapter 3.2.10) into account. These studies were performed by Dr. Marco Bocola from RWTH Aachen University. The results are presented in the following Figure 31.

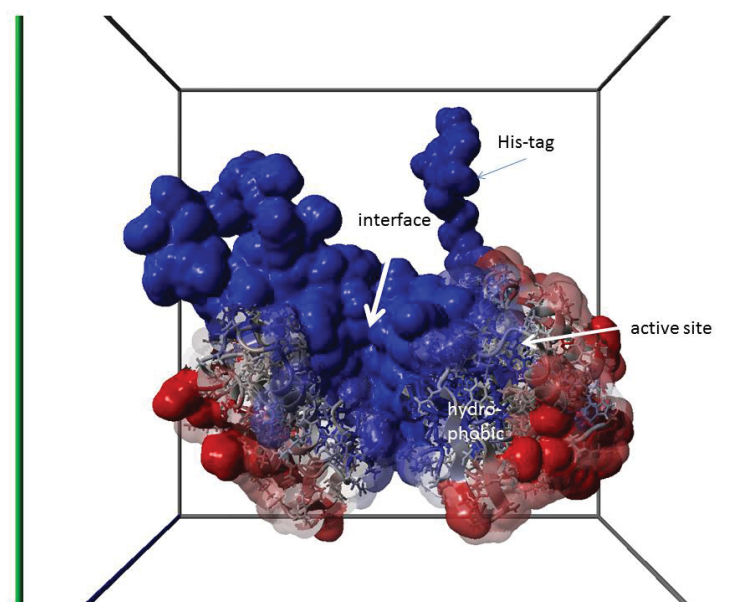


**Figure 31: The electrostatic surface potential (ESP) of the His<sub>6</sub>-AtHNL dimer**

**Modelling was performed based on the X-ray structure of the wt enzyme (pdb: 3DQZ). The hexahistidine tag plus linker was modelled using YASARA [146]. ESP was calculated using AMBER03 [147] partial charges of amino acids at pH 5.5 [148] using particle mesh ewald [149] electrostatics calculations. Positive (blue) and negatively charged (red) residues and surface areas are marked respectively. Non-changed (hydrophobic) residues and areas are shown in grey.**

The distribution of surface charges and hydrophobic patches demonstrates that a large area of the enzyme surface is positively charged, even at pH 5.5. The blue marked area contains several histidine residues (pKa ca. 6), which are predominantly protonated at pH 5.5 and thus either could give rise to an accumulation of negatively charged cyanide ions or, those histidine residues that are not protonated (pka of His-tag was calculated as 5.5) could enable base-catalysis of the cyanohydrin formation. The same could also occur with deprotonated acidic side chains in the red marked areas (Figure 31). Therefore, a base-catalyzed hydrocyanation on the protein surface is likely. Additionally, there is a hydrophobic area close to the large histidine-rich (blue) and the negatively charged (red) area, which could be responsible for the preferred acceleration observed with aromatic 2-hydroxy ketones. In that case one can assume that the aromatic substrates are enriched at this hydrophobic patch, which would increase the probability to form a reactive

---

complex with cyanide. Earlier studies have reported similar catalytic activity on binding of substrate to hydrophobic patches on the surface of BSA [150–152].

As already mentioned above, the protein-accelerating effect was only observed with (*R*)-PAC and (*S*)-HPP, but not with (*R*)-HPP (Appendix 8). The reasons for the differentiation between the two HPP-enantiomers could be explained by different stabilities of the diastereomeric complexes the respective HPP-enantiomers forms with the chiral enzyme surface, although a defined binding region could not be predicted with the applied methods. A similar finding on the HNL from *Prunus amygdalus* and *Manihot esculenta* showed that the addition of imine to a cyanide was not active site catalyzed [153] in contrast to what was reported earlier [154].

The authors showed with docking simulations that the substrate ((*R*) imine and (*S*) imine) did not even fit into the active site of the enzyme and hence these results also hint to a reaction where the active site of enzyme was not involved. Such non-enzymatic catalyzed reactions were also reported by the lipase from *Candida antartica* [155]. Busto et. al. described that the protein mediated nitroaldol addition of aldehydes to nitromethane was also possible with BSA with moderate to high yields [156].

### 4.3 Biotransformations in flow reactors for continuous synthesis of cyanohydrins

A further goal of this project was to transfer the synthesis of cyanohydrins from a batch to a continuous system. Batch processes suffer from some limitations, especially the scale up would mean handling of a large amount of HCN, which arises safety concern (chapter 1.5.5.2). One of the advantages of flow chemistry is to perform reactions involving toxic intermediates. An additional advantage it offers is the immediate modification of unstable products, which is specifically promising for ketone cyanohydrins.

---

In this chapter, the main process parameters were identified and optimized for the multistep chemoenzymatic cascade for the biocatalytic synthesis of O-acylated aldehyde cyanohydrins.

In order to achieve this, it was essential to compartmentalize the reactions and optimize each step separately. The set-up was designed and optimized for the synthesis of (*R*)-mandelonitrile as an example and subsequently applied to further substrates.

The schematic setup is shown in Figure 32. The first step involved the continuous release of HCN, which was used by the second step for the *At*HNL-mediated synthesis of cyanohydrins. The third step comprised of an inline acetylation of the cyanohydrin formed.



**Figure 32: Schematic representation of the 3-step chemoenzymatic cascade**

#### 4.3.1 Step 1- Lipase mediated liberation of HCN

The HNL mediated hydrocyanation requires a cyanide source and in traditional batch reactions described so far, pure HCN was synthesized by the acidification of cyanide salts, which nevertheless renders the system dangerous and imposes high exposure risk. There have been other HCN surrogates previously used for such reactions (chapter 1.5.5).

One optimal alternative to generate HCN was by the hydrolysis of ethyl cyanofornate (ECF). Purkarthofer et al. described the hydrolysis of ECF in micro-aqueous organic solvent using *Pa*HNL immobilized on Celite, which however led only to partial hydrolysis [110]. As an attempt to achieve faster and almost complete hydrolysis, different lipases were screened and tested for the same in a cooperation project with the University of Applied Science, Aachen, Germany in the context of this thesis.

Among these, the lipase from *Candida antartica* (CalB), commercial sold as Novozyme 435 was chosen and optimized because of its low cost, easy availability and robust nature [157]. In an optimized batch reaction 40 mg CalB was sufficient to convert 1.5 M ECF in 2 h at RT.

In order to test for the recyclability, 40 mg of CalB was sealed in a “tea bag” and placed in a 4 ml glass vial followed by the addition of 1 M ECF in 1 ml micro-aqueous MTBE. Four different cycles of the hydrolysis reaction were performed with the same “tea bag” and we see from Figure 33 that the conversion continuously decreased with every cycle and on reaching the fourth cycle, 30 % loss of activity was detected.

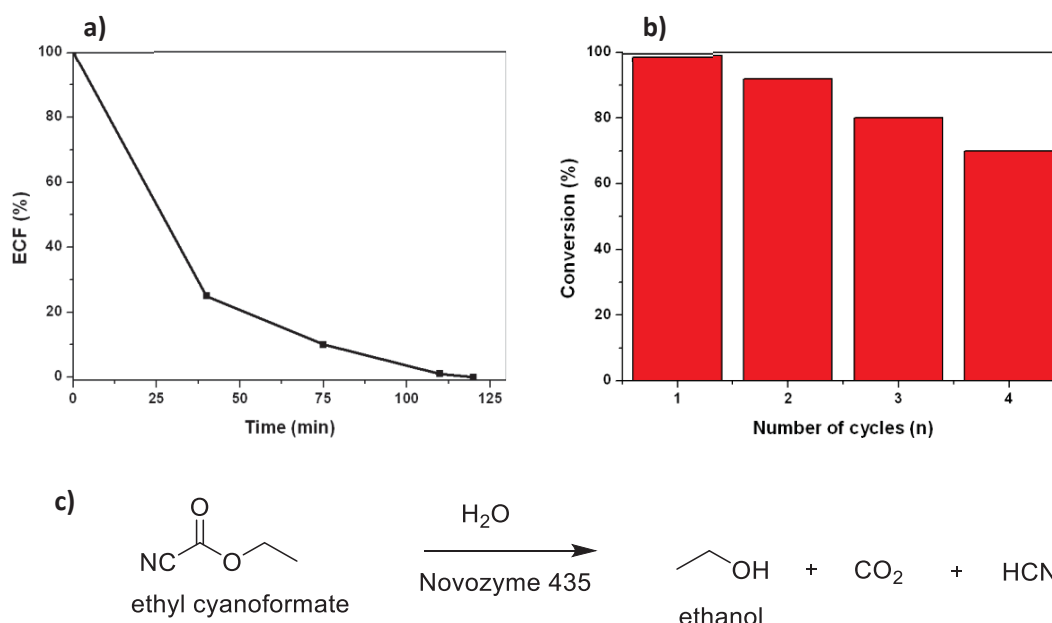


**Figure 33:** a) Generation of HCN by hydrolysis of ECF; b) Recyclability of CalB in batch mode; c) Reaction scheme for the hydrolysis of ECF

**Reaction conditions:** 1 M ECF in MTBE and 40 mg Novozyme 435 (CalB) were stirred for 2 h at RT. The production of HCN was measured by analyzing the depletion of ECF using GC (chapter 3.2.23.1).

To transfer this reaction to a continuous system, a packed-bed reactor (Figure 34) was set up (chapter 3.2.15).

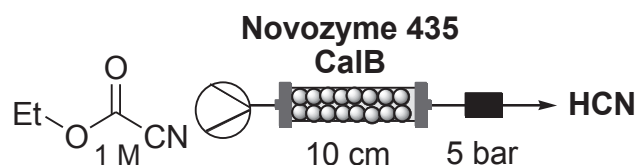


**Figure 34:** Schematic representation of hydrolysis of ECF in a continuous flow set-up.

**Experimental conditions:** 1 M ECF in micro-aqueous MTBE was pumped through a 10 cm long PBR filled with 277 mg CalB (Novozyme 435) with a flowrate of 0.04 ml/min. Conversion was calculated by measuring the depletion of ECF on GC (chapter 3.2.23.1).

The reaction was optimized with respect to various parameters such as column length, catalyst load, residence time and substrate concentration. The results of the optimization are shown in Table 4:

**Table 4: Optimization of hydrolysis of ECF**

Entry	Flow rate (ml/min)	CalB (mg)	Conv. (%)
1	0.15	34	55 <sup>a</sup>
2	0.05	34	56 <sup>a</sup>
3	0.04	277	84 <sup>b</sup>
4	0.04	277	95 <sup>c</sup>
5	0.04	277	97 <sup>d</sup>

<sup>a</sup>A mixture of CalB and Celite has been used to fill the reactor. <sup>b</sup>Dry MTBE has been used. <sup>c</sup>A mixture of MTBE / EtOH (3:1) has been used. <sup>d</sup>Micro-aqueous MTBE has been used.

A good conversion was observed when the PBR was filled with 277 mg CalB and a, ECF concentration of 1 M in dry MTBE was maintained. On adding a small amount of polar solvent like ethanol, almost complete hydrolysis could be achieved with a residence time of 17.5 minutes. The robustness of the system could be greatly improved by switching to micro-aqueous MTBE, where 99 % conversion was achieved. Although the conversions in batch and flow are similar, it

---

is noteworthy that in a continuous system it is more than 5 times faster than in batch. In a batch system, 1 mmol ECF is hydrolyzed to HCN in 90 minutes with 40 mg CalB, whereas 6.6 mmol of the same is hydrolyzed in the same time frame in a continuous system using 277 mg CalB. Therefore 1 mmol requires 17.5 minutes for conversion.

### 4.3.2 Stability of the system

Stability is defined as the time span where the system can be operated without significant loss of activity. This is also termed as “loading” in flow technology. In the optimized setup 1 M ECF was pumped through the reactor for 8 hours and the conversion was monitored via GC at regular time points (Figure 35).

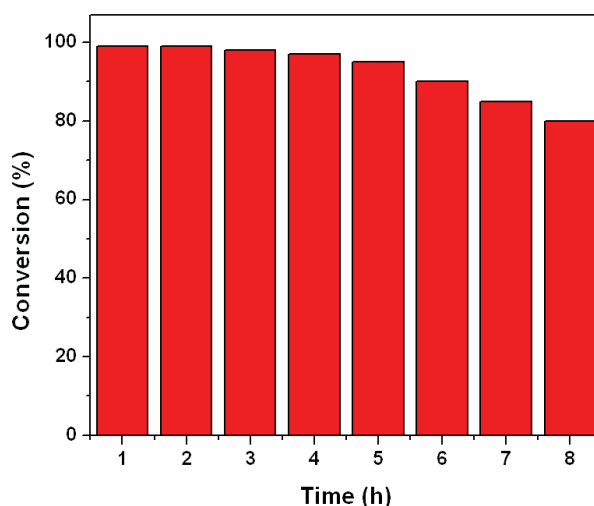


**Figure 35: CalB-catalyzed hydrolysis of ECF in a continuous flow set-up**

**Experimental conditions: 1 M ECF in micro-aqueous MTBE was continuously pumped through a 10 cm PBR filled with 277 mg CalB (Novozyme 435) at 0.04 ml/min. The production of HCN was measured by analyzing the depletion of ECF using GC (chapter 3.2.23.1).**

The process demonstrated a high stability with only a 20 % decrease in conversion after 8 hours. In order to compare the setup with that of a batch, the total product yield over 90 minutes was calculated.

---

In a typical 1 ml batch setup with 1 M ECF and 40 mg CalB (immobilized), 1 mmol of HCN could be produced in 1.5 hours (Figure 33). However, in a flow process 3.6 mmol of product could be achieved in the same time frame. However, if the enzyme specific conversion is calculated, the batch process showed with 0.025 mol HCN/mg CalB the double productivity compared to the flow process (0.012 mol HCN/mg CalB).

The reasons for this is most probably that the enzyme was applied in excess in the flow process and the substrate could have been pumped faster to make full use of the enzyme. From the optimization results (Table 4) we see that the enzyme load was increased more than 7 times, however the flowrate was only decreased by 20 %. Therefore, it is possible that a part of the enzyme was not fully used thereby exhibiting a low specific conversion.

Another explanation for this could be that under these flow conditions, the CalB is washed off from the carrier which is an acrylic resin. Therefore, there is still a lot of optimization potential for the flow process based generation of HCN.

#### 4.3.3 Step 2: *At*HNL-catalyzed continuous synthesis of (*R*)-mandelonitrile

The second step of the cascade was set up with His<sub>6</sub>-*At*HNL to utilize the HCN generated in the first step along with benzaldehyde to produce (*R*)-mandelonitrile (Figure 36). In order to form a packed bed reactor, Celite-His<sub>6</sub>-*At*HNL was used which was already success fully used in batch with excellent conversion and *ee* (chapter 4.1.1.2).

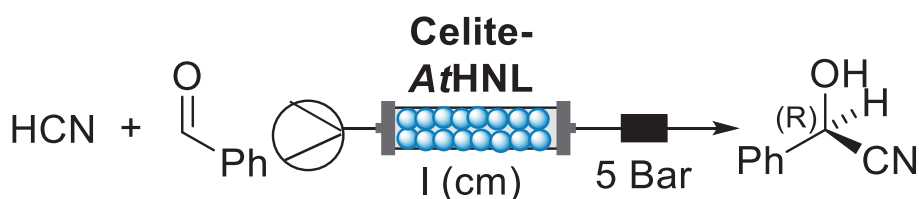


Figure 36: Schematic representation of Celite-His<sub>6</sub>-*At*HNL mediated synthesis of (*R*)-mandelonitrile

Experimental details: A mixture of 500 mM benzaldehyde and 1 M HCN in micro-aqueous MTBE was continuously flown through a 5 cm PBR filled with 100 mg Celite-His<sub>6</sub>-*At*HNL at 0.04 ml/min. Conversions and *ee* were analyzed using GC (chapter 3.2.23.1).

To optimize the setup, the HCN used was first synthesized in batch by hydrolysis of ECF (chapter 3.2.10a). The PBR was set up as described in chapter 3.2.17 and was filled with Celite-His<sub>6</sub>-AtHNL. The set-up was optimized by varying the length of the bed and the composition of the biocatalyst in the PBR. The results are presented in Table 5.

**Table 5: Optimization of the reaction parameters for the Celite-His<sub>6</sub>-AtHNL catalyzed synthesis of (*R*)-mandelonitrile in the flow set-up.**

Entry	Reactor length l (cm)	Flow rate (ml/min)	Celite-His <sub>6</sub> -AtHNL (mg)	Conv. (%)	ee (%)
1	2.5	0.02	50	33	93
2	2.5	0.04	50	20	93
3	7.0	0.04	50 <sup>a</sup>	74	88
4	7.0	0.04	100	85	96

<sup>a</sup>A mixture of Celite-His<sub>6</sub>-AtHNL (50 mg) and pure Celite (50 mg) was used to fill the reactor

From the optimization (Table 5) it is clear that on increasing the contact time between the biocatalyst and the substrates, a good *ee* and a decent conversion was achieved. However, on increasing the biocatalyst/substrate ratio, a positive effect on the conversion and *ee* was seen. For subsequent synthesis reactions in the cascade, a catalyst filling of 100 mg Celite-His<sub>6</sub>-AtHNL (containing 25 mg of pure His<sub>6</sub>-AtHNL) was chosen.

#### 4.3.4 Two-step enzymatic cascade

A fast and robust lipase mediated process for the liberation of HCN was combined with the His<sub>6</sub>-AtHNL-catalyzed synthesis of (*R*)-mandelonitrile from benzaldehyde. The two steps combined as a sequential cascade is schematically represented in Figure 37.

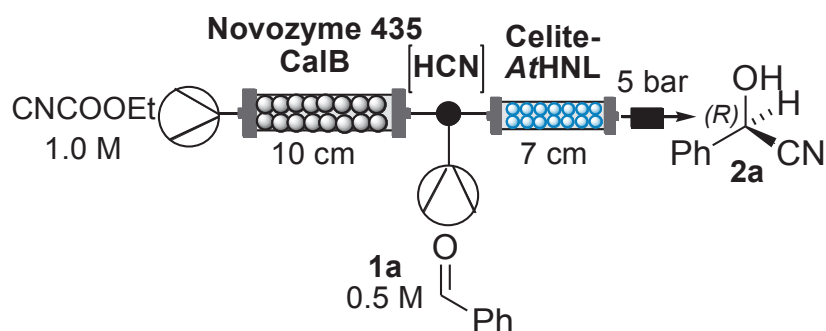


Figure 37: Schematic representation of the 2-step enzymatic cascade for the synthesis of (*R*)-mandelonitrile.

Experimental conditions: 1 M ECF solution in micro-aqueous MTBE was pumped through a PBR of length 10 cm packed with 277 mg CalB. The first output, consisting of 1 M HCN, was mixed with 0.5 M benzaldehyde via a T-shaped mixer. The resulting mixture was passed through a PBR of 7 cm packed with 100 mg of Celite-AtHNL equipped with a back pressure regulator (5 bar).

Using benzaldehyde for the synthesis of (*R*)-mandelonitrile as a proof of principle, excellent conversion (97 %) and *ee* (99 %) were achieved.

#### 4.3.5 Evaluation of whole cell biocatalysis in flow

Although an excellent conversion and *ee* was achieved with the 2-step enzymatic cascade with CalB and Celite-His<sub>6</sub>-AtHNL, the process still is limited by the isolation and purification of the enzyme, which is expensive and time consuming. Therefore, the application of recombinant *E. coli* cells as an alternative biocatalyst is appealing as enzyme purification can be circumvented. The use of recombinant *E. coli* cells containing His<sub>6</sub>-AtHNL for the synthesis of chiral cyanohydrins in micro-aqueous MTBE has been already reported [118]. Lyophilized *E. coli* cells proved to be stable in MTBE for 7 days without loss of enantioselectivity. Excellent conversion and *ee* of 98 % and 99 % respectively were achieved with this setup (Figure 38) for the synthesis of (*R*)-mandelonitrile.

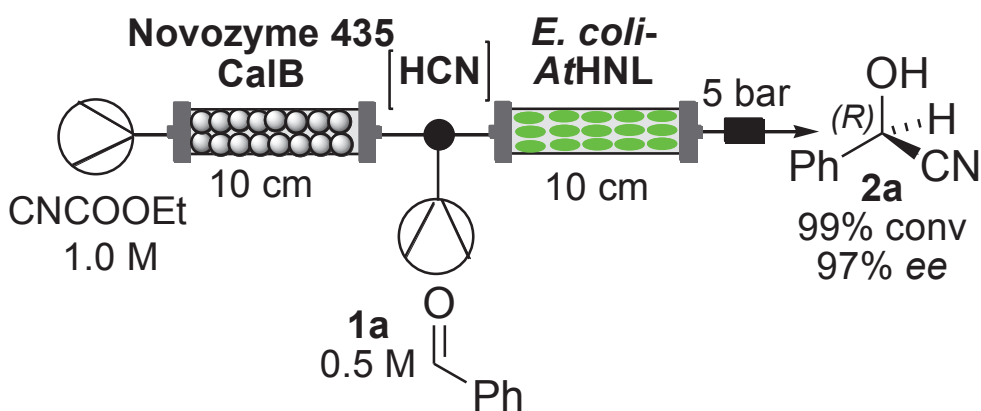


**Figure 38: Schematic presentation of the 2-step cascade**

**Experimental conditions:** 1 M ECF was pumped through a 10 cm column packed with 277 mg CalB at 0.04 ml/min. The outlet of the first reactor was mixed with 0.5 M of benzaldehyde pumped in by a T-shaped mixer. In the second reactor, 250 mg lyophilized *E. coli* cells were packed into a 10 cm column sealed by a nylon mesh (pore size 40  $\mu$ m). The whole system was kept at a pressure of 5 bar. The (*R*)-mandelonitrile formed in the product stream was collected at regular intervals and acetylated offline before analyzing on GC for conversion and *ee*.

On comparing this setup to the previous scheme (Figure 37) with Celite-His<sub>6</sub>-AtHNL, it is interesting to note that 250 mg whole cells contain almost the same amount (20.9 mg) used with Celite-His<sub>6</sub>-AtHNL (25 mg, Figure 37). Thus, enzyme purification and immobilization did not show any advantage with respect to yield and optical purity of the product. Therefore the whole cell system is a good alternative here.

#### 4.3.6 Stability of the two-step enzyme cascade

The two-step enzymatic cascade was set up and optimized with immobilized enzyme and whole cells for the synthesis of (*R*)-mandelonitrile with excellent conversion and *ee*. The stability of the system was then evaluated to determine how long the system could be run with high conversion and *ee*. This is termed as “loading” and is a measure for the total turnover number (the total number of moles that can be converted to product without deactivation of the catalyst). For the lipase catalyzed reaction, a total turnover number in case of the batch and continuous system is

1 mmol and 3.6 mmol, respectively, in 2 h. The two-step cascade was set up with a benzaldehyde concentration of 1 M in micro-aqueous MTBE and the reaction was allowed to proceed continuously under the previously optimized conditions. The product (*R*)-mandelonitrile was collected in fractions of 0.5 ml each and conversion and *ee* were analyzed in regular time intervals via chiral GC (chapter 3.2.23.1). The results are shown in Figure 39.

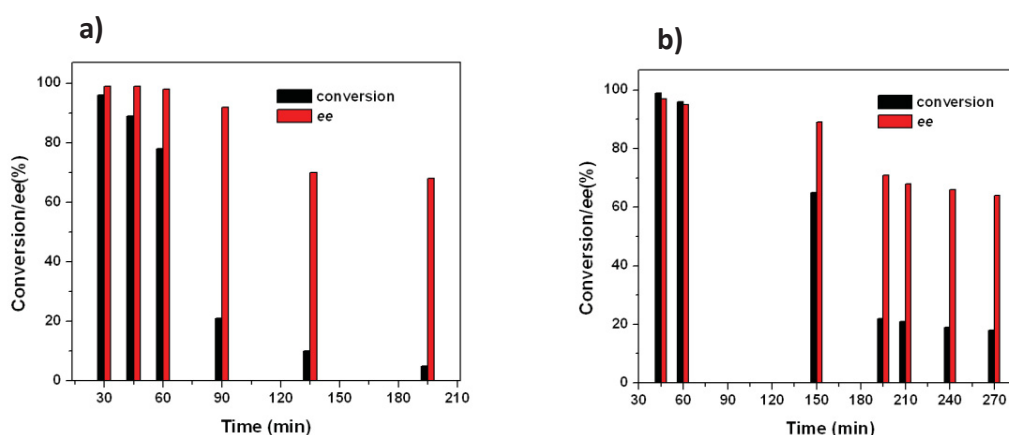


**Figure 39: Conversion and *ee* of the hydrocyanation of benzaldehyde to (*R*)-mandelonitrile in the two-step cascade shown in Figs. 37 and 38 catalyzed by a) Celite-His<sub>6</sub>-AtHNL; b) *E. coli*-His<sub>6</sub>-AtHNL.**

**Experimental conditions:** A 2-step cascade was set up with a) 100 mg Celite-His<sub>6</sub>-AtHNL in a 5 cm PBR (chapter 3.2.18) and b) 250 mg *E. coli*-His<sub>6</sub>-AtHNL in a 10 cm PBR (chapter 3.2.19). The reaction was allowed to proceed continuously and conversions/*ee* were analyzed by GC.

In case of the set-up with Celite-His<sub>6</sub>-AtHNL (Figure 39a), a rapid decrease of the conversion after one hour was observed. The *ee*, however, remained high for 1.5 hours and then slowly decreased towards 70 % in 3 hours. A control experiment was performed with a column filled with Celite (without the enzyme). The control, however, showed only traces of the chemical reaction (less than 2 %). The results can be best explained by leaching out of the active enzyme from the PBR, since the enzyme is weakly bound on the surface of Celite. However, in the batch reaction no leakage of active catalyst into the reaction system was observed [120]. The continuous decrease of conversion can be explained by two effects: firstly, highly concentrated substrate and organic solvent flow continuously through the Celite-enzyme bed thereby making

---

the enzyme prone to unbind from the surface; secondly, the entire system is kept under a pressure of 5 bar which could further facilitate the leaching out of the enzyme from the surface of Celite. Similar stability tests were also performed with lyophilized whole *E. coli* cells containing His<sub>6</sub>-AtHNL (Figure 39b).

The results show a difference in inactivation behavior of Celite-His<sub>6</sub>-AtHNL and enzyme in whole cells. In both reactions the *ee* decreased to 70 % concomitant with a decrease in conversion. However, more activity was retained in case of the whole cell catalyst. Conversion dropped to 3 % after 3 h with Celite-His<sub>6</sub>-AtHNL, whereas with whole cells the conversion dropped rapidly in the first 3 h and then remained steady at 20 % up to 4.5 hours. It is interesting to note that independent of the residual conversion the final product *ee* was 70 %. The decay in *ee* might be due to the enzyme catalyzed cleavage of the (*R*)-product, thereby accumulating the (*S*)-enantiomer.

These results demonstrate that the biocatalyst in whole cells is more stable than the Celite-immobilized enzyme. The total turnover number (TTN) for the flow process with Celite-His<sub>6</sub>-AtHNL is 0.02 mmol per mg enzyme, whereas the TTN for whole cells corresponds to 0.06 mmol per mg enzyme. Therefore, the cells gave a 3 times higher yield than the immobilized enzyme, thereby demonstrating a higher productivity and stability.

#### 4.3.7 Step 3: Inline acetylation as a third step of the cascade

Cyanohydrins are generally unstable at room temperature and ketone cyanohydrins, as tertiary alcohols, are generally less stable than aldehyde cyanohydrins (secondary alcohols). There are many ways to modify a cyanohydrin and in previous studies they have been acetylated before measuring on GC (chapter 1.5.5). In typical batch reactions, acetylation of aldehyde cyanohydrins takes 3-4 hours at room temperature [120].

Since some cyanohydrins degrade faster than the others, an immediate modification is helpful to prevent the degradation of the product back to the starting compounds. Therefore an acetylation module was built in-line to modify the cyanohydrin with an excess of acetic anhydride and

pyridine such that they directly meet the highly concentrated product stream. When highly concentrated reactants are rapidly mixed the reaction rate is much faster compared to a diluted approach, since the probability of a productive interaction increases.

The modification was complete in 20 minutes, which was the time required for the reactants to pass through the 2 ml coil under the flow conditions and the product could be directly analyzed on the GC. The module was established as described in chapter 3.2.20 and it was tested with the synthesis of protected (*R*)-mandelonitrile as an example. The modification in flow takes 20 minutes which was more than 12 times faster than in batch which takes 3 hours, thereby rendering the system fast, efficient and robust.

The three-step cascade was setup with two enzyme-catalyzed steps and a chemical modification step, respectively, according to Figure 40.

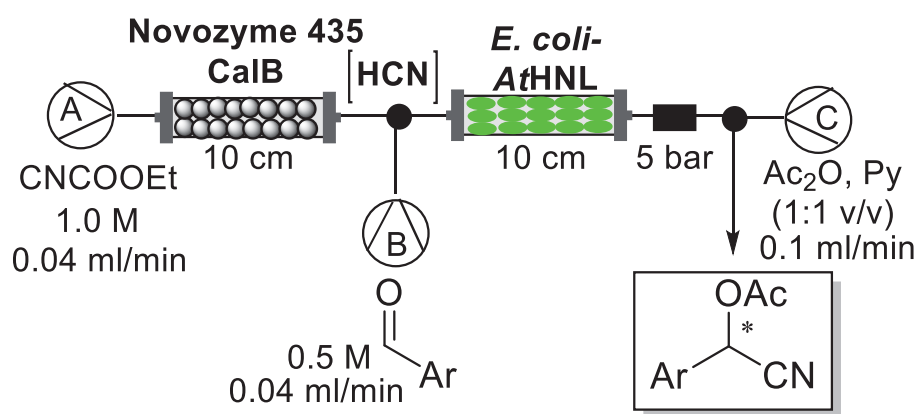


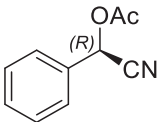
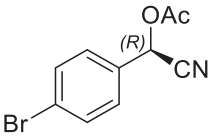
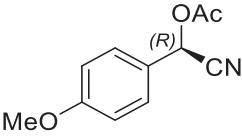
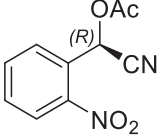
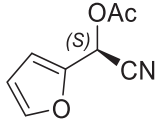
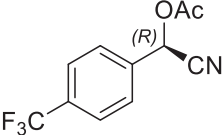
**Figure 40: Schematic presentation of the 3-step cascade**

**Experimental conditions:** 1 M ECF was pumped through a 10 cm column packed with 277 mg CalB at 0.04 ml/min. The outlet of the first reactor was mixed with 0.5 M of benzaldehyde pumped in by a T-shaped mixer. In the second reactor, 250 mg lyophilized *E. coli*-His<sub>6</sub>-AtHNL cells were packed into a 10 cm column sealed by a nylon mesh (pore size 40 μm). The whole system was kept at a pressure of 5 bar. The outflow was mixed with a mixture of pyridine/acetic anhydride (1:1, V/V) pumped by a compact HPLC pump and the resulting solution was passed through a PTFE coil (2 ml).

Pumps A and B were used to flow in 1 M ECF and 0.5 M benzaldehyde, respectively. Two PBRs were installed in omnifit columns with 277 mg CalB (Novozyme 435) and 250 mg *E. coli*\_BL21-His<sub>6</sub>-AtHNL respectively. Pump C was connected to a mixture of acetic anhydride and pyridine via a 2 ml PTFE coil. The product was finally collected in a fraction collector of 0.5 ml each and subsequently analyzed. As a proof of principle, synthesis of O-acetyl-(*R*)-mandelonitrile was achieved with excellent conversion and *ee* of 98 % and 99 %, respectively.

**Table 6: Synthesis of different cyanohydrins in the optimized three-step chemoenzymatic cascade**

**Experimental details: Substrates 1-6 were screened for synthesis of cyanohydrin using the 2-step chemoenzymatic setup as described in Figure 40. Conversions were calculated by depletion of substrate (benzaldehyde and its derivatives)**

No.	Substrate	Product	Conversion (%)	<i>ee</i> (%)
1	benzaldehyde		99	98
2	4-bromobenzaldehyde		99	95
3	4-methoxybenzaldehyde		78	94
4	2-nitrobenzaldehyde		99	70
5	furfural		86	88
6	4-trifluoromethylbenzaldehyde		75	85

---

Subsequently, further substrates were transformed using the optimized 3-step set-up for the synthesis of O-acetylcyanohydrins

(Table 6). Conversions were measured by  $^1\text{H-NMR}$ . High conversions and *ee* were achieved with both electron rich and electron deficit substituents. Excellent to good *ee* were achieved for most of the products except the *ortho*-substituted substrate (**4**) which gave a lower *ee* of 70 %.

---

# Chapter 5

## **SUMMARY**

---

## Summary

In summary the potential of the AtHNL was evaluated with respect to the following regards:

### a) Characterization of AtHNL with a hexahistidine tag (His<sub>6</sub>-AtHNL)

A new His-tagged variant was comparatively characterized to wt-AtHNL with respect to its pH/temperature optima and stability [142]. The His<sub>6</sub>-AtHNL demonstrated similar pH- and temperature optima as the wt-AtHNL, demonstrating that the presence of the His-tag at the N-terminus did not have any influence in the measured range. The addition of the tag not only made the purification protocol fast and efficient, also a 2.2 fold higher expression level of the enzyme was shown compared to its wild type counterpart. Additionally, His<sub>6</sub>-AtHNL was immobilized on Celite and excellent conversion (98 %) and *ee* (98 %) were achieved for the synthesis of (*R*)-mandelonitrile. Celite-His<sub>6</sub>-AtHNL was recyclable up to 4 times and demonstrated a moderate stability in MTBE of seven days with a loss of 10 % in enantioselectivity.

Further, whole *E.coli*\_BL21-His<sub>6</sub>-AtHNL cells were evaluated in micro-aqueous MTBE and exhibited excellent conversion and *ee* for the synthesis of (*R*)-mandelonitrile. Not only a very good recyclability of 4 times was achieved with the whole cells, the whole cell catalyst was also stable for at least 15 days in MTBE without significant loss of activity or enantioselectivity.

### b) aromatic ketones as substrates

Two simple aromatic ketones (acetophenone, 2-fluoroacetophenone) were evaluated as substrates for His<sub>6</sub>-AtHNL in micro-aqueous MTBE. Since the products were not stable at GC temperatures, derivatization of the ketone cyanohydrins was necessary. Acetylation with two different bases and silylation were evaluated for the derivatization of the product. Among them, complete derivatization could be achieved by the silylation of cyanohydrins with BSTFA, although it requires 12-20 hours of incubation time at RT.

---

With both aromatic ketones a maximum conversion of 40 % and 48 % was achieved, respectively, yielding product concentrations of 160-190 mM. The moderate conversions as compared to aldehydes are attributed to the intrinsic bulky nature of ketones, thermodynamic limitation of the reaction and instability of the products. However, these conversions in micro-aqueous MTBE are almost 100 % higher compared to previous studies using other HNLs in aqueous-organic two-phase systems [81].

An interesting behavior of *ee* was observed by following the reaction over several days (Figure 27) where the *ee* remained high for the first 8 hours and then decreased rapidly. This behavior was explained by enzyme-catalyzed product racemization where the enzyme also catalyzes the reverse reaction (cleavage of cyanohydrin) towards the side of the reactants. As a consequence biocatalytic reactions towards ketone cyanohydrins should be carefully controlled and stopped as soon as the equilibrium conversion is reached in order not to impair the product *ee*. Currently, it is not known, whether this effect occurs also with other HNLs as conversion is generally not followed over time and *ee* is only determined when the reaction was stopped. Thus, reported low *ee*-values for ketone cyanohydrins could result from this effect [81, 84, 123].

The evaluation of substrates was further extended to 2-hydroxy ketones. Various 2-hydroxy ketones were screened (Table 2) with His<sub>6</sub>-AtHNL and among them (*R*)-phenylacetylcarbinol (*R*-PAC) and (*S*)-hydroxypropiophenone (*S*-HPP) were studied in detail, as both showed an enzyme-accelerated conversion to the respective cyanhydrine relative to the chemical control.

(*R*)-PAC and (*S*)-HPP were converted to the respective O-acetylated cyanohydrines with 20 % and 30 %, respectively, which was confirmed by mass spectrometric analysis. For both cyanohydrines *ee*-values of 18-22 % were obtained in presence of the enzyme but also with the chemical control. Further control experiments were performed with three inactive variants of AtHNL. His<sub>6</sub>-AtHNL and the inactive active-site variants all showed a weak but clear accelerating of the hydrocyanation, which is most probably not caused by a specific interaction with the active site. Besides, heat-inactivated His<sub>6</sub>-AtHNL and also BSA did not show this accelerating effect.

---

The results suggest a direct influence of the correctly folded enzyme surface [150, 151]. Increasing the enzyme concentration demonstrated a proportional acceleration of the hydrocyanation reaction whereas the *ee* remained constant (Figure 30).

Additional studies were performed to analyze the potential enzyme surface-induced reaction acceleration and subsequently the respective distribution of charges and hydrophobic sites on the enzyme surface were calculated (Figure 31). These findings allow the hypothesis that the hydrophobic substrates could be enriched at a hydrophobic patch close to a basic histidine-rich area, where cyanide could be accumulated. Both, non-protonated histidine residues as well as deprotonated acidic groups could assist in base-catalyzed hydrocyanation.

### c) Biotransformation in flow reactors for the continuous synthesis of cyanohydrins

A three-step chemoenzymatic cascade was developed and optimized for the synthesis of protected *O*-acetylcyanohydrins cyanohydrins. Each step of the cascade was optimized separately and subsequently they were combined and optimized for the synthesis of (*R*)-mandelonitrile as an example. The set-up was then employed for the screening of various aldehyde substrates towards the synthesis of their respective cyanohydrins.

A summary of each of the steps is described below:

As the **first step**, a safer enzymatic method for the liberation of HCN was evaluated with the lipase catalyzed hydrolysis of ECF. Various lipases were screened for the hydrolysis and among them, the commercially available CalB, Novozyme 435 was chosen because of its robust nature and ease of availability [157]. This process was transferred to a continuous mode by setting up a packed bed column reactor (PBR) with Novozyme 435. Starting from 1 M ECF solution in micro-aqueous MTBE a conversion of 99 % was obtained with the optimized set-up (chapter 4.3.1). The continuous system demonstrated a high stability over 8 hours with only 10 % decrease in conversion.

The **second step** involved the His<sub>6</sub>-AtHNL catalyzed synthesis of (*R*)-mandelonitrile. AtHNL was immobilized on Celite and packed into a second column reactor. A pre-mixed solution of 1 M HCN and 0.5 M benzaldehyde in micro-aqueous MTBE was pumped through the column. Product was collected in fractions and analyzed on GC for the formation of (*R*)-mandelonitrile. The set-up was optimized by varying the enzyme load and the flow rate. Excellent conversion and *ee* of 98 % and 95 %, respectively, were achieved with the optimized set-up. Compared to the Celite-immobilisate, whole cell biocatalysis using the respective recombinant *E. coli* cells worked even better. The lyophilized cells could easily be packed into the PBR and high conversion and *ee* were achieved even with the same enzyme load compared to Celite-His<sub>6</sub>-AtHNL. Due to the immobilization of the enzyme inside the cells, the half-life of the whole cell system was almost two times higher (chapter 4.3.6).

The **third step** involved the inline acetylation of the (*R*)-mandelonitrile and further aromatic and heteroaromatic cyanohydrins produced in the second step. A third pump was connected to a mixture of acetic anhydride and pyridine via a coil of 2 ml. A complete modification was observed in 20 minutes which was multiple folds faster than the modification in batch, which took up to 3-4 hours at RT.

All the three steps of the cascade were combined and three different pumps were used for the injection of ECF, the (hetero)aromatic aldehyde and the modifying agents respectively (Figure 41).

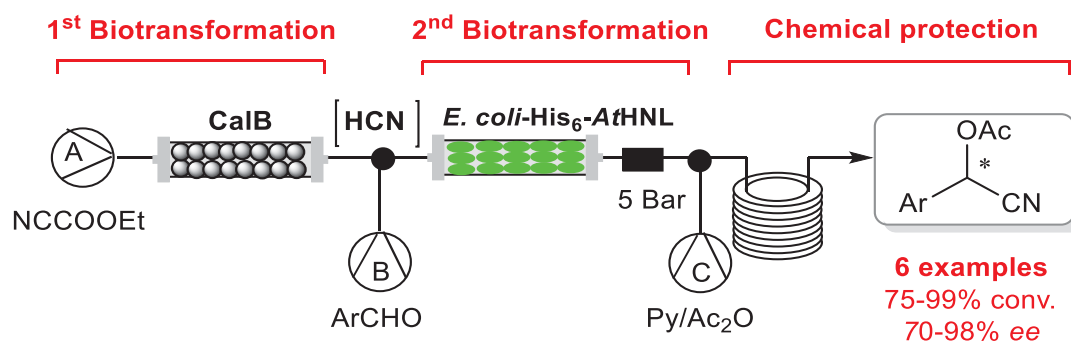


**Figure 41:** Schematic representation of the 3-step chemoenzymatic cascade with lipase, *E.coli*-His<sub>6</sub>-AtHNL and a chemical modification are connected sequentially



# Chapter 6

## **OUTLOOK AND FUTURE PERSPECTIVE**

---

## Outlook

In this thesis, the potential of His<sub>6</sub>-AtHNL has been explored with respect to evaluation of ketones and 2-hydroxy ketones as substrates in a micro-aqueous reaction system and the set-up of a continuous biocatalytic process using the flow-chemistry approach. The reactions can be further improved by multiple ways, for e.g. rational protein engineering to modify the active site of the enzyme active site so as to fit in the desired substrate and product, reaction/solvent engineering that could shift the thermodynamic equilibrium, etc.

The installation of modular biocatalysis can render a process robust, stable and efficient. Flow technology has been used by chemists since decades as a powerful tool for the automated synthesis of compounds, natural compounds etc. It offers advantages of scale up, automation, easier process control, capturing toxic intermediates, etc. Despite its potential and advantages, only a few examples of biocatalysis in flow devices have been reported so far.

In this project this gap was filled by harnessing the potential of both tools: biocatalysis and flow technology. By extending the application of flow technology to realize a multistep chemo-enzymatic cascade, excellent conversion and *ee* was achieved for the synthesis of *O*-acetylcyanohydrins from aromatic and heteroaromatic aldehydes. The elegance of the process lies in the application of whole cells in such flow reactors which also allows circumventing the effort and costs for enzyme production, purification and immobilization, although stability issues (enzyme leakage) have to be addressed in future studies, e.g. by evaluating other immobilization techniques which offer stronger binding of the enzyme onto the carrier. The set-up of such a multistep chemo-enzymatic reactor has set an example and opened multiple doors for new biotransformations in flow technology.

The current set-up built in this project exhibits high potential for the synthesis of aldehyde cyanohydrins. However, for ketones this set-up is most probably even more advantageous, since

---

the in-line modification of ketone cyanohydrins is expected to be much faster compared to the offline modification in batch used in this thesis, thereby preventing decomposition of the respective ketone cyanohydrines.

Another interesting development to the flow reactor would be the safe disposal of the excess of the HCN found in the outlet stream. The excess of HCN can be either neutralized with bleach or recycled for further reactions, possibly by a tube in tube reactor [55].

Considering the industrial impact of this work, it would be logical in the future to transform these cyanohydrins into valuable compounds such as amino alcohols, alpha-hydroxy amides etc.

The modularization of enzymatic cascades in flow reactors renders a biocatalytic process robust and efficient. This is a step forward towards sustainable bioeconomy for the production of bio-based chemicals.

---

# Chapter 7

## REFERENCES

---

## References

1. Sheldon R, van Pelt S: **Enzyme immobilisation in biocatalysis: why, what and how.** *Chem Soc Rev* 2013, **42**:6223–6235.
2. Johannes TW, Simurdiak MR, Zhao H: **Biocatalysis.** In *Encyclopedia of Chemical Processing*; 2006.
3. Bornscheuer UT, Huisman GW, Kazlauskas RJ, Lutz S, Moore JC, Robins K: **Engineering the third wave of biocatalysis.** *Nature* 2012, **485**:185–194.
4. Bommarius AS, Riebel BR: **Biocatalysis, Fundamentals and Applications.** *Wiley-VCH Verlag GmbH* 2005.
5. Pasteur ML: **Mémoire sur la fermentation alcoolique.** *Compt Rend Acad Sci Paris* 1857, **45**:1032–1036.
6. Kühne W: **Über das Verhalten verschiedener organisierter und sog. ungeformter Fermente.** *Verhandlungen des naturhistorisch-medizinischen Vereins zu Heidelberg* 1877, **1**:190–193.
7. Fischer E: **Einfluss der Conformation auf die Wirkung der Enzyme.** *Chem Ber* 1894, **27**:2985–2993.
8. Buchner E: **Alkoholische Gärung ohne Hefezellen (Vorläufige Mitteilung).** *Ber Dtsch Chem Ges* 1897:117–124.
9. Sumner JB: **The chemical nature of enzymes.** *J Wash Acad Sci* 1948, **38**:113–117.

- 
10. Ariëns EJ: **Stereochemistry, a basis for sophisticated nonsense in pharmacokinetics and clinical pharmacology.** *Eur J Clin Pharmacol* 1984, **26**:663–668.
11. Choi J-M, Han S-S, Kim H-S: **Industrial applications of enzyme biocatalysis: Current status and future aspects.** *Biotechnol Adv* 2015, **33**:1443-1454.
12. Narancic T, Davis R, Nikodinovic-Runic J, O' Connor KE: **Recent developments in biocatalysis beyond the laboratory.** *Biotechnol Lett* 2015, **37**:943–954.
13. Denard CA, Ren H, Zhao H: **Improving and repurposing biocatalysts via directed evolution.** *Curr Opin Chem Biol* 2015, **25**:55–64.
14. Schmid A, Dordick JS, Hauer B, Kiener A, Wubbolts M, Witholt B: **Industrial biocatalysis today and tomorrow.** *Nature* 2001, **409**:258–268.
15. Sigrist R, da Costa BZ, Marsaioli AJ, de Oliveira LG: **Nature-inspired enzymatic cascades to build valuable compounds.** *Biotechnol Adv* 2015:1–18.
16. Cossins BP, Jacobson MP, Guallar V: **A new view of the bacterial cytosol environment.** *PLoS Comput Biol* 2011, **7**:e1002066.
17. Rariy R V., Klivanov AM: **On the Relationship Between Enzymatic Enantioselectivity in Organic Solvents and Enzyme Flexibility.** *Biocatal Biotrans* 2000, **18**:401–407.
18. Cantone S, Hanefeld U, Basso A: **Biocatalysis in non-conventional media—ionic liquids, supercritical fluids and the gas phase.** *Green Chemistry* 2007, **9**:954-971.
19. Klivanov A: **Why are enzymes less active in organic solvents than in water?** *Trends Biotechnol* 1997, **15**:97–101.

- 
20. Griebenow K, Klivanov AM: **On protein denaturation in aqueous-organic mixtures but not in pure organic solvents.** *J Am Chem Soc* 1996, **118**:11695–11700.
21. Klivanov AM: **Improving enzymes by using them in organic solvents.** *Nature* 2001, **409**:241–246.
22. Bell G, Halling PJ, Moore BD, Partridge J, Rees DG: **Biocatalyst behaviour in low-water systems.** *Trends Biotechnol* 1995, **13**:468–473.
23. Nikolova P, Ward OP: **Whole cell biocatalysis in nonconventional media.** *J Ind Microbiol* 1993, **12**:76–86.
24. Wescott CR, Klivanov AM: **The solvent dependence of enzyme specificity.** *Biochem Biophys Acta - Protein Struct Mol Enzymol* 1994, **1206**:1–9.
25. Carrea G, Ottolina G, Riva S: **Role of solvents in the control of enzyme selectivity in organic media.** *Trends Biotechnol* 1995, **13**:63–70.
26. Broos J, Engbersen JFJ, Verboom W, Hoek A Van, Reinhoudt DN: **Flexibility of Enzymes Suspended in Organic Solvents Probed by Time-Resolved Fluorescence Anisotropy.** 1995, **117**:12657-12663.
27. Klivanov AM: **Enzymatic catalysis in anhydrous organic solvents.** *Trends Biochem* 1989, **14**:141–144.
28. Vermue MH, Tramper J: **Biocatalysis in non-conventional media: Medium engineering aspects (Technical Report).** *Pure Appl Chem* 1995, **67**:345–373.
29. Affleck R, Xu ZF, Suzawa V, Focht K, Clark DS, Dordick JS: **Enzymatic catalysis and dynamics in low-water environments.** *Proc Natl Acad Sci U S A* 1992, **89**:1100–1104.

- 
30. Sheldon R: **Reactions In Non-Conventional Media For Sustainable Organic Synthesis**. In *NATO Advanced Study Institute on New Methodologies and Techniques for a Sustainable Org Chem* 2008, **246**:1–28.
31. Žnidaršič-Plazl P: **Enzymatic microreactors utilizing non-aqueous media**. *Chim Oggi/Chemistry Today* 2014, **32**:54–60.
32. Grünwald P: *Biocatalysis: Biochemical Fundamentals and Applications*. London: Imperial College Press; 2009.
33. Cao L: **Immobilised enzymes: Science or art?** *Curr Opin Chem Biol* 2005, **9**:217–226.
34. Hanefeld U, Gardossi L, Magner E: **Understanding enzyme immobilisation**. *Chem Soc Rev* 2009, **38**:453–468.
35. End N, Schöning K-U: **Immobilized biocatalysts in industrial research and production**. *Curr Chem* 2004, **242**:273–317.
36. Brady D, Jordaan J: **Advances in enzyme immobilisation**. *Biotechnol Lett* 2009, **31**:1639–1650.
37. Sheldon RA: **Cross-linked enzyme aggregates as industrial biocatalysts**. *Org Process Res Dev* 2011, **15**:213–223.
38. Van Langen LM, Selassa RP, van Rantwijk F, Sheldon RA: **Cross-linked aggregates of (R)-oxynitrilase: a stable, recyclable biocatalyst for enantioselective hydrocyanation**. *Org Lett* 2005, **7**:327–329.
39. Chaplin M, Bucke C: *Enzyme Technology*. Cambridge University Press; 1990.

- 
40. Jones E, McClean K, Housden S, Gasparini G, Archer I: **Biocatalytic oxidase: Batch to continuous.** *Chem Eng Res Des* 2012, **90**:726–731.
41. Rao NN, Lütz S, Würges K, Minör D: **Continuous biocatalytic processes.** *Org Proc Res Dev* 2009, **13**:607–616.
42. Liese A, Seelbach K, Wandrey C: *Industrial Biotransformations, Second Edition.* Wiley-VCH Verlag GmbH & Co. KGaA; 2006.
43. Rios GM, Belleville MP, Paolucci D, Sanchez J: **Progress in enzymatic membrane reactors - A review.** *J Membrane Sci* 2004, **242**:189–196.
44. Shin JS, Kim BG, Liese A, Wandrey C: **Kinetic resolution of chiral amines with  $\omega$ -transaminase using an enzyme-membrane reactor.** *Biotechnol Bioeng* 2001, **73**:179–187.
45. Wichmann R, Wandrey C, Bückmann AF, Kula MR: **Continuous enzymatic transformation in an enzyme membrane reactor with simultaneous NAD(H) regeneration.** *Biotechnol Bioeng* 2000, **67**:791–804.
46. Prazeres DMF, Cabral JMS: **Enzymatic membrane bioreactors and their applications.** *Enzyme Microb. Tech.* 1994, **16**:738–750.
47. Ingham RJ, Battilocchio C, Fitzpatrick DE, Sliwinski E, Hawkins JM, Ley S V: **A systems approach towards an intelligent and self-controlling platform for integrated continuous reaction sequences.** *Angew Chemie Int Ed* 2015, **54**:144–148.
48. Ley S V, Fitzpatrick DE, Ingham RJ, Myers RM: **Organic Synthesis: March of the Machines.** *Angew Chemie Int Ed* 2015, **54**:3449–3464.

- 
49. Ley S V, Baxendale IR: **New tools and concepts for modern organic synthesis.** *Nat Rev Drug Discov* 2002, **1**:573–586.
50. Pastre JC, Browne DL, Ley S V: **Flow chemistry syntheses of natural products.** *Chem Soc Rev* 2013, **42**:8849–8869.
51. Hartwig J, Metternich JB, Nikbin N, Kirschning A, Ley S V: **Continuous flow chemistry: a discovery tool for new chemical reactivity patterns.** *Org Biomol Chem* 2014, **12**:3611–3615.
52. Wegner J, Ceylan S, Kirschning A: **Flow chemistry - A key enabling technology for (multistep) organic synthesis.** *Adv Synth Catal* 2012, **354**:17–57.
53. Tamborini L, Romano D, Pinto A, Contente M, Iannuzzi MC, Conti P, Molinari F: **Biotransformation with whole microbial systems in a continuous flow reactor: Resolution of (RS)-flurbiprofen using *Aspergillus oryzae* by direct esterification with ethanol in organic solvent.** *Tetrahedron Lett* 2013, **54**:6090–6093.
54. Fornera S, Bauer T, Schlüter AD, Walde P: **Simple enzyme immobilization inside glass tubes for enzymatic cascade reactions.** *J Mater Chem* 2012, **22**:502-511.
55. Tomaszewski B, Schmid A, Bühler K: **Biocatalytic Production of Catechols Using a High Pressure Tube-in-Tube Segmented Flow Microreactor.** *Org Process Res Dev* 2014, **18**:1516–1526.
56. Delville MME, Koch K, van Hest JCM, Rutjes FPJT: **Chemoenzymatic flow cascade for the synthesis of protected mandelonitrile derivatives.** *Org Biomol Chem* 2015, **13**:1634–1638.
57. Cowen RC: **Microbes in industry. The revolution in biotechnology.**  
<http://www.csmonitor.com/1981/1028/102834.html> .

- 
58. Wöhler, F. Liebig J: **Über die Bildung des Mandelöls**. *Ann Pharm* 1837, **22**:1–24.
59. Rosenthaler L: **Enzyme effected asymmetrical synthesis**. *Biochem Z* 1908, **14**:238–253.
60. Stumpf P.K. and Conn EE: *The Biochemistry of Plants*. York London Toronto Sydney San Francisco: Academic Press Inc.; 1988.
61. Nahrstedt A: **Cyanogenic compounds as protecting agents for organisms**. *Plant Syst Evol* 1985, **150**:35–47.
62. Conn EE: **Biosynthesis of cyanogenic glycosides**. *Naturwissenschaften* 1979, **66**:28–34.
63. Seigler DS: **Isolation and characterization of naturally occurring cyanogenic compounds**. *Phytochemistry* 1975, **14**:9–29.
64. Poulton JE: **Localization and catabolism of cyanogenic glycosides**. *Ciba Found Symp* 1988, **140**:67–91.
65. Conn EE: **Cyanogenic Compounds**. *Annual Review of Plant Physiology* 1980, **31**:433–451.
66. Hickel A, Hasslacher M, Griengl H: **Minireview. Hydroxynitrile lyases: Functions and properties**. *Physiol Plant* 1996, **98**:891–898.
67. Gracia R, Shepherd G: **Cyanide poisoning and its treatment**. *Pharmacotherapy* 2004, **24**:1358–1365.
68. Zagrobelny M, Bak S, Rasmussen AV, Jørgensen B, Naumann CM, Møller BL: **Cyanogenic glucosides and plant-insect interactions**. *Phytochemistry* 2004, **65**:293–306.
69. Poulton JE: **Cyanogenesis in plants**. *Plant Physiol* 1990, **94**:401–405.

- 
70. Bordo D, Bork P: **The rhodanese/Cdc25 phosphatase superfamily Sequence–structure–function relations.** *EMBO Rep* 2002, **3**:741–746.
71. Lieberei R, Selmar D, Biehl B: **Metabolization of cyanogenic glucosides in *Hevea brasiliensis*.** *Plant Syst Evol* 1985, **150**:49–63.
72. Selmar D: **Zwei Wege zur Metabolisierung Cyanogenic Glycoside.** Doctoral thesis, University of Braunschweig, Germany; 1986.
73. Horeis G: **The hydroxynitrile lyase from flax.** Doctoral thesis, University of Graz; 2008.
74. Wehtje E, Adlercreutz P, Mattiasson B: **Formation of C-C bonds by mandelonitrile lyase in organic solvents.** *Biotechnol Bioeng* 1990, **36**:39–46.
75. Lanfranchi E, Steiner K, Glieder A, Hajnal I, Sheldon R A, van Pelt S, Winkler M: **Mini-review: recent developments in hydroxynitrile lyases for industrial biotechnology.** *Recent Pat Biotechnol* 2013, **7**:197–206.
76. Effenberger F: **Synthesis and Reactions of Optically Active Cyanohydrins.** *Angew Chemie Int Ed* 1994, **33**:1555–1564.
77. Gregory RJH: **Cyanohydrins in Nature and the Laboratory: Biology, Preparations, and Synthetic Applications.** *Chem Rev* 1999, **99**:3649–3682.
78. Fischer T, Pietruszka J: **Key building blocks via enzyme-mediated synthesis.** *Top Curr Chem* 2010, **297**:1–43.
79. North M: **Synthesis and applications of non-racemic cyanohydrins.** *Tetrahedron Asymmetry* 2003, **14**:147–176.

- 
80. Griengl H, Klempier N, Pöchlauer P, Schmidt M, Shi N, Zabelinskaja-Mackova AA: **Enzyme catalysed formation of (S)-cyanohydrins derived from aldehydes and ketones in a biphasic solvent system.** *Tetrahedron* 1998, **54**:14477–14486.
81. Von Langermann J, Mell A, Paetzold E, Daußmann T, Kragl U: **Hydroxynitrile lyase in organic solvent-free systems to overcome thermodynamic limitations.** *Adv Synth Catal* 2007, **349**:1418–1424.
82. Bühler H, Bayer A, Effenberger F: **A convenient synthesis of optically active 5,5-disubstituted 4-amino- and 4-hydroxy-2(5H)-furanones from (S)-ketone cyanohydrins.** *Chemistry* 2000, **6**:2564–2571.
83. Albrecht J, Jansen I, Kula MR: **Improved purification of an (R)-oxynitrilase from *Linum usitatissimum* (flax) and investigation of the substrate range.** *Biotechnol Appl Biochem* 1993, **17 ( Pt 2)**:191–203.
84. Roberge C, Fleitz F, Pollard D, Devine P: **Synthesis of optically active cyanohydrins from aromatic ketones: evidence of an increased substrate range and inverted stereoselectivity for the hydroxynitrile lyase from *Linum usitatissimum*.** *Tetrahedron Asymm* 2007, **18**:208–214.
85. Zagrobelny M, Bak S, Møller BL: **Cyanogenesis in plants and arthropods.** *Phytochemistry* 2008, **69**:1457–1468.
86. Sharma M, Sharma NN, Bhalla TC: **Hydroxynitrile lyases: At the interface of biology and chemistry.** *Enzyme Microb Technol* 2005, **37**:279–294.
87. Hussain Z, Wiedner R, Steiner K, Hajek T, Avi M, Hecher B, Sessitsch A, Schwab H: **Characterization of two bacterial hydroxynitrile lyases with high similarity to cupin superfamily proteins.** *Appl Environ Microbiol* 2012, **78**:2053–2055.

- 
88. Hajnal I, Łyskowski A, Hanefeld U, Gruber K, Schwab H, Steiner K: **Biochemical and structural characterization of a novel bacterial manganese-dependent hydroxynitrile lyase.** *FEBS J* 2013, **280**:5815–5828.
89. Gerstner E, Mätzke V, Pfeil E: **Zur chemischen und biologischen Systematik der Rosaceen - Untersuchung des Flavinsystems D-Oxynitrilase.** *Naturwissenschaften* 1968, **55**:561–563.
90. Dreveny I, Gruber K, Glieder A, Thompson A, Kratky C: **The hydroxynitrile lyase from almond: A lyase that looks like an oxidoreductase.** *Structure* 2001, **9**:803–815.
91. Dreveny I, Kratky C, Gruber K: **The active site of hydroxynitrile lyase from *Prunus amygdalus*: modeling studies provide new insights into the mechanism of cyanogenesis.** *Protein Sci* 2002, **11**:292–300.
92. Cheng IP, Poulton JE: **Cloning of cDNA of *Prunus serotina* (R)-(+)-Mandelonitrile Lyase and Identification of a Putative FAD-Binding Site.** *Plant Cell Physiol* 1993, **34**:1139–1143.
93. Jorns MS: **Mechanism of catalysis by the flavoenzyme oxynitrilase.** *J Biol Chem* 1979, **254**:12145–12152.
94. Hasslacher M, Kratky C, Griengl H, Schwab H, Kohlwein SD: **Hydroxynitrile lyase from *Hevea brasiliensis*: Molecular characterization and mechanism of enzyme catalysis.** *Proteins Struct Funct Genet* 1997, **27**:438–449.
95. Wajant H, Forster S, Bottinger H, Effenberger F, Pfizenmaier K: **Acetone cyanohydrin lyase from *Manihot esculenta* (cassava) is serologically distinct from other hydroxynitrile lyases.** *Plant Sci* 1995, **108**:1–11.
96. Ollis DL, Cheah E, Cygler M, Dijkstra B, Frolow F, Franken SM, Harel M, Remington SJ, Silman I, Schrag J: **The alpha/beta hydrolase fold.** *Protein Eng* 1992, **5**:197–211.

- 
97. Gruber K, Gartler G, Krammer B, Schwab H, Kratky C: **Reaction mechanism of hydroxynitrile lyases of the  $\alpha/\beta$ -hydrolase superfamily: The three-dimensional structure of the transient enzyme-substrate complex certifies the crucial role of Lys236.** *J Biol Chem* 2004, **279**:20501–20510.
98. Hanefeld U, Straathof AJJ, Heijnen JJ: **Study of the (S)-hydroxynitrile lyase from *Hevea brasiliensis*: Mechanistic implications.** *Biochem Biophys Acta - Protein Struct Mol Enzymol* 1999, **1432**:185–193.
99. Bühler H, Effenberger F, Förster S, Roos J, Wajant H: **Substrate specificity of mutants of the hydroxynitrile lyase from *Manihot esculenta*.** *ChemBioChem* 2003, **4**:211–216.
100. Wajant H, Mundry KW, Pfizenmaier K: **Molecular cloning of hydroxynitrile lyase from *Sorghum bicolor* (L.). Homologies to serine carboxypeptidases.** *Plant Mol Biol* 1994, **26**:735–746.
101. Kuroki GW, Conn EE: **Mandelonitrile lyase from *Ximenia americana* L.: stereospecificity and lack of flavin prosthetic group.** *Proc Natl Acad Sci U S A* 1989, **86**:6978–6981.
102. Breithaupt H, Pohl M, Bönigk W, Heim P, Schimz KL, Kula MR: **Cloning and expression of (R)-hydroxynitrile lyase from *Linum usitatissimum* (flax).** *J Mol Catal B Enzym* 1999, **6**:315–332.
103. Tateno H, Winter HC, Petryniak J, Goldstein IJ: **Purification, characterization, molecular cloning, and expression of novel members of jacalin-related lectins from rhizomes of the true fern *Phlebodium aureum* (L) J. Smith (polypodiaceae).** *J Biol Chem* 2003, **278**:10891–10899.
104. Han SQ, Ouyang PK, Wei P, Hu Y: **Enzymatic synthesis of (R)-cyanohydrins by a novel (R)-oxynitrilase from *Vicia sativa* L.** *Biotechnol Lett* 2006, **28**:1909–1912.

- 
105. Sakurai T, Margolin AL, Russell AJ, Klivanov AM: **Control of enzyme enantioselectivity by the reaction medium.** *J Am Chem Soc* 1988, **110**:7236–7237.
106. Schmitke JL, Wescott CR, Klivanov a. M: **The mechanistic dissection of the plunge in enzymatic activity upon transition from water to anhydrous solvents.** *J Am Chem Soc* 1996, **118**:3360–3365.
107. Brattsen LB, Samuelian JH, Long KY, Kinciad SA, Evans CK: **Cyanide as a feeding stimulant for the southern army worm, *Spodoptera eridania*.** *Ecol Entomol* 1983, **8**:125–132.
108. Van Langen LM, Van Rantwijk F, Sheldon RA: **Enzymatic Hydrocyanation of a Sterically Hindered Aldehyde. Optimization of a Chemoenzymatic Procedure for (*R*)-2-Chloromandelic Acid.** *Org Process Res Dev* 2003, **7**:828–831.
109. Veum L, Hanefeld U, Pierre A: **The first encapsulation of hydroxynitrile lyase from *Hevea brasiliensis* in a sol-gel matrix.** *Tetrahedron* 2004, **60**:10419–10425.
110. Purkarthofer T, Skranc W, Weber H, Griengl H, Wubbolts M, Scholz G, Pöchlauer P: **One-pot chemoenzymatic synthesis of protected cyanohydrins.** *Tetrahedron* 2004, **60**:735–739.
111. Andexer J, von Langermann J, Mell A, Bocola M, Kragl U, Eggert T, Pohl M: **An *R*-selective hydroxynitrile lyase from *Arabidopsis thaliana* with an  $\alpha/\beta$ -hydrolase fold.** *Angew Chemie Int Ed* 2007, **46**:8679–8681.
112. Wagner UG, Hasslacher M, Griengl H, Schwab H, Kratky C: **Mechanism of cyanogenesis: The crystal structure of hydroxynitrile lyase from *Hevea brasiliensis*.** *Structure* 1996, **4**:811–822.

- 
113. Hughes J, Carvalho FJ, Hughes MA: **Purification, characterization, and cloning of alpha-hydroxynitrile lyase from cassava (*Manihot esculenta* Crantz).** *Arch Biochem Biophys* 1994;496–502.
114. Andexer JN, Langermann J V., Kragl U, Pohl M: **How to overcome limitations in biotechnological processes - examples from hydroxynitrile lyase applications.** *Trends Biotechnol* 2009, **27**:599–607.
115. Andexer JN, Staunig N, Eggert T, Kratky C, Pohl M, Gruber K: **Hydroxynitrile Lyases with  $\alpha/\beta$ -Hydrolase Fold: Two Enzymes with Almost Identical 3D Structures but Opposite Enantioselectivities and Different Reaction Mechanisms.** *ChemBioChem* 2012, **13**:1932–1939.
116. Guterl JK, Andexer JN, Sehl T, von Langermann J, Frindi-Wosch I, Rosenkranz T, Fitter J, Gruber K, Kragl U, Eggert T: **Uneven twins: Comparison of two enantiocomplementary hydroxynitrile lyases with  $\alpha/\beta$ -hydrolase fold.** *J Biotechnol* 2009, **141**:166–173.
117. Okrob D, Metzner J, Wiechert W, Gruber K, Pohl M: **Tailoring a Stabilized Variant of Hydroxynitrile Lyase from *Arabidopsis thaliana*.** *Chembiochem* 2012, **13**:797–802.
118. Scholz KE, Kopka B, Wirtz AA, Pohl M, Jaeger KE, Krauss U: **Fusion of a flavin-based fluorescent protein to hydroxynitrile lyase from *Arabidopsis thaliana* improves enzyme stability.** *Appl Environ Microbiol* 2013, **79**:4727–4733.
119. Kopka B, Diener M, Wirtz A, Pohl M, Jaeger K-E, Krauss U: **Purification and simultaneous immobilization of *Arabidopsis thaliana* hydroxynitrile lyase using a family 2 carbohydrate-binding module.** *Biotechnol J* 2015, **10**:811-819.
120. Okrob D, Paravidino M, Orru RVA, Wiechert W, Hanefeld U: **Hydroxynitrile lyase from *Arabidopsis thaliana*: Identification of reaction parameters for enantiopure cyanohydrin synthesis by pure and immobilized catalyst.** *Adv Synth Catal* 2011, **353**:2399–2408.

- 
121. Scholz KE, Okrob D, Kopka B, Grünberger A, Pohl M, Jaeger KE, Krauss U: **Synthesis of chiral cyanohydrins by recombinant *Escherichia coli* cells in a micro-aqueous reaction system.** *Appl Environ Microbiol* 2012, **78**:5025–5027.
122. Brovetto M, Gamemara D, Saenz Méndez P, Seoane GA: **C-C bond-forming lyases in organic synthesis.** *Chem Rev* 2011, **7**:4346–4403.
123. Diebler J, von Langermann J, Mell A, Hein M, Langer P, Kragl U: **Synthesis of aliphatic and alpha-halogenated ketone cyanohydrins with the hydroxynitrile lyase from *Manihot esculenta*.** *ChemCatChem* 2014, **6**:987–991.
124. Effenberger F, Heid S: **(R)-oxynitrilase catalyzed synthesis of (R)-ketone cyanohydrins.** *Tetrahedron Asymm* 1995, **6**:2945–2952.
125. Kiljunen E, Kanerva LT: **(R)- and (S)- Cyanohydrins Using Oxynitrilases in Whole Cells Almond Meal or bicolor Shoots.** *Science* 1996, **7**:1105–1116.
126. Studier FW, Moffatt BA: **Use of bacteriophage T7 RNA polymerase to direct selective high-level expression of cloned genes.** *J Mol Biol* 1986, **189**:113–130.
127. Bertani G: **Studies on lysogenesis. I. The mode of phage liberation by lysogenic *Escherichia coli*.** *J Bacteriol* 1951, **62**:293–300.
128. Hanahan D: **Studies on transformation of *Escherichia coli* with plasmids.** *J Mol Biol* 1983, **166**:557–580.
129. Studier FW: **Protein production by auto-induction in high-density shaking cultures.** *Protein Expr and Purif* 2005, **41**:207–234.

- 
130. Laemmli UK: **Cleavage of structural proteins during the assembly of the head of bacteriophage T4.** *Nature* 1970, **227**:680–685.
131. Candiano G, Bruschi M, Musante L, Santucci L, Ghiggeri GM, Carnemolla B, Orecchia P, Zardi L, Righetti PG: **Blue silver: A very sensitive colloidal Coomassie G-250 staining for proteome analysis.** *Electrophoresis* 2004, **25**:1327–1333.
132. Hochuli E, Bannwarth W, Döbeli H: **Genetic Approach to Facilitate Purification of Recombinant Proteins with a Novel Metal Chelate Adsorbent.** *Nature* 1988, **6**:1321–1325.
133. Billingsley ML, Pennypacker KR, Hoover CG, Brigati DJ, Kincaid RL: **A rapid and sensitive method for detection and quantification of calcineurin and calmodulin-binding proteins using biotinylated calmodulin.** *Proc Natl Acad Sci U S A* 1985, **82**:7585–7589.
134. Bauer M, Griengl H, Steiner W: **Kinetic studies on the enzyme (S)-hydroxynitrile lyase from *Hevea brasiliensis* using initial rate methods and progress curve analysis.** *Biotechnol Bioeng* 1999, **62**:20–29.
135. Datta S, Christena LR, Rajaram YRS: **Enzyme immobilization: an overview on techniques and support materials.** *3 Biotech* 2012, **3**:1–9.
136. Butler LG: **Enzymes in non-aqueous solvents.** *Enzyme Microb. Tech.* 1979, **1**:253–259.
137. Wachtmeister J, Jakoblinnert A, Kulig J, Offermann H, Rother D: **Whole-Cell Teabag Catalysis for the Modularisation of Synthetic Enzyme Cascades in Micro-Aqueous Systems.** *ChemCatChem* 2014, **6**:1051–1058.
138. Płotka JM, Biziuk M, Morrison C, Namieśnik J: **Pharmaceutical and forensic drug applications of chiral supercritical fluid chromatography.** *TrAC - Trends Anal Chem* 2014, **56**:74–89.

- 
139. Kadam ST, Kim SS: **One-pot three components synthesis of O-acetylcyanohydrins with TMSCN, acetic anhydride and carbonyl compounds under solvent-free condition.** *Tetrahedron* 2009, **65**:6330–6334.
140. Khan NH, Agrawal S, Kureshy RI, Abdi SHR, Mayani VJ, Jasra R V.: **Easily recyclable polymeric V(V) salen complex for the enantioselective O-acetyl cyanation of aldehydes.** *J Mol Catal A Chem* 2007, **264**:140–145.
141. Sakai T, Wang K, Ema T: **Lipase-catalyzed dynamic kinetic resolution giving optically active cyanohydrins: use of silica-supported ammonium hydroxide and porous ceramic-immobilized lipase.** *Tetrahedron* 2008, **64**:2178–2183.
142. Frese A: **Evaluation of (R)- and (S)-selective hydroxynitrile lyase variants in a microaqueous organic solvent.** Master thesis, Heinrich-Heine-Universität Düsseldorf; 2014.
143. Pohl M, Wechsler C MM: **Acyloln, benzoin, and related reactions.** In *Biocatalysis in Organic Synthesis 2*. Edited by Faber, K, Fessner, W-D, Turner N. Georg Thieme Verlag, Stuttgart, Germany; 2014:93–131.
144. Sharma N, Sharma UK, Kumar R, Katoch N, Kumar R, Sinha AK: **First bovine serum albumin-promoted synthesis of enones, cinnamic acids and coumarins in ionic liquid: An insight into the role of protein impurities in porcine pancreas lipase for olefinic bond formation.** *Adv Synth Catal* 2011, **353**:871–878.
145. Go MK, Malabanan MM, Amyes TL, Richard JP: **Bovine serum albumin-catalyzed deprotonation of [1-<sup>13</sup>C] Glycolaldehyde: Protein reactivity toward deprotonation of the alpha-hydroxy alpha-carbonyl carbon.** *Biochemistry* 2010, **49**:7704–7708.
146. Krieger E, Vriend G: **YASARA View - molecular graphics for all devices - from smartphones to workstations.** *Bioinformatics* 2014, **30**:2981–2982.

- 
147. Duan Y, Wu C, Chowdhury S, Lee MC, Xiong G, Zhang W, Yang R, Cieplak P, Luo R, Lee T, Caldwell J, Wang J, Kollman P: **A Point-Charge Force Field for Molecular Mechanics Simulations of Proteins Based on Condensed-Phase Quantum Mechanical Calculations.** *J Comput Chem* 2003, **24**:1999–2012.
148. Krieger E, Dunbrack RL, Hooft RWW, Krieger B: **Assignment of protonation states in proteins and ligands: Combining pKa prediction with hydrogen bonding network optimization.** *Methods Mol Biol* 2012, **819**:405–421.
149. Essmann U, Perera L, Berkowitz ML, Darden T, Lee H, Pedersen LG: **A smooth particle mesh Ewald method.** *J Chem Phys* 1995, **103**:8577–8593.
150. Kikuchi K, Thorn SN, Hilvert D: **Albumin-catalyzed proton transfer.** *J Am Chem Soc* 1996, **118**:8184–8185.
151. Koh S-WM, Means GE: **Characterization of a small apolar anion binding site of human serum albumin.** *Arch Biochem Biophys* 1979, **192**:73–79.
152. Means GE, Bender ML: **Acetylation of human serum albumin by p-nitrophenyl acetate.** *Biochemistry* 1975, **14**:4989–4994.
153. Torrel G, Jin J, Hanefeld U: **Hydroxynitrile Lyases Do Not Catalyse the Promiscuous Addition of Cyanide to Imines.** *ChemCatChem* 2013, **5**:1304–1307.
154. Lee T, Ahn Y: **Enzymatic introduction of cyanide into imine for constructing optically active compound by (R)-oxy-nitrilase in almond meal.** *Bull Korean Chem Soc* 2002, **23**:1490–1492.
155. Evitt AS, Bornscheuer UT: **Lipase CAL-B does not catalyze a promiscuous decarboxylative aldol addition or Knoevenagel reaction.** *Green Chemistry* 2011:1141.

- 
156. Milner SE, Moody TS, Maguire AR: **Biocatalytic approaches to the Henry (nitroaldol) reaction.** *Eur J Org Chem* 2012:3059–3067.
157. Ismayilova U: **Coimmobilisierung von Hydroxynitril-Lyase mit Lipasen und Reaktionen damit.** Bachelor thesis, Aachen University of Applied Sciences; 2014.
158. Kahlow UH, Schmid RD, Pleiss J: **A model of the pressure dependence of the enantioselectivity of *Candida rugosalipase* towards (+/-)-menthol.** *Protein Sci* 2001, **10**:1942–1952.

---

## Appendix

### **Appendix 1: Gene and amino acid sequences for His<sub>6</sub>-AtHNL**

#### **Gene sequence**

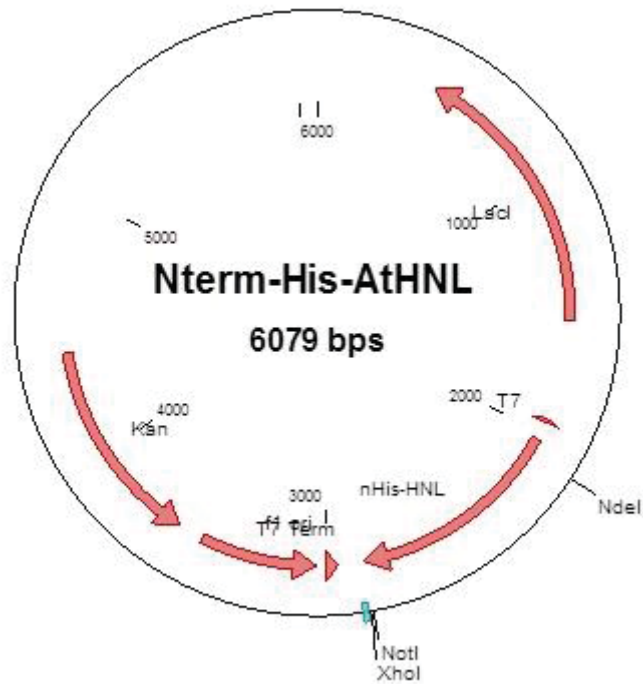
ATGGGCAGCAGCCATCATCATCATCACAGCAGCGGCCTGGTGCCGCGCGGCAGCCATATGGAGAG  
GAAACATCACTTCGTGTTAGTTCACAACGCTTATCATGGAGCCTGGATCTGGTACAAGCTCAAGCCCCTC  
CTTGAATCAGCCGGCCACCGCGTACTGCTGTCGAACTCGCCGCTCCGGGATCGACCCACGACCAATCC  
AGGCCGTTGAAACCGTCGACGAATACTCCAACCGTTGATCGAAACCCTCAAATCTCTCCAGAGAACGA  
AGAGGTAATTCTGGTTGGATTAGCTTCGGAGGCATCAACATCGCTCTCGCCGCCGACATATTTCCGGCG  
AAGATTAAGGTTCTTGTGTTCTCAACGCCTTCTTGCCCGACACAACCCACGTGCCTTCTCACGTTCTGGA  
CAAGTATATGGAGATGCCTGGAGGTTTGGGAGATTGTGAGTTTTATCTCATGAAACAAGAAATGGGAC  
GATGAGTTTATTGAAGATGGGACCAAATTCATGAAGGCACGTCTTTACCAAATTTGCCATAGAGGAT  
TACGAGCTGGCAAAAATGTTGCATAGGCAAGGGTCATTTTTACAGAGGATCTATCAAAGAAAGAAAAG  
TTTAGCGAGGAAGGATATGGTTCGGTGCAACGAGTTTACGTAATGAGTAGTGAAGACAAAGCCATCCCC  
TGCGATTTCAATTCGTTGGATGATTGATAATTTCAACGTCTCGAAAGTCTACGAGATCGATGGCGGAGATC  
ACATGGTGATGCTCTCAAACCCCAAAAACCTTTGACTCTCTCTGCTATTGCCACCGATTATATGTAA

#### **Amino acid sequence**

MGSSHHHHHSSGLVPRGSHMERKHHFVLVHNAYHGAWIWKLPKPLESAGHRVTAVELAASGIDPRPIQ  
AVETVDEYSKPLIETLKSLPENEEVILVGFSGGINIALAADIFPAKIKVLVFLNAFLPDTHVPSHVLDKYMEMP  
GGLGDCEFSSHETRNGTMSLLKMGPKFMKARLYQNCPIEDYELAKMLHRQGSFFTEDLSKKEKFSEEGYGSV  
QRVYVMSSDKAIPCDFIRWMIDNFNVSQVYEIDGGDHMVMLSKPQKLFDSLAIATDYM

---

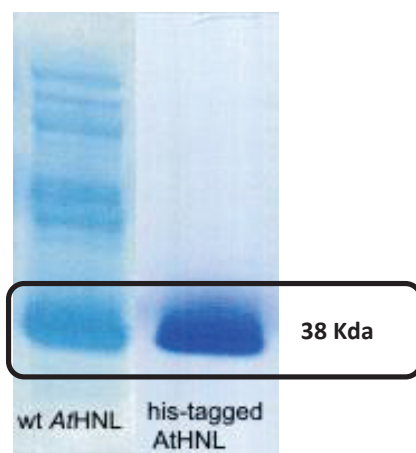
## Appendix 2: Plasmid map



## Appendix 3: Comparison of lyophilized wt AtHNL and His<sub>6</sub>-AtHNL

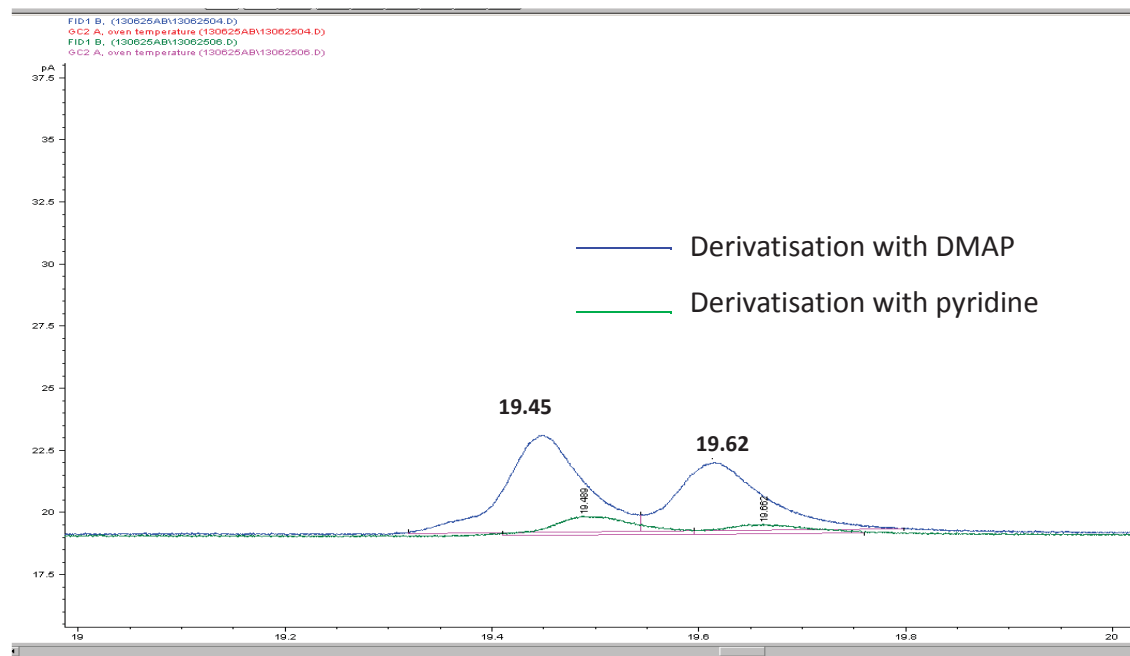
wt-AtHNL was purified via Anion exchange chromatography [120]. His<sub>6</sub>-AtHNL was purified via IMAC [142].

20 µg lyophilized enzyme were loaded on a SDS-Gel and SDS-Page was carried out .



#### **Appendix 4: Comparison of acetylation with pyridine and dimethyl aminopyridine**

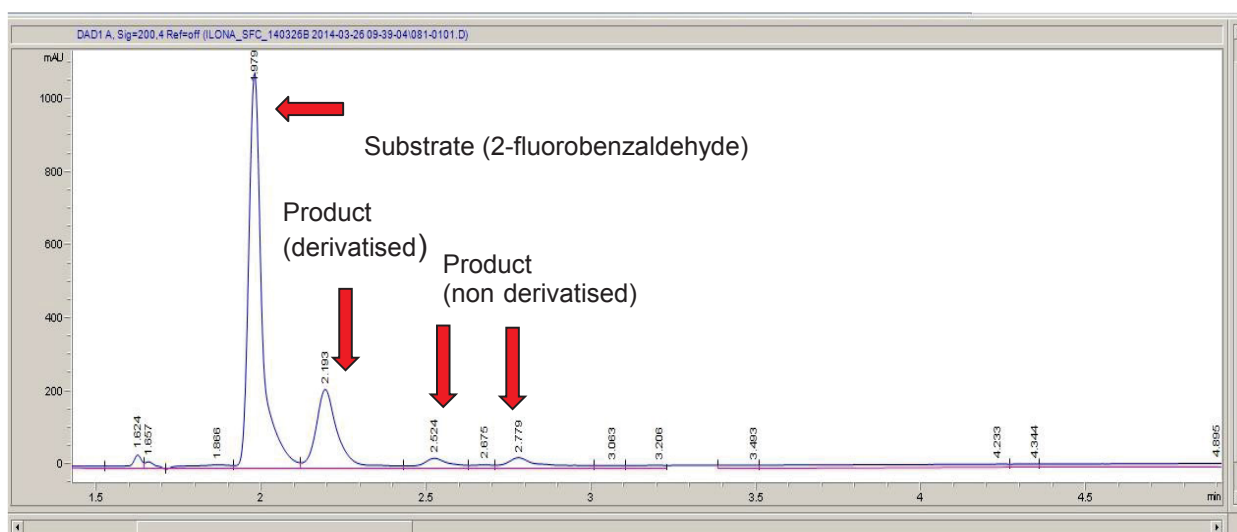
The GC chromatogram for a comparison of product acetylation with pyridine and 4-dimethyl aminopyridine (DMAP) (chapter 4.2.1). Acetophenone cyanohydrin was synthesized followed by subsequent acetylation with pyridine and 4-dimethyl aminopyridine (DMAP) (chapter 3.2.12)



The product peaks shown in the GC chromatogram above.

## Appendix 5: Completeness of derivatization by silylation

The following SFC chromatogram shows the completeness of derivatization by silylation (chapter 4.2.1). The SFC method is described in chapter 3.2.23.3.1

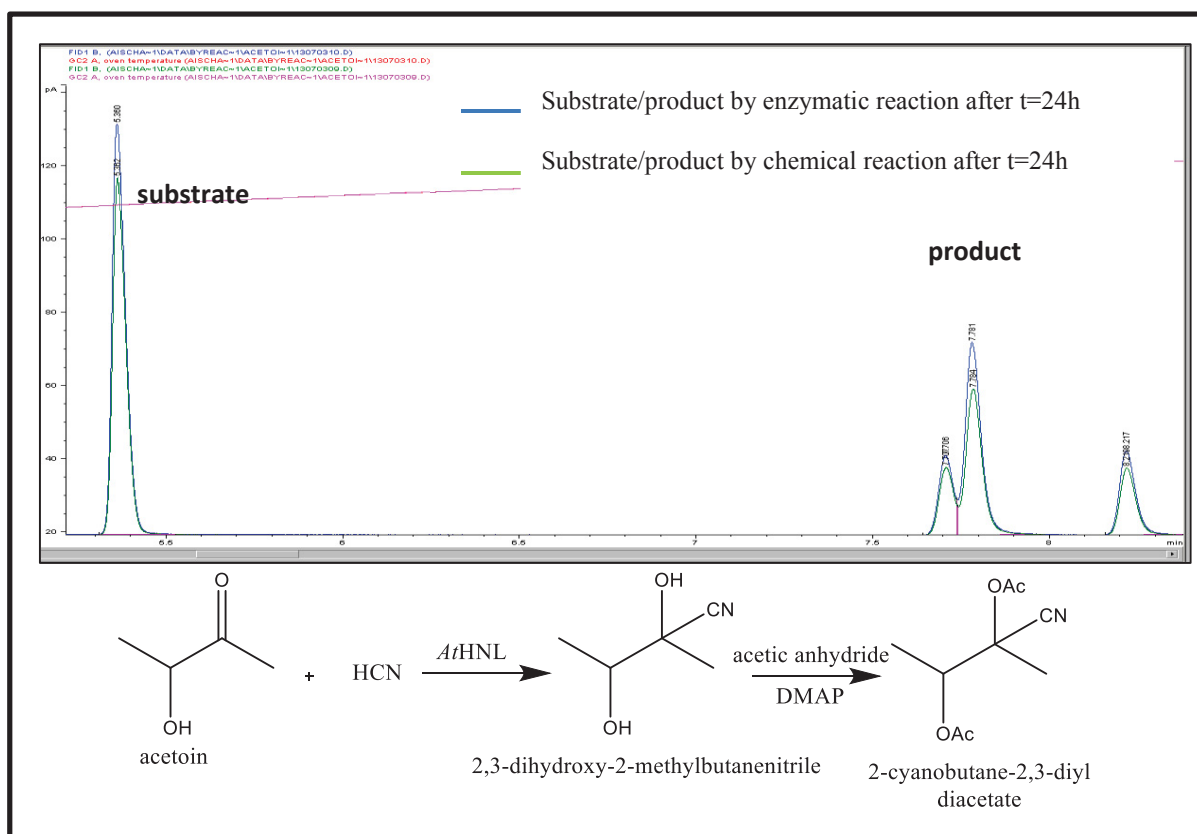


Compound	Structure	Retention time
2-F-acetophenone		2.0 min
2-(2-fluorophenyl)-2-((trimethylsilyl)oxy)propanenitrile		2.19 min*
2-(2-fluorophenyl)-2-hydroxypropanenitrile		2.6 min and 2.7 min

\*the peaks for the derivatised product could not be separated on the SFC

## Appendix 6: GC chromatogram of acetoin-cyanohydrin

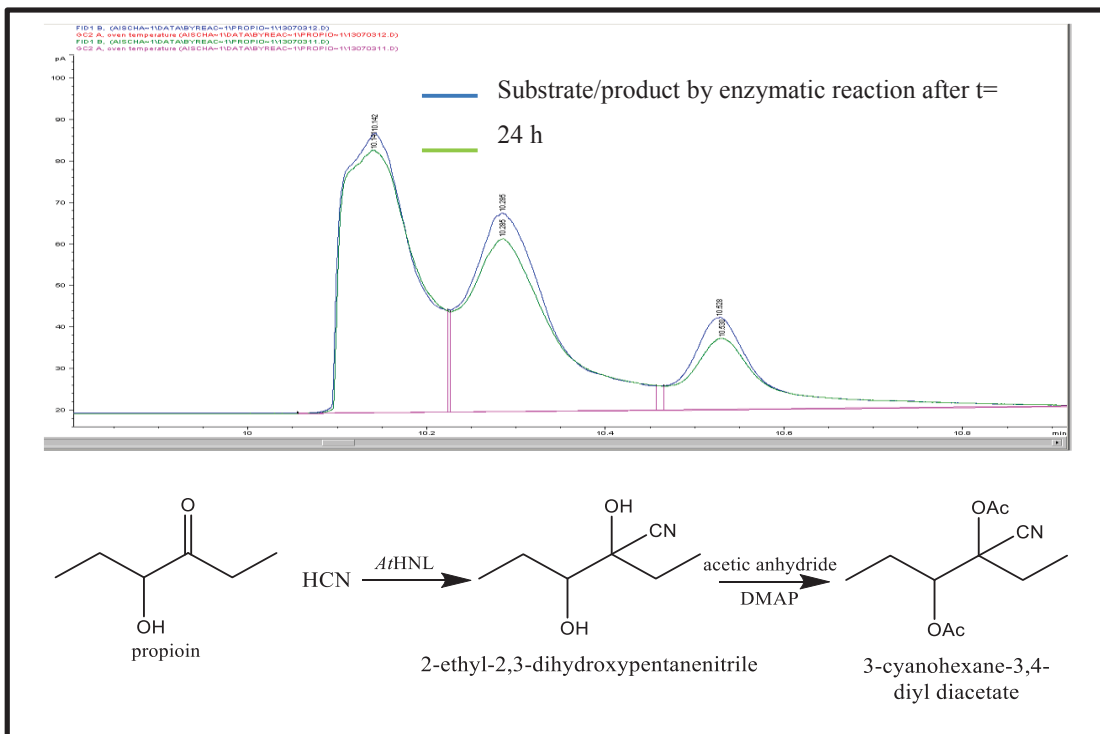
The following chromatogram shows the synthesis of acetoin cyanohydrin in presence and absence of enzyme (chapter 4.2.2). The synthesis reaction was carried out as described in chapter 3.2.12



The conversion was the same in presence (enzymatic) and absence(chemical) of the enzyme.

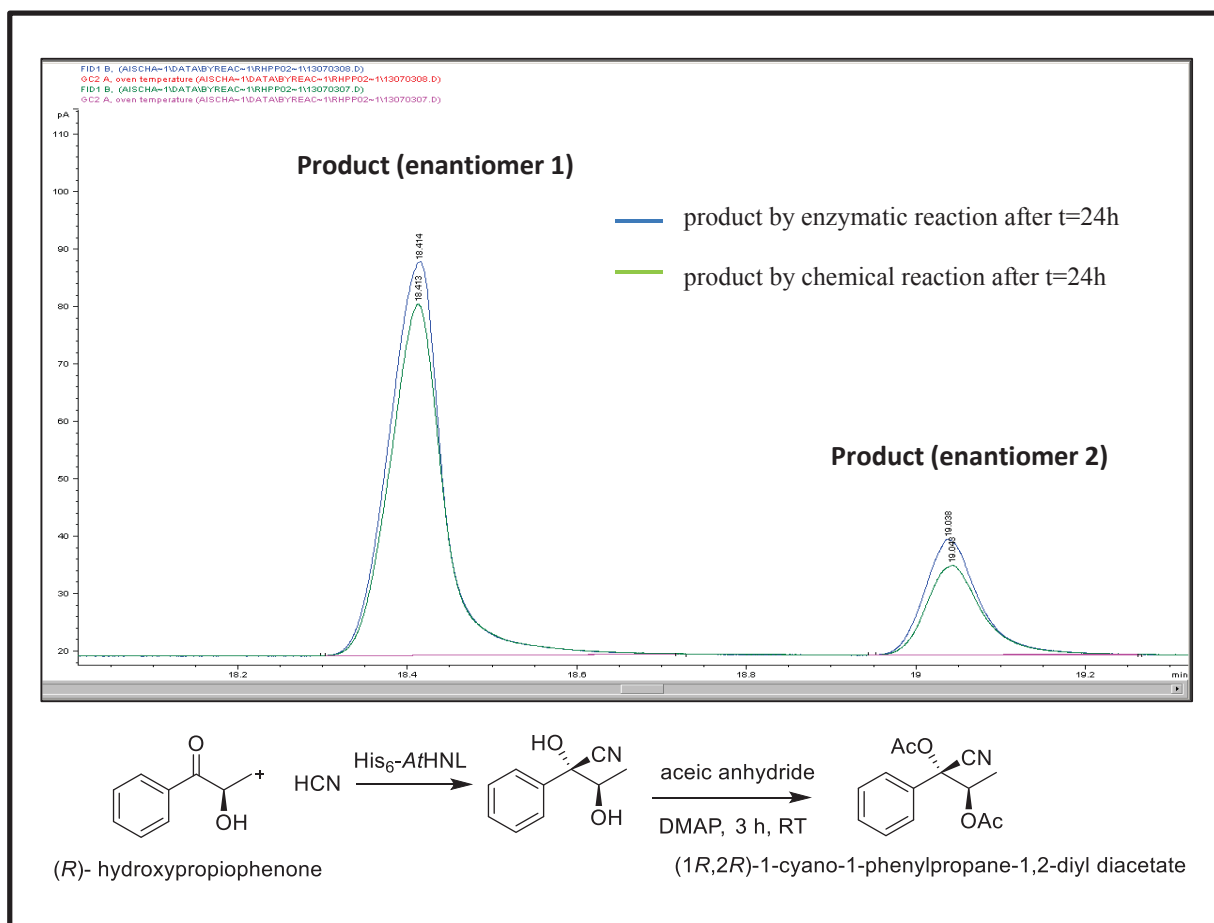
## Appendix 7: GC chromatogram of propioin-cyanohydrin

The following chromatogram shows the synthesis of propioin cyanohydrin in presence and absence of enzyme (chapter 4.2.2). The synthesis reaction was carried out as described in chapter 3.2.12



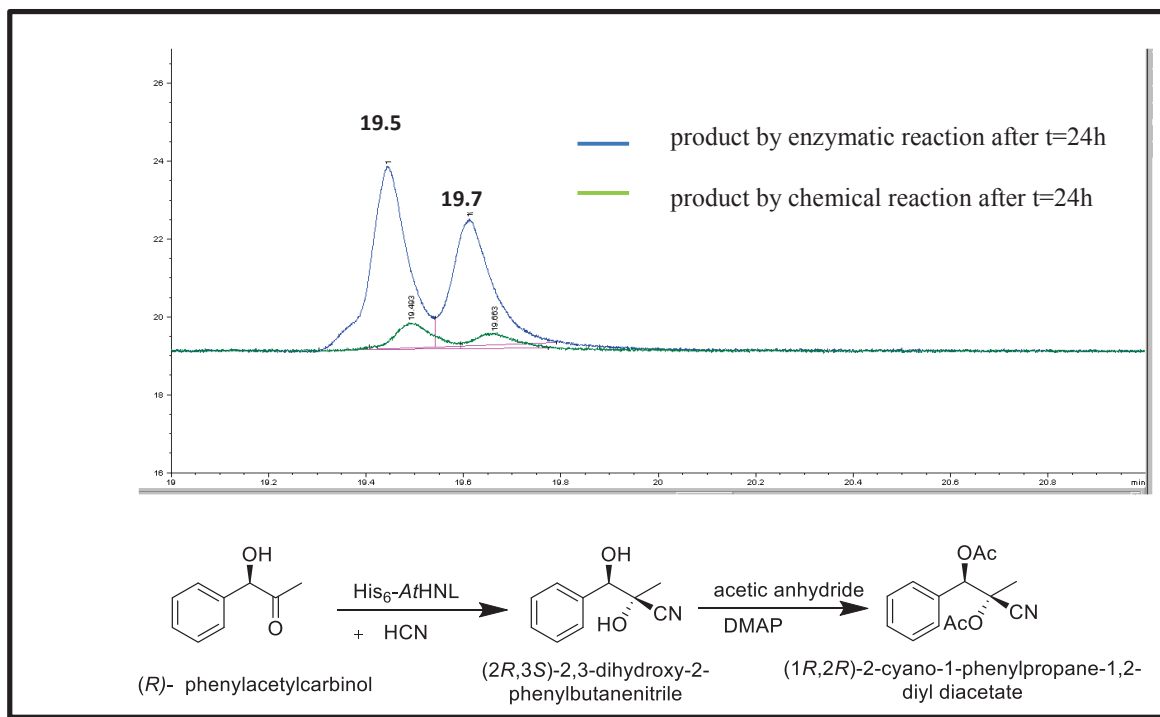
## Appendix 8: Chromatogram for (*R*)-HPP cyanohydrin

The GC chromatogram for *R*-HPP cyanohydrin synthesis is as shown below. *R*-HPP cyanohydrin was synthesized as described in chapter 3.2.12.



The chromatogram shows the conversion in presence and absence of enzyme (chapter 4.2.2)

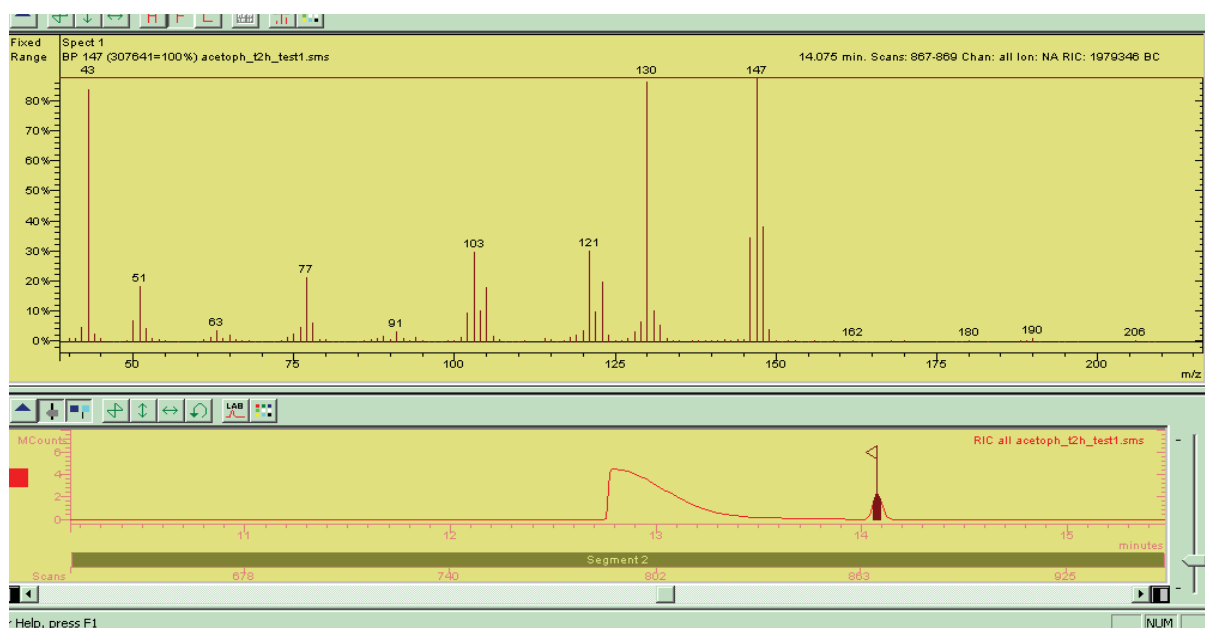
## Appendix 9: Chromatogram for (*R*)- phenylacetylcarbinol (PAC)

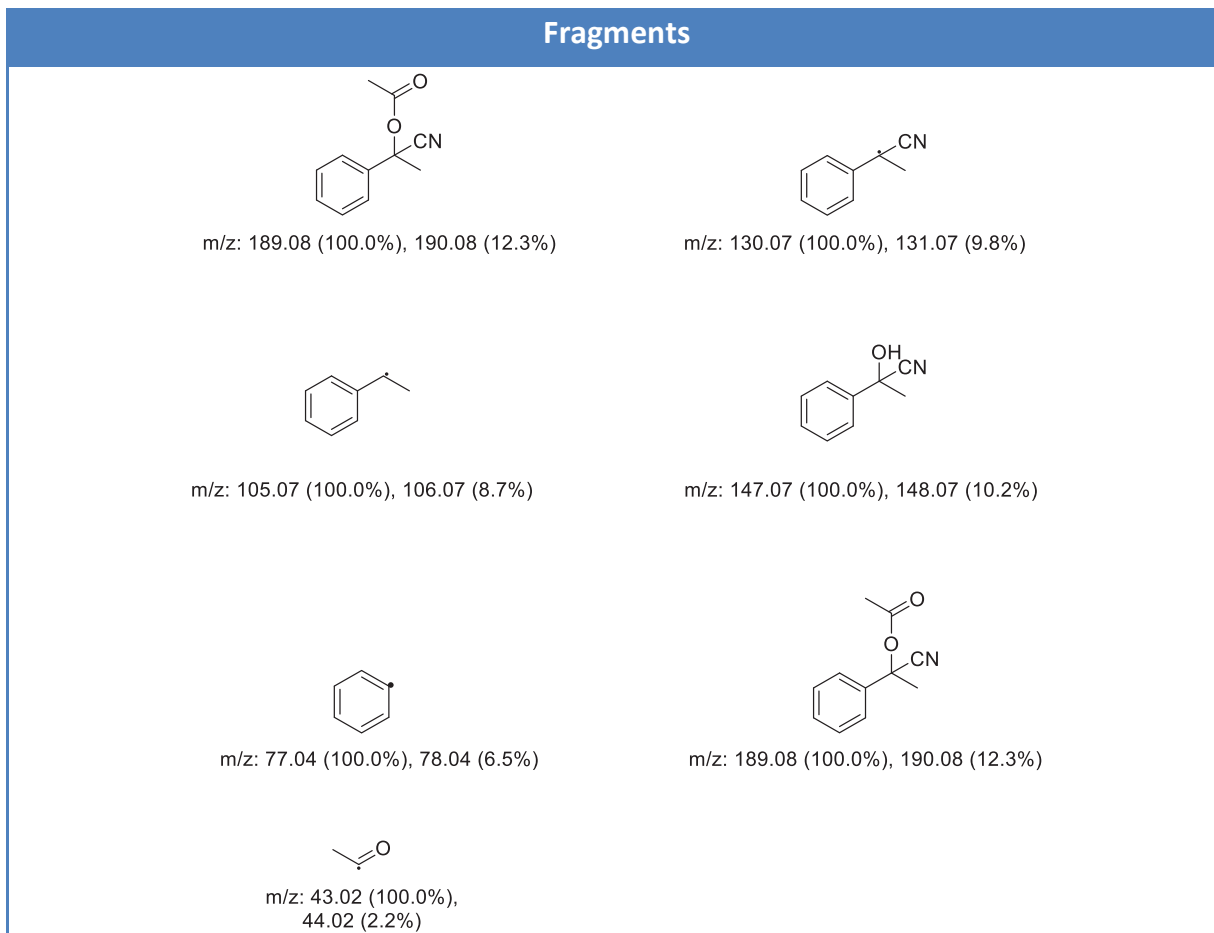


The following chromatogram shows the synthesis of *R*-PAC cyanohydrin in presence and absence of enzyme (chapter 4.2.2). The synthesis reaction and derivatization was carried out as described in chapter 3.2.12

## Appendix 10: Mass spectrometry of acetylated acetophenone cyanohydrin

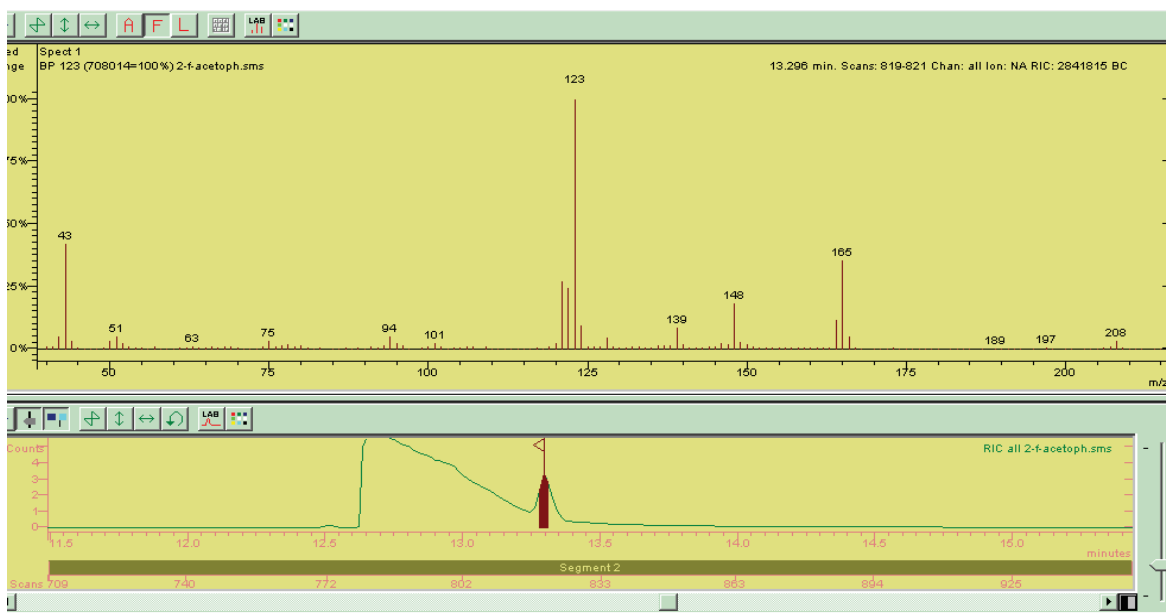
The following figure shows the mass spectra and the fragments for acetophenone cyanohydrin (chapter 4.2.1). Acetophenone cyanohydrin was synthesized as described in chapter 3.2.12 and the method for MS was described in chapter 3.2.23.4





### **Appendix 11: Mass spectrometry of 2-F-acetophenone cyanohydrin**

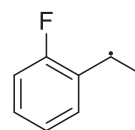
The following figure shows the mass spectra and the fragments for 2-F-acetophenone cyanohydrin (chapter 4.2.1). 2-F-acetophenone cyanohydrin was synthesized as described in chapter 3.2.12 and the method for MS was described in chapter 3.2.23.4



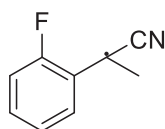
### Fragments



m/z: 207.07 (100.0%), 208.07 (12.3%)



m/z: 123.06 (100.0%), 124.06 (8.7%)



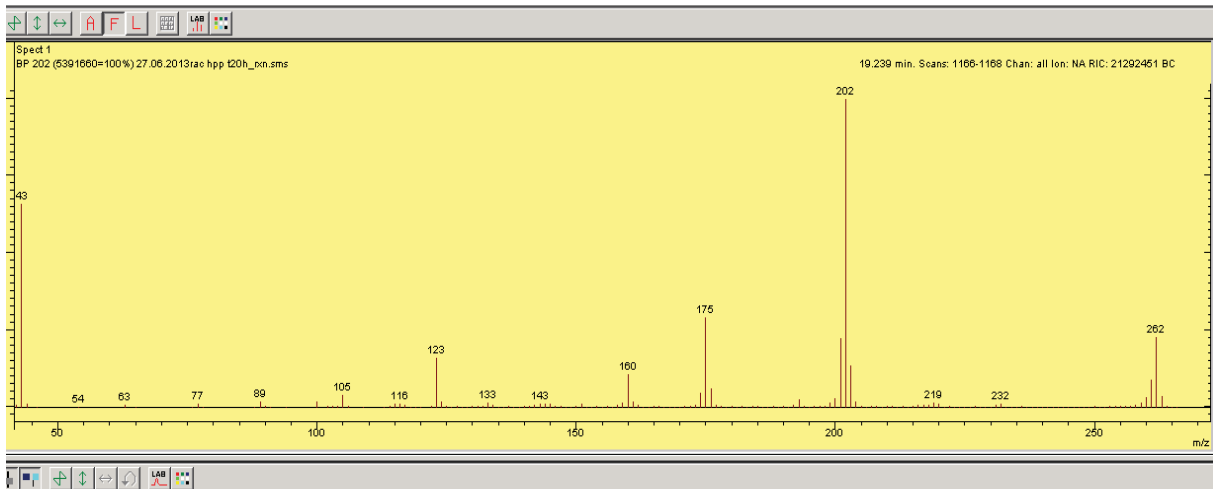
m/z: 148.06 (100.0%), 149.06 (9.8%)



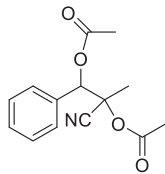
m/z: 43.02 (100.0%),  
44.02 (2.2%)

### Appendix 12: Mass spectrometry of (S)-HPP- cyanohydrin

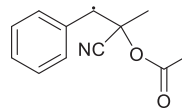
The following figure shows the mass spectra and the fragments for (S)-HPP- cyanohydrin (chapter 4.2.2). (S)-HPP cyanohydrin was synthesized as described in chapter 3.2.12 and the method for MS was described in chapter 3.2.23.4



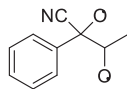
## Fragments



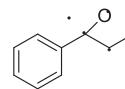
m/z: 261.10 (100.0%), 262.10 (15.7%), 263.11 (1.1%)



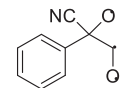
m/z: 202.09 (100.0%), 203.09 (13.2%), 204.09 (1.2%)



m/z: 175.06 (100.0%), 176.07 (11.0%)



m/z: 133.07 (100.0%), 134.07 (9.9%)



m/z: 160.04 (100.0%), 161.04 (10.2%)

## Appendix 13: Mass spectrometry of (R)-PAC-cyanohydrin

The following figure shows the mass spectra and the fragments for (R)-PAC cyanohydrin (chapter 4.2.2). (R)-PAC cyanohydrin was synthesized as described in chapter 3.2.12 and the method for MS was described in chapter 3.2.23.4

